APPENDIX O11.2

Hydrodynamic and Water Quality Modelling in Spencer Gulf: Calibration Report (report by BMT WBM, 2008)

See overleaf for report.

BMT WBM

Hydrodynamic and Water Quality Modelling in Spencer Gulf: Calibration Report

R.B15583.004.04.Calibration.doc
December 2008

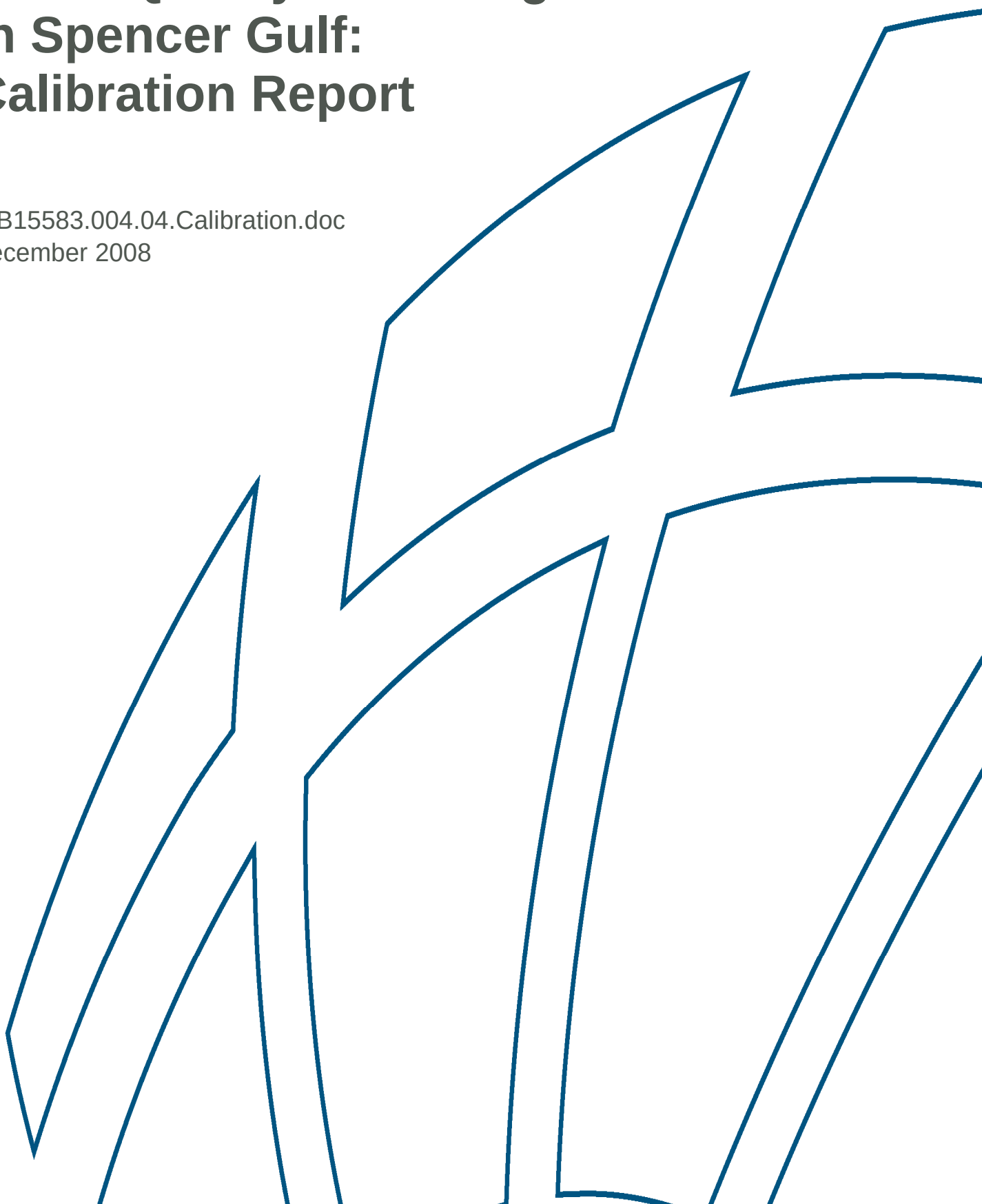

Hydrodynamic and Water Quality Modelling In Spencer Gulf: Calibration Report

Prepared For:	BHP Billiton/Arup
Prepared By:	BMT WBM Pty Ltd (Member of the BMT group of companies)

Offices

Brisbane
Denver
Karratha
Melbourne
Morwell
Newcastle
Perth
Sydney
Vancouver

CONTENTS

LIST OF FIGURES

LIST OF TABLES

1 INTRODUCTION

1.1 Study Background

BHP Billiton (BHP) is considering the construction of a desalination facility in the Spencer Gulf region of South Australia (see Figure 1-1) to supply water to the proposed expansion of the Olympic Dam project. This desalination facility will produce a brine wastewater stream, which will require discharge to Spencer Gulf. Due to the requirements for such a discharge, WBM and the Centre for Water Research at the University of Western Australia were commissioned to develop, calibrate, validate and apply a detailed three-dimensional (3-D) hydrodynamic and transport model in order to assist with the following assessments:

- How brine mixes/behaves near any proposed outfalls, and how the outfalls are designed to ensure no unacceptable environmental impacts in the area where high effluent concentrations may occur. Note that this task relates to mixing/plume behaviour timescales of the order of minutes to hours;
- How brine may travel in the nearshore coastal zone between potential outfall and intake locations, especially with respect to local environmental impacts and potential short-circuiting between the intake and the outfall. Note that this task relates to mixing and plume behaviour timescales of the order of days to months; and
- How the proposed discharge may affect sites distant from potential outfall locations, and in particular, how potentially increased salinity levels in the Upper Spencer Gulf region may affect long-term circulation and transport processes. Note that this task relates to oceanographic timescales of the order of months to years (or even decades).

In regard to the study, key performance parameters/objectives that were defined to quantify acceptable or unacceptable impacts and system performance were as follows:

- In respect to environmental impacts, a key target will be to comply with the SA EPA objective of concentrations from an outfall being within 10% of ambient levels within 100 metres of the discharge (at the edge of a defined 'mixing zone'). This will require both 'far field' (whole of Spencer Gulf) assessments of long-term pollutant accumulation and 'near field' assessments (within several hundred metres) of diffuser configurations and initial waste plume behaviour;
- Potential LD50 (abbreviation for "Lethal Dose, 50%" or median lethal dose of a substance required to kill half the members of a tested population. LD50 figures are frequently used as a general indicator of a substance's toxicity) impacts of constituents that may be present in the wastewater discharge are also of concern. We note that given the timeframe and data sets available to this model study, water quality and toxicant modelling was not possible. As such, separate eco-toxicological assessments have been used to define critical brine and effluent concentrations that are of commensurate impact to an LD 50; and
- In respect to operation, that there be minimal recirculation between the proposed intake and outfall locations. This will require 'mid field' assessments of plume behaviour, in a zone several kilometres around the intake/outfall system.

Given the above, this project has encompassed both far, mid and near field modelling.

By way of general background, we highlight that our modelling work has had to rely heavily upon available data for calibration purposes. We were able to collect a concurrent wind/tide/current/water quality data set encompassing a five-week midwinter period, however, there was a need to rely on previous data to quantify, long-term, seasonal behaviour and oceanographic processes in Spencer Gulf. Fortunately, such receiving water/environmental data were available, however, concurrent model forcing data (tide, wind, solar radiation, etc) were in many cases not available. Hence some of our model comparisons are qualitative (e.g. comparing seasonal behaviour patterns for the mid 1980s, when oceanographic data were available with predicted behaviour for the early 2000's when concurrent forcing data were available), while some are quantitative (e.g. directly comparing recorded data and model results for simultaneous time periods).

Also by way of background, we highlight at this point that the ELCOM (Estuary, Lake and Coastal Ocean Model) model was applied by the study for specific reasons outlined in Section 5.1 of this report. ELCOM is a recognised and widely applied model, and was ideally suited to the needs of this project.

1.2 Proposed Project Details

The proposed seawater reverse osmosis desalination (SWRO) plant will source 'raw' water from Spencer Gulf, with the preferred location for the plant being at Port Bonython (Figure 1-2), though this project will also assess the implications of locating the plant at Port Augusta.

The feasibility of the SWRO plant is dependent, among other factors, on it being demonstrated that there is no undue detrimental impact of the return of wastewater (brine) from the desalination process to the marine environment. The wastewater discharge will have an increased level of salinity and turbidity in respect to background water quality, and will also contain chemical substances used for antifouling purposes.

1.3 Locality Description

1.3.1 General Details

The study is focused on the Port Bonython/Point Lowly area in Spencer Gulf, as this is the presently preferred location of the SWRO plant. In order to adequately assess long-term accumulation and mixing processes, and also to accommodate other potential discharge locations and areas of environmental significance, the study must address the whole of Spencer Gulf.

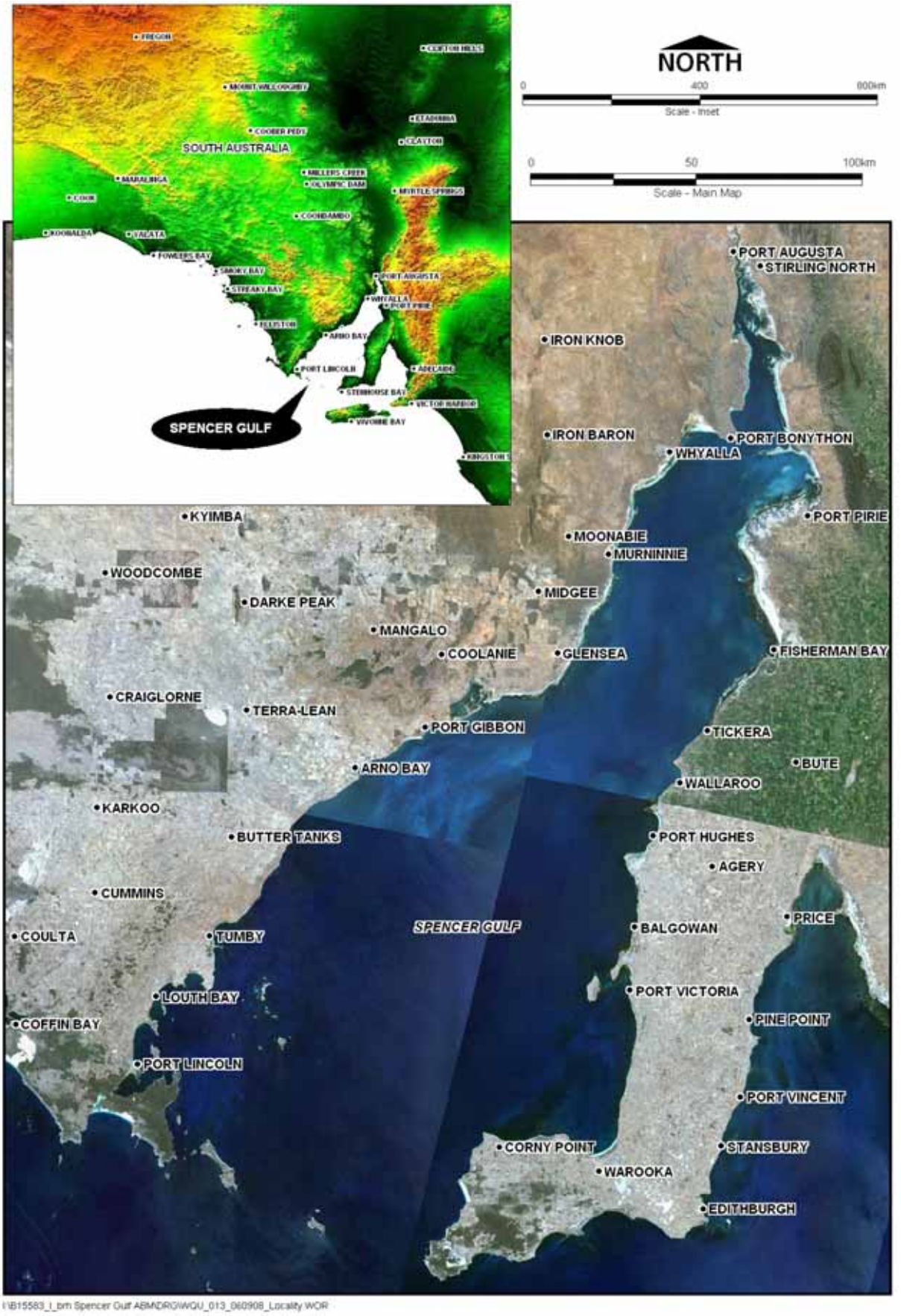

Figure 1-1 Spencer Gulf Locality Plan

Figure 1-2 Port Bonython Locality Plan

1.3.2 Oceanographic Processes

Spencer Gulf is a large (length approximately 300km, mean width approximately 60km), relatively shallow (mean depth approx 22m) semi-enclosed sea, adjacent to the South Australian coast. The key area of interest to this study is the area of Spencer Gulf north of approximately latitude 34 deg S, which can broadly be referred to as Northern Spencer Gulf. This section of the Gulf has a mean depth of approximately 13m, with the mean depth decreasing to approximately 7m north of Point Lowly. Strong evaporation results in a net northward transport of water in order to supply the evaporated volume and as a result a large north-south salinity gradient develops, with salinity approaching 48g/L in the very north of the Gulf during summer. It has been found that the water column is generally vertically mixed except in the case of dodge tides and light winds (Nunes and Lennon 1986) when density driven gravitational circulation can produce stratification for short periods of time.

Local meteorology governs temperature responses in the region, not interaction with the continental shelf. North-south temperature gradients in the water column are up to 2°C from Port Bonython to the head of the Gulf, with the temperature range at Port Augusta ranging between 12 and 24°C over the annual cycle. There is a noticeable temperature lag from north to south, with the shelf lagging the northern Gulf by approximately 40 days with a reduced range (~4°C) compared to the head of the Gulf (~12°C). Associated with the temperature range, the salinity at Port Augusta varies between 43-48 g/L, with the range decreasing to 38-39 g/L 160km south of Port Augusta (Nunes and Lennon 1986).

In the northern Gulf, isohalines run approximately east-west. To the south of Whyalla, isohalines are generally oriented north-south (or more accurately, NNW-SSE), suggesting a cyclonic (clockwise) gyre (Nunes and Lennon 1986). A simple scaling based on the nondimensional Rossby number (R=U/Lf, where U is velocity, f is the Coriolis parameter, and L is a length scale), reflecting the balance between inertia and the Coriolis force, demonstrates why this phenomenon is observed. Nunes and Lennon (1986) observe a velocity scale of ~2 cm/s, f = 7.92e-5 rad/s (T_f = 22 hours) for this latitude, and the scale of the isohaline deviation is ~ 10 km, which gives a Rossby number of ~ 0.01. This indicates that the earth's rotation plays a significant role in the dynamics of the flow. In the southern hemisphere, flows affected by the earth's rotation move with the coastline to the left, which is what is observed with the saline discharge from the Gulf along the eastern shoreline and the fresher inflow along the western shore leading to the cyclonic (clockwise) gyre.

A second mechanism for salt removal observed in the Gulf eventuates from the fortnightly stratification of northern Gulf waters due to the weak neap tides (Nunes Vaz et al 1990). This results in the periodic formation of high salinity fluid packets that flow southwards, initially close to the coast but moving increasingly westward (Nunes Vaz et al 1990).

1.4 Project Team

A joint team from WBM and the Centre for Water Research (CWR) at the University of Western Australia undertook the study. Key project team members and the roles they played in the study are as follows:

- WBM
  - Tony McAlister - Project manager, modelling overview and direction, client liaison
  - Dr Michael Barry - Modelling
  - Craig Morgan - Field data collection
  - Nicole Le Muth - Data collation and review
  - Bruce Harris - Mapping and GIS support
- CWR
  - Dr Jason Antenucci – Modelling
  - Dr Peter Yeates – Modelling

1.5 Report Structure

It is noted that, for various reasons, this report has been prepared and reviewed over a period of almost three years. During this period, the underlying numerical models have been progressively reviewed and interrogated in a number of ways to assess their predictive capabilities relative to a range of expected or previously measured phenomena. In part, the intent of these additional works has also been to assess the robustness and reliability of the models.

For a range of reasons it was determined that, throughout this iterative process, the original calibration report (i.e. the first version of this report issued at the end of 2006) not be altered substantially from its original form. Rather, it was decided that appendices be added progressively to the report to strengthen and support various aspects of the modelling study, both in response to reviewer feedback and as part of works to generally improve the modelling framework.

As a result, the report is presented in its final form as essentially the original calibration report (with some minor alterations) and two consolidated Appendices. Where appropriate, references to the Appendices are made in the main body of the report to assist the reader.

2 PROJECT OVERVIEW

The modelling study was broken into three stages, each with specific tasks and objectives. The stages were:

- Stage 1: Review and Data Collection
- Stage 2: Model Development and Initial Impact Assessments
- Stage 3: Detailed Impact Assessments

The tasks and objectives of each of these stages are summarised below. For reference, we provide Figure 2-1 which illustrates the spatial extents of the far, mid and near field models referred to in this report. The near field delineation refers to the approximate areas from which forcing data was extracted for subsequent model execution. We note that no detailed near field modelling was conducted for the potential discharge location at Port Augusta as far and midfield modelling work indicated that such an outfall may have unacceptable impacts on the northern reaches of Spencer Gulf.

Only stages 1 and the model development component of Stage 2 are presented in this report, with modelling assessments presented in subsequent reports.

2.1 Stage 1 - Data Review and Data Collection

Tasks/Objectives:

- Review past studies and available data
- Define additional data requirements
- Collect additional calibration and verification data

2.2 Stage 2 – Model Development and Initial Impact Assessments

Tasks/Objectives (only model development presented here):

- Using available data, set-up, calibrate and validate a suitable far field 3D hydrodynamic model suitable for initial impact investigations. This task was divided into the following sub-tasks:
    - Reproduce observed north-south salinity gradient using the far field model.
    - Reproduce observed large scale gyre characteristics (isohalines) from an initial east-west isohaline distribution using the far field model.
    - Reproduce observed minimal vertical stratification based on ambient meteorological conditions and tidal forcing using far field model.
    - Reproduce observed seasonal north-south lag in temperature and salinity gradients using far field model.
- Nest mid field model within far field model domain within the region of Port Bonython.

- Couple near field model for negatively buoyant plumes to be generated by the diffuser with mid field model.

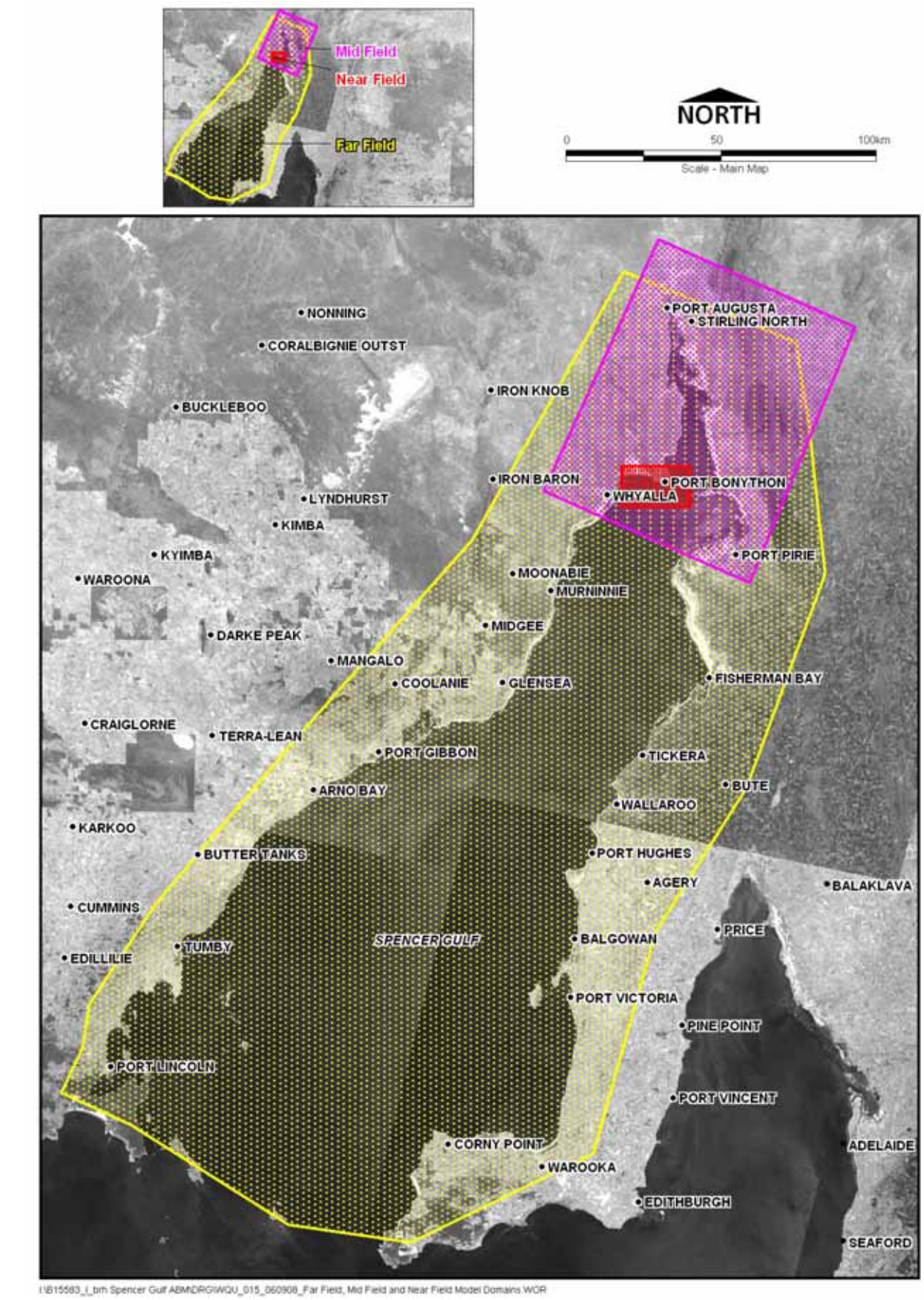

Figure 2-1 Far Field, Mid Field and Near Field Model Domains

- Undertake comparative assessment of several intake/outfall sites for mean spring and neap tides and assess impact on salinity, temperature and brine dispersion. This task was divided into the following sub-tasks:
  - Run far field model to generate boundary conditions for mid field model for period of interest.
  - Simulate various intake/outfall sites with mid field model.
- Investigate potential for recirculation of return water from the outfall to the intake. This task was divided into the following sub-tasks:
  - Determine 'worst-case' scenario conditions for diffuser performance.
  - Run mid field model to determine likelihood for recirculation.

2.3 Stage 3 - Detailed Impact Assessments

Tasks/Objectives (presented in subsequent reports):

- Detailed Plume Dispersion Study.
  - Detailed assessment of medium term (several day) plume dispersion at selected intake/outlet configurations.
  - Recirculation requires high resolution in the vicinity of the diffuser; simulation durations were relatively short (several days), and encompassed summer and winter circulation patterns.
- Salinity build-up study.
  - Detailed assessment of the potential for long-term salinity build-up. This task utilised the far field model used in Stage 2 to ensure the model was capable of reproducing flushing and salinity generation mechanisms in the Gulf.
- Salinity profile study.
  - Assessment of the impacts of preferred discharge locations on brine dispersion and stratification processes in the immediate vicinity of the outfall, focusing on worst-case conditions of high temperatures (summer), low wind and dodge tides.
- Study of hypersaline bottom current.
  - Assessment of interaction of desalination plant with hypersaline bottom current. As part of Stage 2, the far field model reproduced the basic flushing mechanisms of the Gulf, in particular the hypersaline bottom current. In this stage, results from the mid field model were used to determine a saline boundary condition in the vicinity of Pt Bonython, and this saline boundary condition was investigated in the context of its impact on the hypersaline bottom current.

Recommend performance requirements for diffuser design. Performance requirements for the diffuser design were defined based on achieving maximum dilution of the plume given the background flow. This effect will be based primarily on the momentum available, the depth of the diffuser, the (negative) buoyancy between the plume and ambient waters, and the seasonal variation in the plume dynamics as a result of seasonal variations in ambient salinity.

3 DATA REVIEW

3.1 Previous Studies

As part of the data review, a search of all pertinent journals and reference reports was undertaken to identify important background information regarding the study site and hydrodynamic processes occurring within Spencer Gulf. These references were collated and examined in detail to identify relevant information for use in the study. The following list of references was reviewed and collated for use in this study:

- Bullock, D.A. (1975) The General Water Circulation of Spencer Gulf, South Australia in the period February to May. *Transections of the Royal Society of South Australia Incorporated* **99**(1), 43-53, 28 February 1975;
- Petrusevics, P., Harvey, M., Body, P. and Belperio, A. (Iron Triangle Study Group) (1983) Oceanography Study Report. Department of Environment and Planning, South Australia;
- Coast and Marine Branch, Department of Environment and Heritage (2003) Focus: A Regional Perspective of Spencer Gulf. Department of Environment and Heritage, Adelaide;
- Rangelands INRM Group (2004) Supplement to Rangelands Integrated Natural Resource Management Plan and Investment Strategy, Upper Spencer Gulf Area (Draft). Department of Water, Land and Biodiversity Conservation, Adelaide;
- Natural Systems Research Pty Ltd (NSR) 1981, Cooper Basin Liquids Project. Oil Spill Trajectory Study. Final Report, Prepared for SANTOS Ltd;
- Natural Systems Research Pty Ltd (NSR) 1982, Cooper Basin Liquids Project. Oil Spill Trajectory Study. Tidal Currents, Prepared for SANTOS Ltd;
- Steedman RK & Associates 1983, Review of Northern Spencer Gulf Water Circulation & Dispersion prepared for SA Dept Environment & Planning;
- Whyalla Investment Park DoEF Report, extract received from Arup;
- PB and SARDI Research and Development, Technical Review for Aquaculture Management Plans – Phase 2 – Volume A – Upper Spencer Gulf, Section 7 – Fitzgerald Bay, extract received from Arup;
- 2004 Technical Report: An Ecologically Representative System of Marine Protected Areas in SA, Section 8.10, extract received from Arup;
- Gostin, V.A., Hails, J.B., and Belperio, A.P. The Sedimentary Framework of Northern Spencer Gulf, South Australia. *Marine Geology* 61 111-118, 1984;
- Nunes, R.A. and Lennon, G.W. Physical Property Distributions and Seasonal Trends in Spencer Gulf, South Australia. *Australian Journal of Marine and Freshwater Research* 37 39-53, 1986;
- Lewis G. D., Noye, B.J. and Bills, P.J. Oil Spill Trajectory Modelling in Northern Spencer Gulf, The University of delaide, Adelaid, South Australia;
- Mickley, M. (2006) Environmental Considerations for The Disposal of Desalination Concentrates. Retrieved on 14 July 2006 from http://www.mickleyassoc.com/protected/disposalfull.html;

- EPRI Community Environment Centre Project Staff (1994) Modelling of Brine Disposal in Oceans, St. Louis, Missouri, EPRI Community Environment Centre;
- Gaylard, S. (2004) Ambient Water Quality of the Gulf St Vincent Metropolitan Coastal Waters Report No. 2 1995-2002. Environmental Protection Authority, Adelaide;
- Easton A.K. A Reappraisal of the Tides in Spencer Gulf, South Australia. *Australian Journal of Marine and Freshwater Research*. 29 467-77, 1978;
- Corbin, T. and Wade, S. (2004) Heavy Metal Concentrations in Razor Fish (*Pinna bicolor*) and Sediments Across Northern Spencer Gulf. Environmental Protection Authority, Adelaide;
- Nunes, R. A. (1985) Catalogue of Data From A Systematic Programme of Oceanographic Measurements in Northern Spencer Gulf From 1982 to 1985 (Cruise Report No. 9). Flinders Institute for Atmospheric and Marine Sciences, Flinders University of South Australia;
- Bye, J. A. T. and Harbison P. (1987) Hydrological Observations in Far Upper Spencer Gulf, South Australia, During 1986 (Cruise Report No. 13). Flinders Institute for Atmospheric and Marine Sciences, Flinders University of South Australia; and
- Bye, J. A. T. and Harbison P. (1989) Hydrological Observations in Spencer Gulf and the Pirie-Torrens Plains, South Australia, During 1987 and 1988 (Cruise Report No. 15). Flinders Institute for Atmospheric and Marine Sciences, Flinders University of South Australia.

3.2 Bathymetric Data

A thorough review was conducted of all available bathymetric data for Spencer Gulf, with particular attention being given to the Upper Gulf region. A wide range of relevant data sets were identified, primarily from local Admiralty and navigation charts. These data were digitised and corrected to Australian Height Datum (AHD) from the various chart and low water datums that had been used in order to create a single, high-quality digital elevation model (DEM) of Spencer Gulf. This DEM, illustrated in Figure 3-1, was subsequently used for construction of all models used by the study. Further detail around Port Bonython is shown in Figure 3-2.

3.3 Tidal Data

3.3.1 Historical Tidal Data

All available historic tide data for the region has been investigated and sourced where appropriate. Investigations revealed three primary organisations from which recorded tide data could be sourced. A brief summary of each data source is outlined below:

- **National Tide Centre (NTC), Bureau of Meteorology**. The NTC commenced operation in January 2004, replacing many of the functions of the former National Tidal Facility of Australia (NTFA) operated by Flinders University of South Australia. The NTF ceased operations in December 2003, and consequently tide data has since been managed by the NTC. Apart form the standard ports (Wallaroo, Whyalla, Port Pirie and Port Lincoln) and Port Augusta, all other tide data in the Spencer Gulf Region held by NTC has been recorded by Flinders University Students using pressure sensors, hence no Tide Gauge Zero/Australian Height Datum/Lowest Astronomical Tide relationships were available.

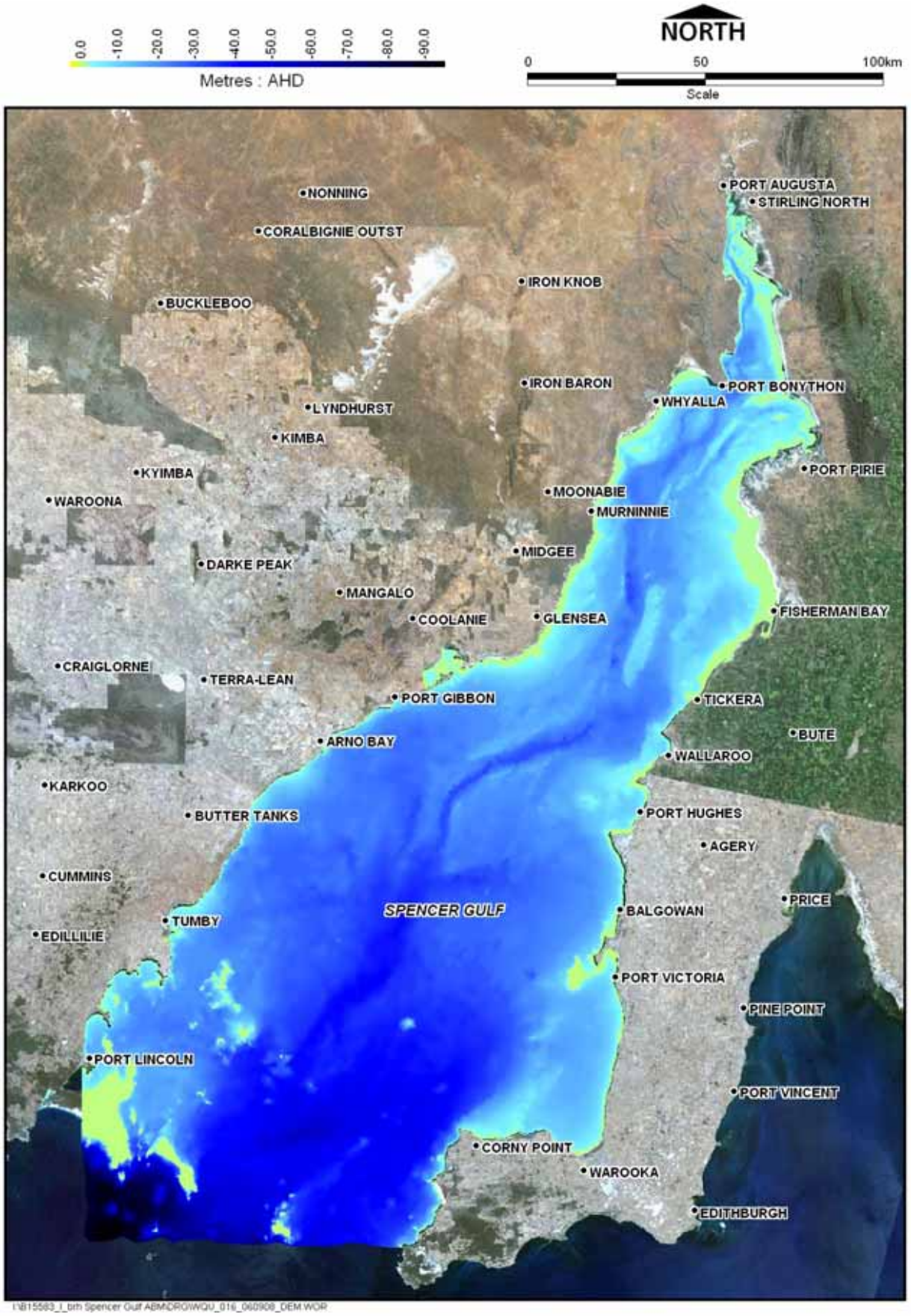

Figure 3-1 Spencer Gulf DEM

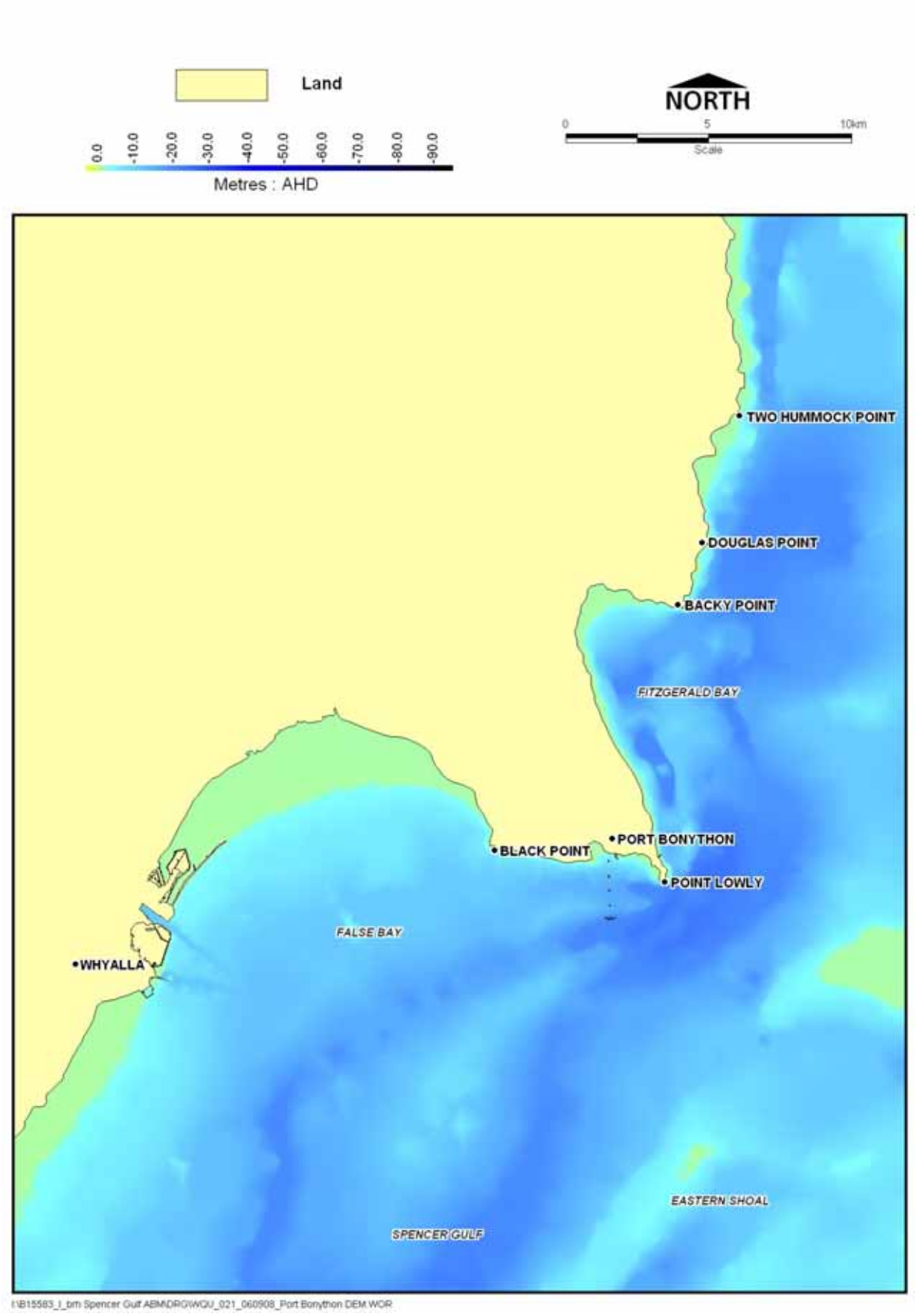

Figure 3-2 Spencer Gulf DEM, Port Bonython Detail

- **Flinders Ports Corporation (FPC)**. The FPC has historically recorded tide levels using analogue charts which would then be passed to the NTC at Flinders University (now NTF BOM) who would digitise this information into hourly tides. Between January 1996 and November 2004, FPC began converting to digital tide gauges, making 5-minute digital data available for standard ports that can be sourced directly through FPC.
- **Australian Hydrographic Services (AHS), Royal Australian Navy**. The Australian Hydrographic Office of AHS maintains the national hydrographic data collection. This accumulation of data is used to provide the national navigation chart series. NTC is the primary source of tide information provided to the AHS, however AHS holds data for some tide gauges in the Spencer Gulf region that the NTC does not have.

Historical tide data was obtained from NTC and AHS. Data was not sourced from FPC due to the high cost of obtaining data. If required, this data will be sourced at a later date when known time frames of interest have been established to minimise expenses. Table 3-1 summarises the information available from Flinders Port Corporation if data is required to be sourced at a later date. It is noted that FPC's standard fee for the full dataset of recorded data is $396 per year per port, but as more data is requested the cost per year to obtain decreases. It is also less expensive to obtain data in larger time increments.

It is also noted that FPC has also recently installed a digital tide gauge at Port Bonython. Communications with Greg Pearce (HydroSurvey Australia, FPC) on 15 June, 2006 have indicated that some equipment calibration is still required before the data at Port Bonython is considered reliable. The locations of tide gauge data sourced from NTC and AHS are displayed below in Table 3-1.

Table 3-1 Digital 5 minute data available from the Flinders Port Corporation

Port	Data Start Date	Data End Date	Recording Period
Port Lincoln	September 1996	July 2006	9.9 years
Wallaroo	November 1997	July 2006	8.7 years
Port Pirie	February 1999	July 2006	7.5 years
Whyalla	November 2004	July 2006	1.75 years

In total, tide data within the Spencer Gulf Region was sourced for 14 locations from NTC, and 9 locations from AHS, giving a total of 23 locations where tide data has been collected through the Gulf. A summary of the data received from NTC and AHS for these locations is detailed in Figure 3-3Figure 3-3, Table 3-2 and Table 3-3.

Figure 3-3 Tide Gauge Locations

Table 3-2 Summary of Tide Data Received from the National Tide Centre

Tide Gauge Location	Original Data Source	Data Start Date	Data Finish Date	Approximate Recording Period	Distance of TGZ below 0m AHD
Port Augusta	FPC	15/11/1976	31/12/1983	7 yrs	**2.025**
Redcliff (Beacon 5)	Flinders University	8/04/1983	21/07/1983	3.5 mths	**Unknown**
Port Bonython	Flinders University	8/12/1983	31/12/1984	1 yr	**Unknown**
Whyalla	FPC	1/01/1987	31/12/1992	6 yrs	**1.741**
Port Pirie	FPC	1/01/1982	31/12/1992	11 yrs	**1.933**
Yarraville Shoal	Flinders University	1/03/1974	6/04/1974	1 mth	**Unknown**
Franklin Harbour	Flinders University	27/06/1989	4/10/1989	3 mths	**Unknown**
Wallaroo	FPC	1/11/1982	31/12/1992	11 yrs	**1.602**
Arno Bay	Flinders University	6/06/1983	5/06/1984	1 yr	**Unknown**
Port Lincoln	FPC	1/01/1982	30/12/1992	11 yrs	**1.024**
Taylors Landing	Flinders University	8/04/1983	22/03/1984	1 yr	**Unknown**
Point Turton	Flinders University	30/12/1954	24/11/1955	1 yr	**Unknown**
Thistle Island	Flinders University	28/11/1985	19/01/1987	2 yrs	**Unknown**
Wedge Island	Flinders University	26/09/1982	18/10/1984	2 yrs	**Unknown**

Table 3-3 Summary of Tide Data Received from the Australian Hydrographic Centre

Location	Start Date	Finish Date	Approx Recording Period	Recorded Time Increment	MSL above LAT	LAT above TGZ
Althorpe Island	3/03/1997	10/04/1997	5 weeks	10 mins	0.55	2.26
Port Victoria	2/04/1991	7/04/1991	1 week	Hourly	0.83	1.49
Cape Elizabeth	10/03/1978	7/04/1978	4 weeks	Hourly	0.85	2.54
Backy Point	14/11/1973	9/12/1973	4 weeks	10 mins	0.88	1.16
Reevesby Island	17/09/1995	13/11/1995	4 weeks	10 mins	1.01	1.41
Thistle Island – East of	2/03/1990	4/04/1990	5 weeks	Hourly	1.35	0.09
Thistle Island – East of	17/11/1992	18/01/1993	9 weeks	10 mins	1.53	0.99
Middle Bank South Beacon	12/05/2005	30/06/2005	7 weeks	10 mins	0.73	1.73
Tiparra Reef Light	18/05/2005	17/07/2005	4 weeks	Hourly	0.72	0.08
Western Shoal Beacon	13/05/2005	7/07/2005	3 weeks	Hourly	0.68	0.77

MSL: Mean Sea Level LAT: Lowest Astronomical Tide TGZ: Tide Gauge Zero

It was noted that no tidal information was sourced from NTC at Port Bonython Jetty in 1986, as suggested in the Whyalla Investment Park DoEF. Paul Davill (NTC) was consulted and WBM were advised that this data was most likely not included due to inaccuracies in the data or possibly the failure to pass this data on when Flinders University ceased operations of the NTF in December 2003.

3.3.2 Synthetic Tide Data

In addition to the collection of historical tide data, predicted artificial tide data were also synthesised to establish boundary conditions with which to run the hydrodynamic and advection-dispersion model of the Spencer Gulf. Data were synthesised for four locations bordering the southern boundary of the Spencer Gulf, namely:

- Taylors Landing;
- Whalers Bay;
- Wedge Island; and
- Pondalowie Bay.

These data were synthesised utilising tidal constituents sourced from Seafarer Tides (http://www.hydro.gov.au/seafarer/tides/tides.html) into the commonly used software IOS Tide. Seafarer Tides is an official Australian Hydrographic Service product that provides users with tidal constituents (and visualisation thereof) for a large number of primary and secondary Australian ports. Tidal data were synthesised for a 6 year period between January 2000 and December 2006.

3.4 Meteorological Data

3.4.1 Meteorological Data Collection

As part of the data collation and review stage for the Spencer Gulf study, all available meteorological data for the region were sourced from the Bureau of Meteorology (BOM) in South Australia and the BOM in Victoria.

Data were collected for all stations within close proximity of the coastline bordering Spencer Gulf. In total, the BOM confirmed nine stations in the location of interest in which meteorological data could be obtained. Figure 3-4 shows the location of these stations. Station data were requested at these locations for the longest duration possible and in the smallest time increments available for the following parameters:

- Rainfall;
- Air Temperature;
- Relative Humidity;
- Wind Speed;
- Wind Direction;
- Cloud Cover; and
- Solar Radiation.

Figure 3-4 Location of Meteorological Stations

The BOM in South Australia provided a mixture of three hourly, hourly and half hourly data for the above listed parameters, apart from solar radiation. Solar Radiation data was only available from the Climate Information Services BOM in Melbourne, Victoria.

Solar radiation is only monitored at two locations on the ground in South Australia:

1. Adelaide; and
2. Mount Gambia.

Half hourly surface based solar radiation data were obtained for these two locations from BOM Victoria. However, as these locations are some distance from Spencer Gulf, the BOM offered to provide satellite derived daily data at our locations of interest. These data could be derived from either latitude and longitude information or BOM station locations. WBM requested satellite derived daily solar radiation data from the BOM station locations shown previously. WBM also obtained data for Moonta derived from latitude longitude information for comparison with the Moonta BOM site data.

Wind frequency analyses and wind roses were also obtained from BOM for Whyalla Aero, however these were of little use.

3.4.2 Meteorological Data Review

Review of the available station data revealed that due to different monitoring periods (refer to Table 3-5 and 3-6), it is not possible to select a period including data from all stations. This is not unusual for modelling studies.

The station data were also interrogated to determine the most appropriate period for subsequent forcing of ELCOM simulations. The period between July 2003 and June 2006 (approximately 3 years) was identified as a possible candidate. This period excludes Port Augusta Power Station and Port Lincoln only, with the following stations included in the data set:

- Port Augusta Aero;
- Whyalla Aero;
- Cleve;
- Neptune Island;
- Moonta (Warburto Point);
- Minlaton Aero; and
- Stenhouse Bay.

Table 3-4 Hourly and Half Hourly Station Data Summary

Station Name	First Year Data	Last Year Data	Hourly/ Half Hourly Intervals	% Complete Between First & Last	% Values with 'N' Quality[1]	Parameters Available[2]						
						Rainfall	Air Temp	Relative Humidity	Wind Speed	Wind Direction	Cloud Cover	Solar Radiation
Port Augusta Aero	2001	2006	Hourly	52	100	✓	✓	✓	✓	✓	×	×
Whyalla Aero	1982	2006	Half Hourly	98	100	✓	✓	✓	✓	✓	×	×
Neptune Island	1962	2006	Half Hourly	75	100	✓	✓	✓	✓	✓	×	×
Moonta (Warburto Point)	2003	2006	Half Hourly	99	100	×	×	×	✓	✓	×	×
Minlaton Aero	2001	2006	Hourly	53	100	✓	✓	✓	✓	✓	×	×
Stenhouse Bay	1996	2006	Hourly	54	100	✓	✓	✓	✓	✓	×	×
Adelaide	2003	2006	Half Hourly	Unknown	Unknown	N/A	N/A	N/A	N/A	N/A	N/A	✓
Mt Gambier	1993	2006	Half Hourly	Unknown	Unknown	N/A	N/A	N/A	N/A	N/A	N/A	✓

[1] N': not quality controlled
[2] Note: Data may not extend for the entire recording duration.

Table 3-5 Three Hourly Station Data Summary

Station Name	First Year Data	Last Year Data	% Values with 'Y' Quality[1]	% Values with 'N' Quality[2]	% Values with 'S' Quality[3]	Parameters Available[4]						
						Rainfall	Air Temp	Relative Humidity	Wind Speed	Wind Direction	Cloud Cover	Solar Radiation
Port Augusta Aero	2001	2006	95	5	0	✓	✓	✓	✓	✓	×	×
Port Augusta Power Station	1962	1997	99	0	0	✓	✓	✓	✓	✓	✓	×
Whyalla Aero	1982	2006	85	2	13	✓	✓	✓	✓	✓	✓	×
Cleve	1957	2006	99	1	0	✓	✓	✓	✓	✓	✓	×
Port Lincoln	1951	2002	87	0	13	✓	✓	✓	✓	✓	✓	×
Neptune Island	1962	2006	99	1	1	✓	✓	✓	✓	✓	✓	×
Moonta (Warburto Point)	2003	2006	94	6	0	×	×	×	✓	✓	×	×
Minlaton Aero	2001	2006	96	4	0	✓	✓	✓	✓	✓	×	×
Stenhouse Bay	1996	2006	98	2	0	✓	✓	✓	✓	✓	×	×

[1] 'Y': quality controlled and acceptable
[2] 'N': not quality controlled
[3] 'S': quality controlled and considered suspect
[4] Note: Data may not extend for the entire recording duration.

Table 3-6 Daily Satellite Derived Solar Radiation Data

Station Name	First Year Data	Last Year Data	% Complete Between First & Last	% Values with 'Y' Quality[1]	% Values with 'N' Quality[2]
Port Augusta Aero	1990	2006	61	72	28
Whyalla Aero	1990	2006	61	72	28
Cleve	1990	2006	60	73	27
Port Lincoln	1990	2006	60	73	27
Neptune Island	1990	2006	-	-	-
Moonta (Warburto Point)	1990	2006	59	72	28
Minlaton Aero	1990	2006	59	72	28
Stenhouse Bay	1990	2006	59	72	28

[1] 'Y': quality controlled and acceptable
[2] 'N': not quality controlled

Data sets at the above stations were examined for any large gaps or spurious data during the July 2003 to June 2006 period. The following discrepancies were noted:

- The station Moonta contains only wind speed and wind direction;
- No cloud data extends over this period for any stations apart from Cleve;
- Spurious data and large data gaps exist in relative humidity between November 2003 – January 2006 at Neptune Island. Periods identified with missing or spurious relative humidity data between this period include:
    - 7/11/03 - 28/11/03
    - 1/7/04 - 1/11/04
    - 23/11/04 - 1/1/05
    - 1/2/05 - 31/8/05
    - 1/11/05 - 31/1/06
- No solar radiation data are available at Neptune Island; and
- Existing solar radiation data has an uncertainty of between 20-25%.

Importantly, it must be noted that due to the lack of ground monitoring solar radiation stations in South Australia, solar radiation data available to use at these sites are satellite derived daily values only, and are less reliable than direct measurements. Additionally, it is noted that the quality of the data between 2001-2006 are potentially suspect due to the installation of a new satellite imagery system. Quality testing of the radiation data acquired during this period indicates uncertainty as high as 20-25%, based on static comparison with station data.

As longer term ELCOM modelling will also be undertaken for the Spencer Gulf study, meteorological data was again examined to help identify a period of approximately 10 years of continuous data.

Of the stations holding long term meteorological data, Port Augusta Power Station and Whyalla Aero were identified as the two most relevant stations for calibration/verification purposes due to their respective locations at the top of the gulf and nearest to the project site (Port Bonython).

Data collected for Whyalla Aero commences in July 1982 whilst data collected at Port Augusta Power Station finishes in June 1997. Therefore the search for a continuous data set was restricted to within this 15 year timeframe. The quality of data at all points with recordings available during this timeframe was examined, with particular emphasis placed on the following parameters:

- Relative Humidity;
- Wind Speed; and
- Wind Direction.

A potentially useful long term data set for the above parameters without any large gaps or spurious data was found to be the period between 9 July 1982 and 9 January 1991. This data set has a relatively ‘continuous’ (no large data gaps) duration of approximately 8.5 years for the following five locations:

- Port Augusta Power Station;
- Whyalla Aero;
- Cleve;
- Port Lincoln; and
- Neptune Island.

It is noted however that no satellite derived solar radiation information is available prior to 1990, and therefore no solar radiation data are available for this period.

3.5 Water Quality Data

A search of available salinity and temperature water quality data was undertaken to aid in calibration of the Spencer Gulf model. Investigations revealed that the most comprehensive temperature and salinity data was reported on by R. A. Nunes in December 1985 in a report entitled *Catalogue of Data From A Systematic Programme of Oceanographic Measurements in Northern Spencer Gulf From 1982 to 1985* ("Cruise Report No. 9"). Flinders Institute for Atmospheric and Marine Sciences, Flinders University of South Australia, published this report.

An electronic copy of the data from the Cruise Report was obtained from the author, Dr Rick Nunes-Vaz. Dr Nunes Vaz also kindly provided separate temperature, salinity and current timeseries data at a range of locations within the Gulf to assist in assessing model robustness. These are presented in Appendix B.

Discussions with the South Australian EPA indicated that water quality data collected in the Spencer Gulf is limited to ambient water quality at Port Hughes and a monthly monitoring program in the Northern Spencer Gulf that has only recently commenced.

Daily historic data for sea surface temperature were also sourced from the CSIRO website. These data were collected using satellite imagery and are accurate for an area of approximately $1km^2$ and to a temperature of approximately 1 degree Celsius.

4 DATA COLLECTION

4.1.1 Overview

A comprehensive data collection program was developed to enable the provision of high quality, concurrent and locally specific (to Port Bonython) information to both inform and support the modelling. This data collection program encompassed the following activities:

- deployment of a bottom mounted Acoustic Doppler Current Profiler (ADCP) adjacent to the end of the jetty structure at Port Bonython;
- deployment of tidal water level gauges on the jetty at Port Bonython, and in the marina basin just to the north of Point Lowly;
- deployment of surface and bottom mounted conductivity/temperature/density (CTD) probes midway along the jetty at Port Bonython;
- performance of several boat mounted ADCP transects to investigate local current patterns around the area of the preferred intake and outfall location;
- the collection and analysis of several water samples in the region to assist in quantifying ambient water quality levels; and
- the deployment of the temporary wind speed and direction recording station on the jetty at Port Bonython for the duration of all field data collection.

The relevant locations of the sites at which data were collected are illustrated in Figure 4-1. The data that were collected are presented and discussed in subsequent sections of this chapter. Appendix B presents a summary of a secondary bottom-mounted ADCP deployment over the summer period of 2007-2008.

4.1.2 Bottom Mounted ADCP

Water currents were measured at a location approximately 1km south-south east of the Port Bonython wharf using an Acoustic Doppler Current Profiler (ADCP) mounted on the seafloor. A 600kHz Workhorse Sentinel Model ADCP manufactured by RD Instruments was mounted within a specialised gimballed frame (a Sea Spider manufactured by Ocean Sciences Inc: http://www.oceanscience.com/spider.html) to measure and record water currents for an approximate 1 month deployment period. The Sea Spider frame containing the ADCP was positioned using the survey vessel “Viking” and a professional diving team from Whyalla Diving Services.

In the bed-mounted configuration, the ADCP is programmed to measure water currents through the water column above the instrument at regular time intervals through the deployment period. Each ensemble consists of many ‘pings’, which are averaged to provide the average current speed and direction within each bin. The ADCP was configured for regular 6-minute measurements of water speed and direction using an ensemble of 50 pings. Water velocities were measured and recorded in 1.0m bins using a water salinity of 40g/L. The ADCP was equipped with an on-board battery and had sufficient internal memory capacity for a deployment in excess of 90 days.

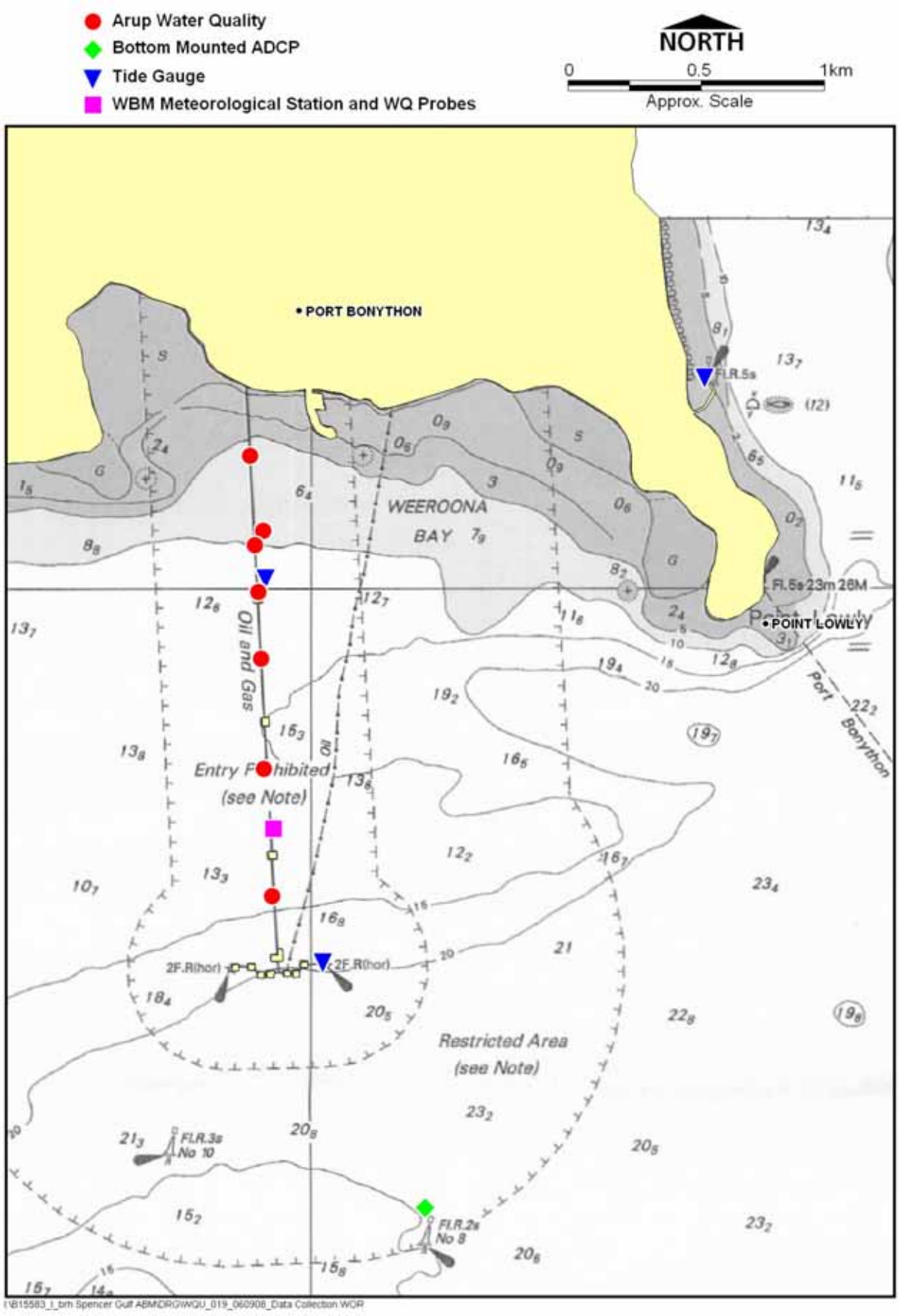

Figure 4-1 Data Collection Locations

The bottom mounted ADCP was deployed on this 12/7/2006 and retrieved on the 20/8/2006. The instrument was deployed in just over 20 metres of water, and provided a high quality data set for use by the study. This data set is illustrated in Figure 4-3 and Figure 4-4 for depth averaged current speed and direction and Figure 4-5 and Figure 4-6 for depth contoured current speed and direction results.

4.1.3 Tide Gauges

Tidal water level measurements were obtained from the deployment of 3 fully submersible Greenspan model PS2100 water level recorders. All were absolute pressure sensing instruments with a 2-atmosphere range (10m water depth) and included measurement of water temperature. Factory calibration of all three pressure sensors was based upon freshwater, so the difference in density between freshwater and denser saline water from Spencer Gulf was taken into account during data reduction.

Two recorders were installed on the afternoon of 12th July 2006, with one being positioned approximately 3m below low water on a raked pile of the outer mooring dolphin at the Port Bonython wharf (758504.4mE, 6343847.6mN – GDA94). The second was positioned on a raked pile close to shore (758320.3mE, 6345364.0mN – GDA94) at a similar depth. A third instrument was placed on a steel frame and lowered into position below the Port hand navigation marker at the entrance to the Point Lowly Boat Harbour (760061.9m E, 6346110.6mN – GDA94). The third instrument is estimated as being approximately 2m below low water.

For each instrument, water level (and temperature) measurements were collected every 6 minutes, based upon an average of 8 measurements each 2 seconds apart to reduce the influence of waves upon the recorded data. Each of the instruments had an inbuilt data logger with the capability to store in excess of 60 days worth of data.

Upon retrieval of the instruments, the internally recorded data were downloaded using a laptop computer with installed Smartcom for Windows Software (Greenspan Technology 2006).

The results of the tidal water level data collection are presented in Figure 4-7. Note that these data have not been corrected to AHD for presentation in this report.

4.1.4 Water Quality Instruments

A combined water quality measurement and wind measurement station was established on the Port Bonython trestle at a location (758325.0m E, 6344376.0mN - GDA94) approximately 1.7km offshore. The water depth at the measurement location was approximately 12m below low water datum.

The installed equipment consisted of two Greenspan Model CS304 water quality probes, each capable of measuring water temperature, electrical conductivity, pH and dissolved oxygen. The instruments were each affixed on a taught chain lowered below the trestle with the upper instrument (Instrument 1) being positioned 11m above the seabed and the lower instrument (Instrument 2) positioned 2m above the seabed. In this way, the instruments were able to measure differences in the water quality at the upper and lower horizons of the depth profile. The instruments were interfaced to a Campbell Scientific Model 200 data logger housed within a small weatherproof box mounted at deck level on the trestle. The weather proof box contained two 12V DC gel Cell batteries

used to power the data logger and a GSM mobile phone modem allowing data from the data logger to be downloaded at regular intervals during the deployment period using "LoggerNet" Version 3.2 (Campbell Scientific Inc, 2005). Sensor communication was via SDI-12 protocol and the sensors were powered only when a reading is required. Water quality measurements were made every 6 minutes following a 20 second sensor warm-up period.

Battery power to the data logger was augmented with power from a small 10W solar panel, mounted on the adjoining handrail. The data logger was also connected to an RM Young Model 05106 - MA Marine Model Wind Sensor that was mounted on a 2m mast. The data logger interrogated the wind sensor at 10 second intervals to log the wind speed and direction from which a 6-minute average wind speed and direction was calculated and stored. The wind direction standard deviation and maximum gust were also recorded. The data logger had an approximate capacity of 12 days of combined water quality and wind speed records, after which the memory wraps over the earliest recorded information.

Representative results of the water quality data collection are presented in Figure 4-8 to Figure 4-10.

4.1.5 ADCP Profiling

Currents in the vicinity of Port Bonython were measured using a boat-mounted Acoustic Doppler Current Profiler (ADCP). The survey vessel "Viking" owned by Whyalla Diving Services was equipped with a 1200kHz Workhorse Sentinel Model ADCP manufactured by RD Instruments and a TRIMBLE Model ProXRS dGPS and Model TSC1 data collector for navigation and position fixing.

ADCP current measurements were undertaken during the peak of ebb tide flow conditions between approximately 2200hrs 14th July 2006 and 0300hrs on the 15th July 2006. A large range ebb tide was selected for the measurement period so that the potential for eddy formation would be high. ADCP measurements were conducted along selected north-south trending transects (parallel to the Port Bonython trestle) varying in length from approximately 3.0 to 3.3km. The vessel was driven at slow speed (approximately 6km/h) along each transect, with each transect requiring approximately 30 minutes for completion. A total of 7 ADCP transects were completed for the evening with the seventh transect being run in a diagonal south-easterly direction from the shoreward end of the Port Bonython trestle to an end point south of Pont Lowly. Corresponding differential global positioning system (DGPS) vessel tracks were recorded for transects 2-6. The ADCP was also equipped with bottom tracking capabilities (see below), although this feature becomes unreliable as a navigation and positioning tool when water velocities are sufficiently high to mobilise bed sediments.

The ADCP transmits bursts of sound (pings) at a known frequency (in this instance, 1200kHz) into the water column. Each complete set of pings is called an ensemble. The sound is scattered by plankton sized particles (reflectors) carried by the water currents and some is received by the ADCP which also listens for reflected echoes from the transmitted sound. As echoes are received from deeper in the water column the ADCP assigns different water depths (depth cells or bins) to corresponding parts of the return echo. This enables the ADCP to define vertical profiles of current velocity. The motion of the reflectors relative to the ADCP causes the echo to change frequency by an amount which is proportional to their velocity. The ADCP measures the frequency change, the Doppler shift and thus constructs vertical current velocity profiles for the water profile.

In a vessel mounted configuration the ADCP looks down through the water column and measures current profiles continuously as the vessel travels along a transect. The current profiles, which are initially measured relative to the ADCP, are then converted to earth-referenced currents. This can be achieved because the ADCP also has the capability of measuring its own motion relative to the earth using the Doppler shift of echoes received from the seafloor (bottom tracking). The bottom tracking feature also allows the ADCP to directly measure the distance travelled between individual current profiles along a given transect. The long channel measured velocity is then used to calculate the discharge (flow) for each bin. In the instance where a transect is undertaken across a channel, the discharges for the bins are progressively summed as the vessel moves from one side of the channel to the other to give a total discharge for the cross section.

The ADCP was configured for measurements of water speed and direction in 0.5m bins using a water salinity of 40g/L. ADCP output was sent to an on-board laptop computer and current measurement and navigation data were displayed and recorded in real time using the RD Instruments software package WinRiver.

The results of the ADCP profiling are presented in Figure 4-11.

4.1.6 Echo Sounding

Extensive echo sounding transects were undertaken as part of the data collection program. These were executed primarily to cross-check the accuracy of the DEM data in the vicinity of the proposed outfall. Other parties involved in the design of the outfall pipe network and associated infrastructure also expressed an interest in collecting this data. The echo sounding transects and interpolated DEM are shown in Figure 4-2.

4.1.7 Water Quality Profiling and Sampling

Project Managers Arup sought the collection of *in-situ* water quality data from the water profile at several locations from shore along the trestle alignment (see F). To this extent, *In-situ* water quality measurements were collected from the survey vessel “Viking” owned by Whyalla Diving Services. The vessel was positioned below the trestle alignment at the required location using a differential Global Positioning System (dGPS) for navigation. The water quality measurement parameters included secchi disc (m), water temperature (ºC), electrical conductivity (mS/cm), salinity (g/L), pH, dissolved oxygen (mg/L), redox (mV), turbidity (NTU) and chlorophyll. Measurements were collected using a secchi disc and a YSI Model 6600 water quality instrument equipped with a YSI Model 650 MDS data collector. Water quality profile measurements were collected at 1m depth increments from near the water surface to the seafloor. Data recorded to the data collector was later downloaded to a lap top computer. Representative results are shown in Figure 4-12.

A set of water samples from a depth of 5m (mid-depth in the water column) was also collected for laboratory analysis of the major ions.

4.1.8 Meteorological Data

The results of the meteorological data collection are presented in Figure 4-13 and Figure 4-14.

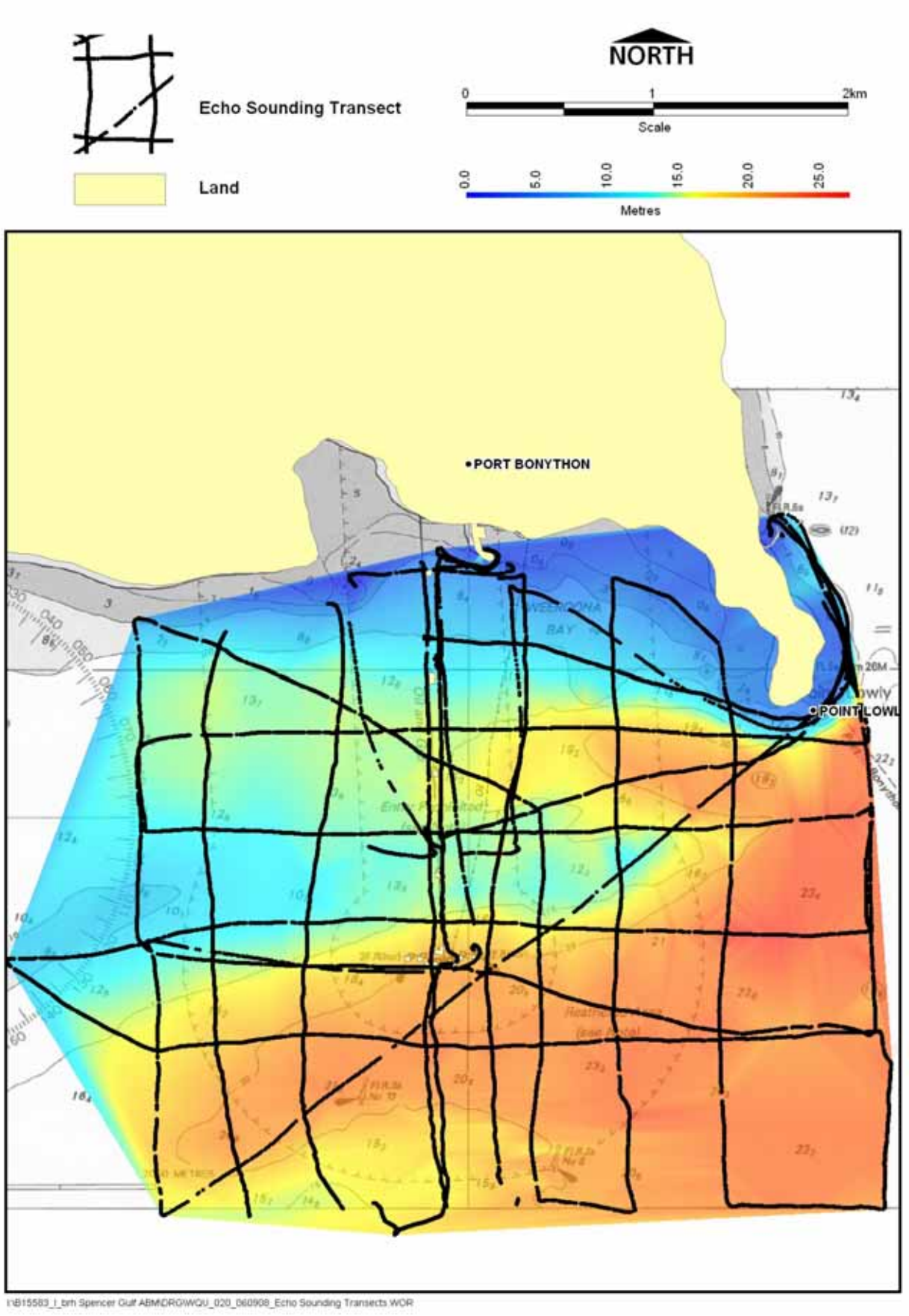

Figure 4-2 Echo Sounding Transects

4.1.9 Summary / Discussion

The data collected for this study and presented in this section of our report provide a detailed record of oceanographic processes in the vicinity of Port Bonython, albeit for a period of several weeks in winter 2006. Key observations that can be made from this data set are as follows:

- the local Admiralty charts are sufficiently accurate for modelling;
- throughout the more than five weeks of ADCP deployment, which encompassed several periods of small/dodge tides, there was nearly always some prevailing current moving past the site;
- stratification to any significant degree, either as major temperature (> ~1^{o}C difference), salinity (> ~1g/L difference) or current velocity differentials between surface and bottom locations, was minimal and not persistent at elevated levels. For example, the largest salinity differences observed from top to bottom were approximately 1.4 g/L (and there was never an inversion), but these were transient, with the average salinity difference being only approximately 0.5 g/L., which is relatively small. The temperature signals showed a very small (~ 0.1 ^{o}C differential), and the observed inversion around 20th July occurred simultaneously with a peak in salinity stratification; and
- ADCP profiling showed strong variations in current speed and direction over relatively short distances, and also highlighted the formation of a tide eddies in the lee of Point Lowly, which may be important in respect to brine accumulation from potential discharge locations in this vicinity.

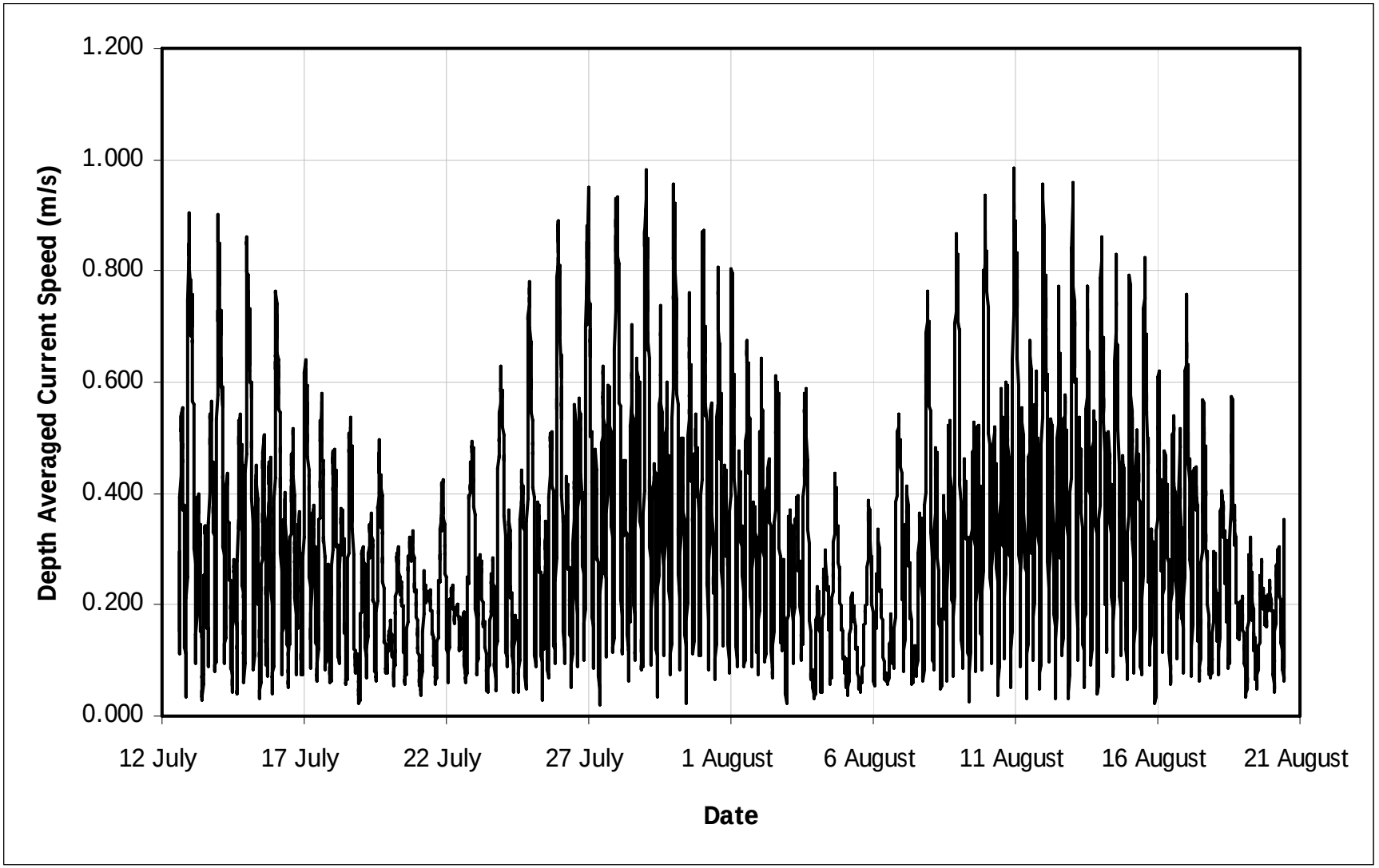

Figure 4-3 Depth Averaged ADCP Tidal Current Data

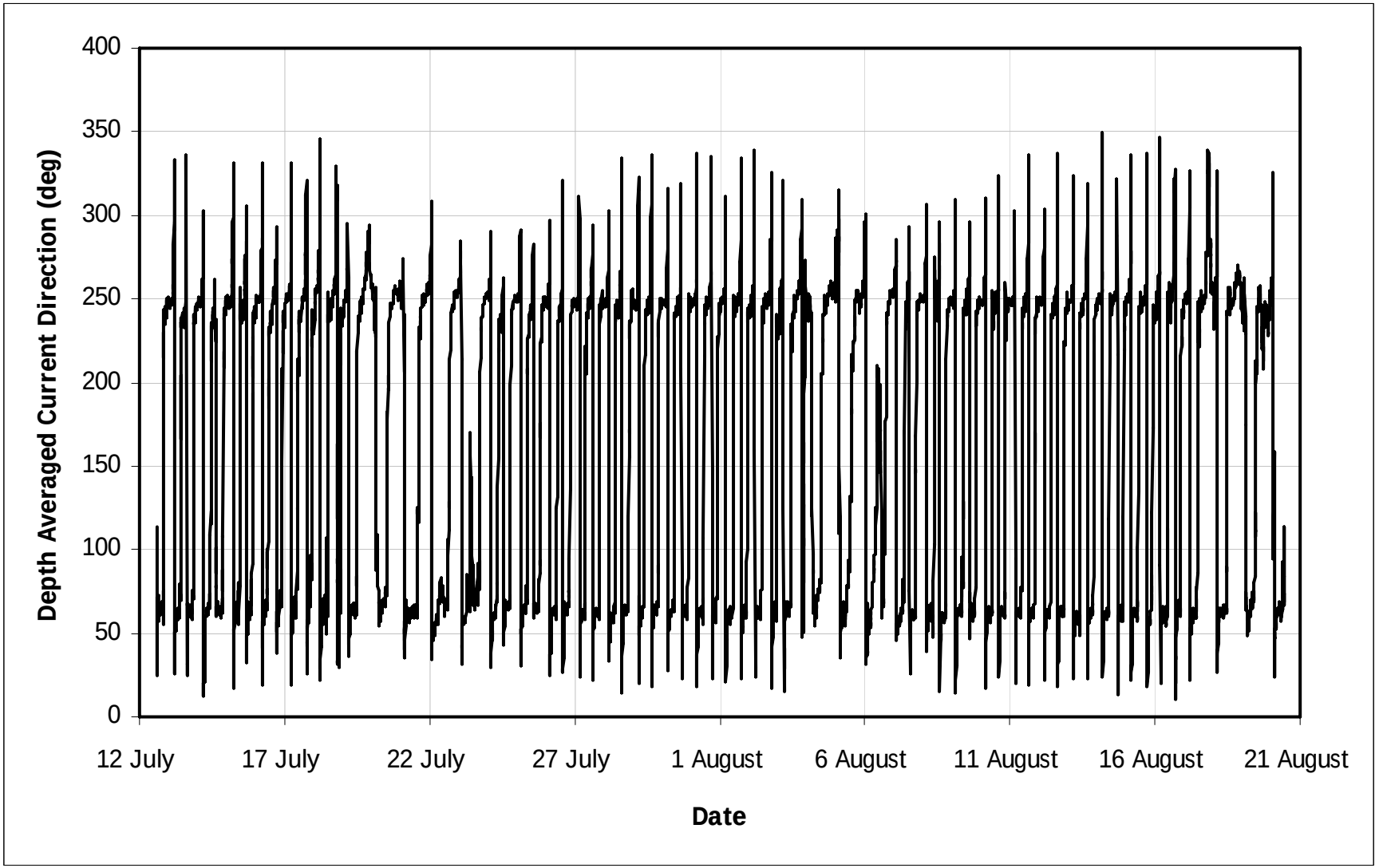

Figure 4-4 Depth Averaged ADCP Tidal Direction Data

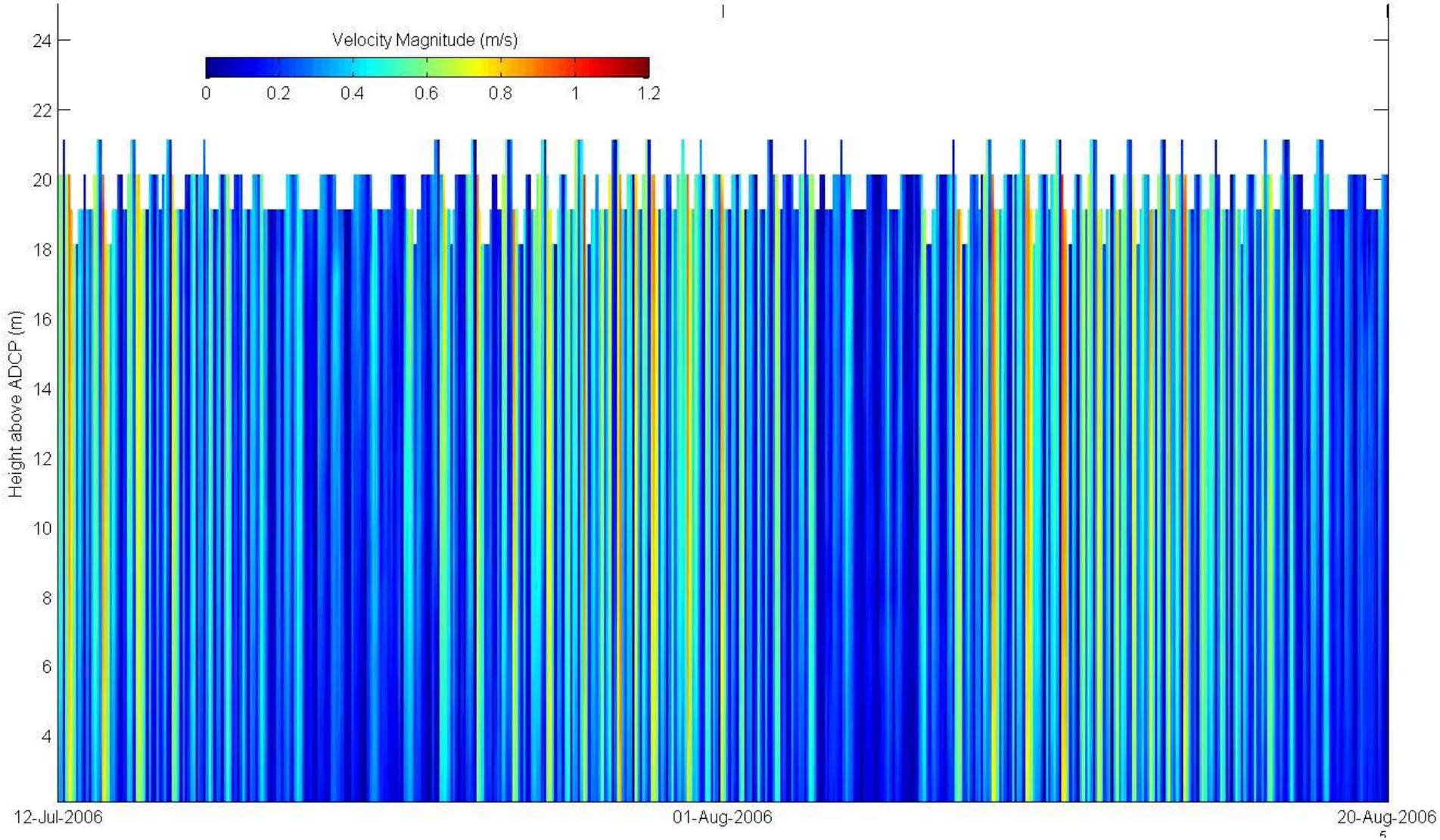

Figure 4-5 Contoured ADCP Tidal Current Data

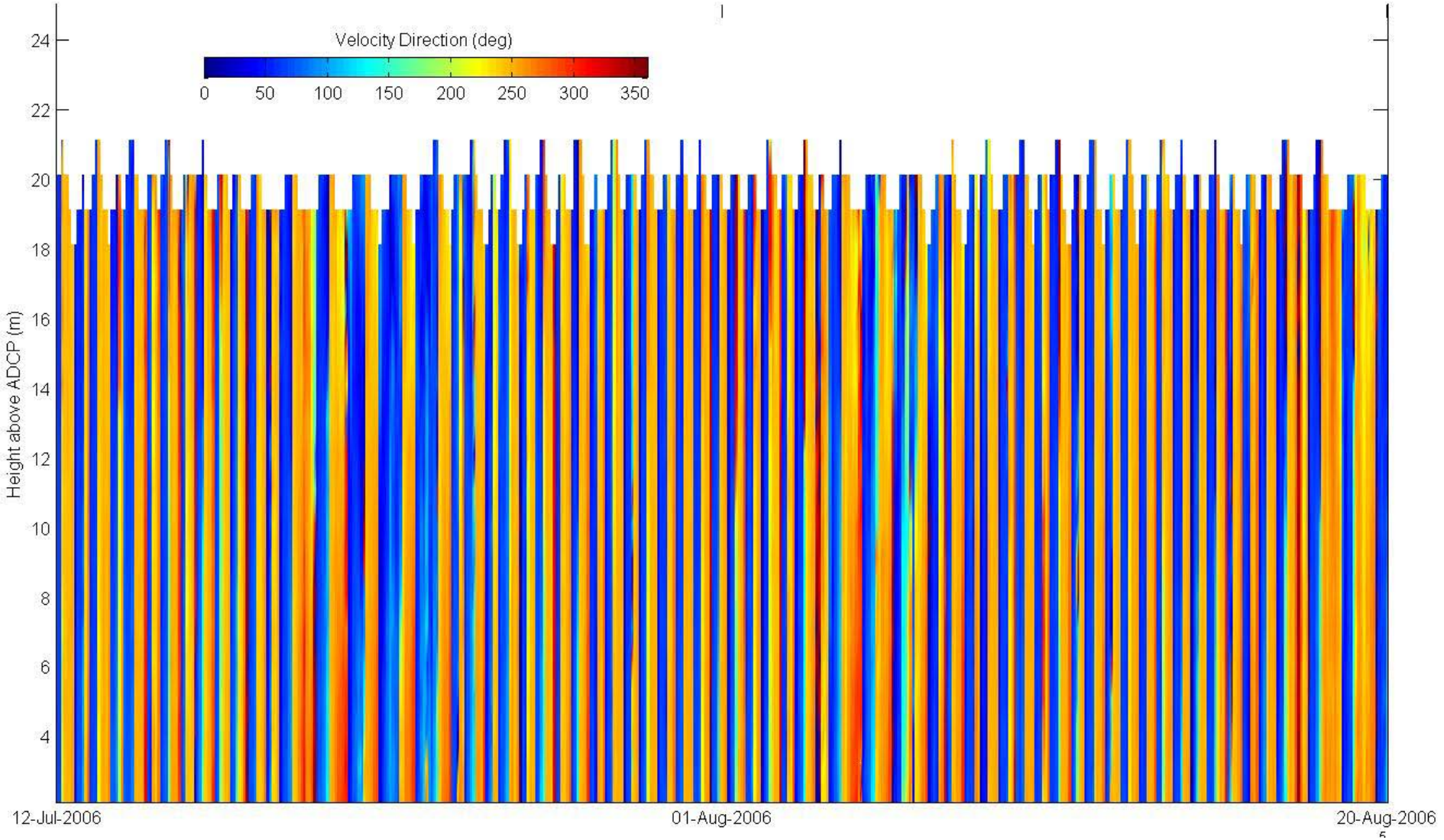

Figure 4-6 Contoured ADCP Tidal Direction Data

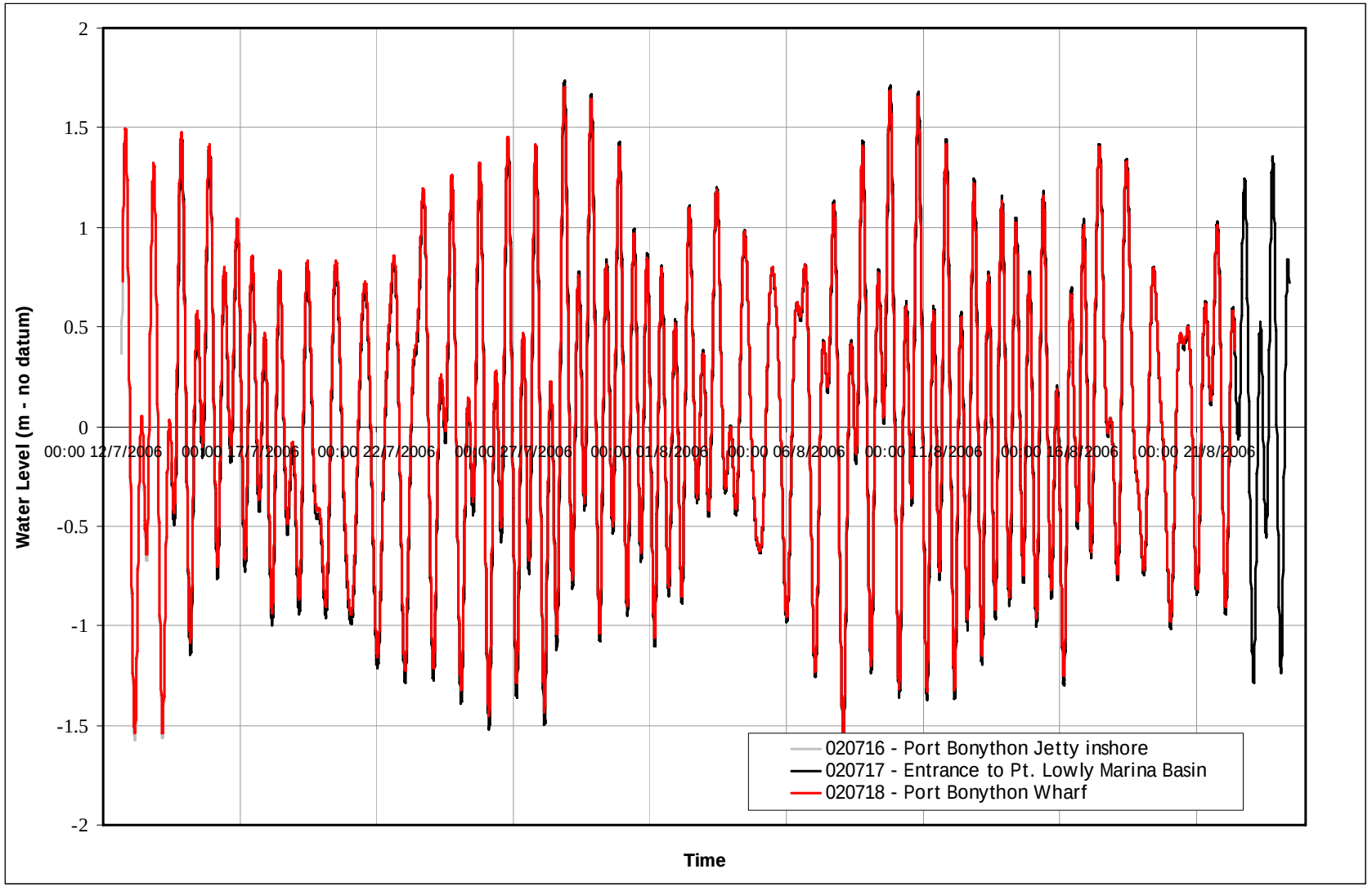

Figure 4-7 Recorded Tidal Water Level Data

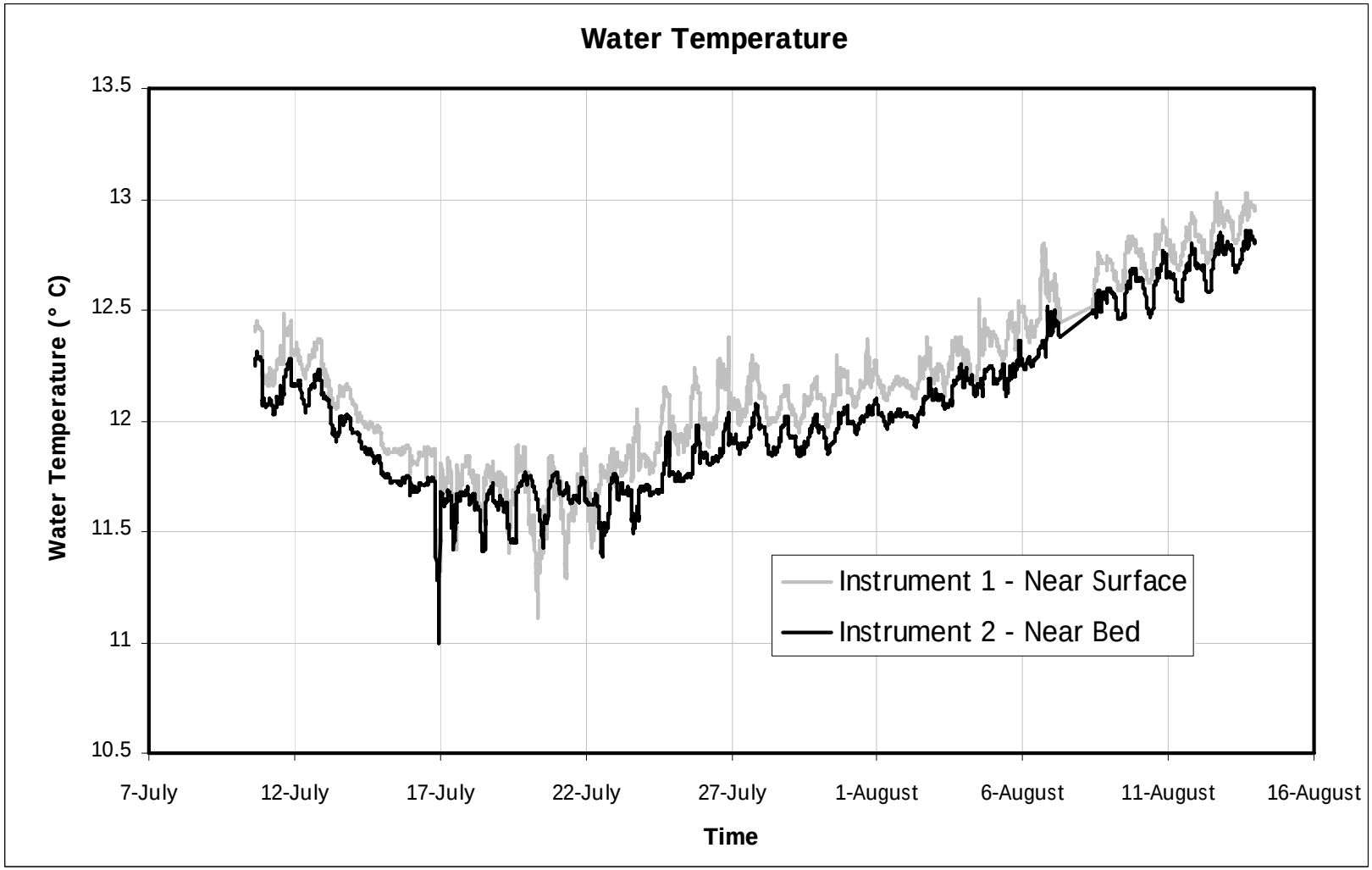

Figure 4-8 Recorded Water Temperature Data

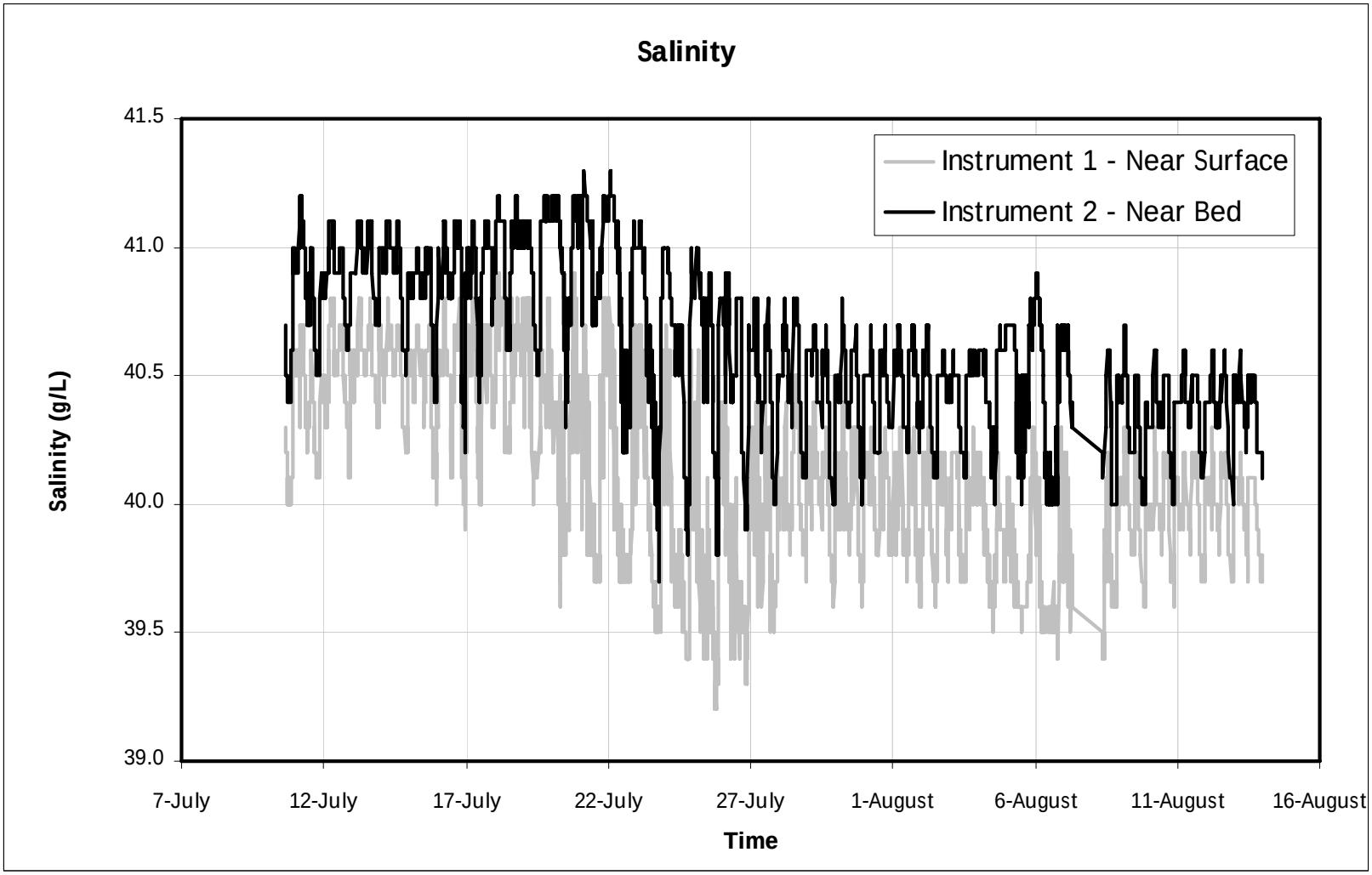

Figure 4-9 Computed Salinity

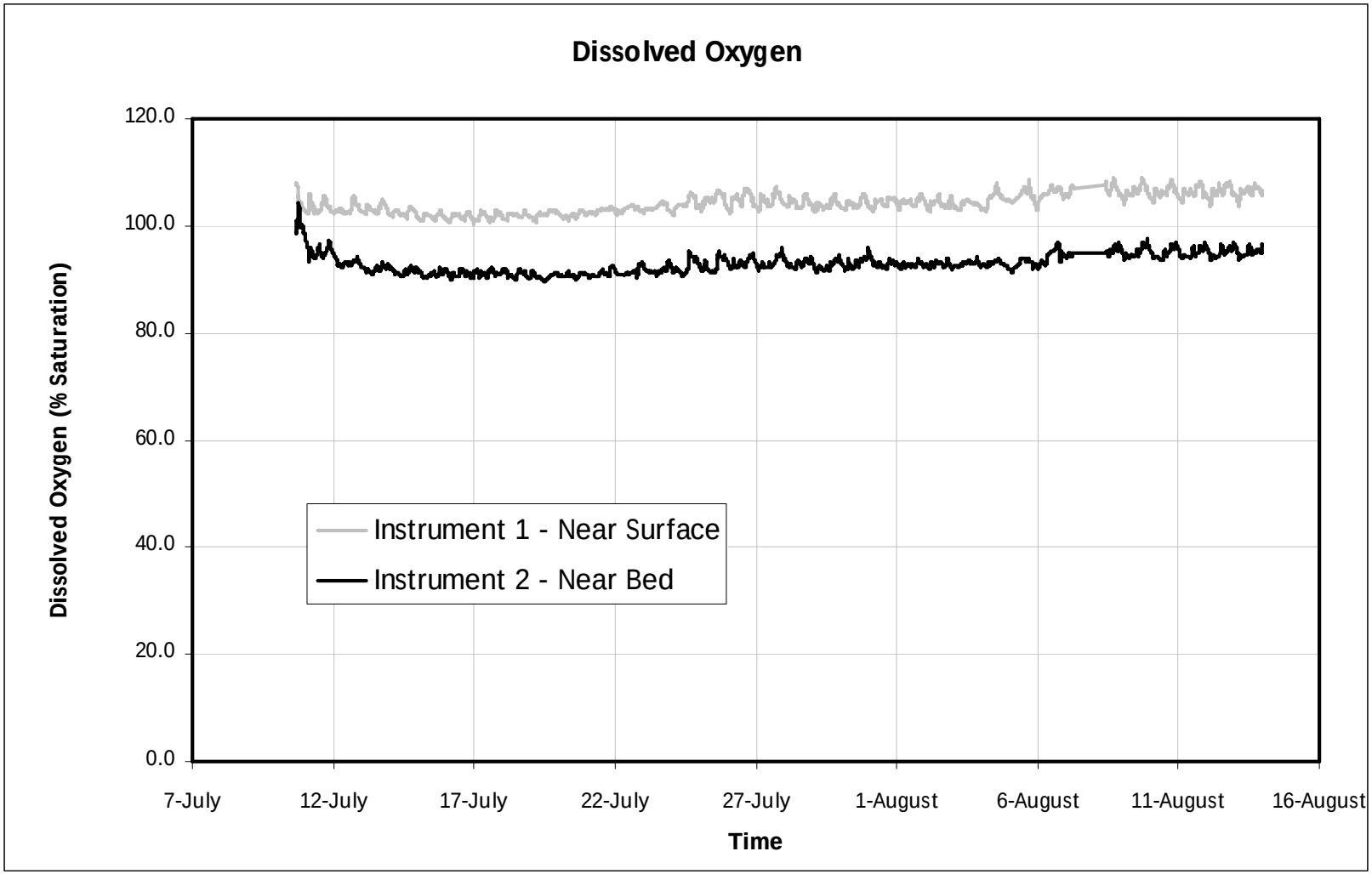

Figure 4-10 Recorded Water Dissolved Oxygen Data

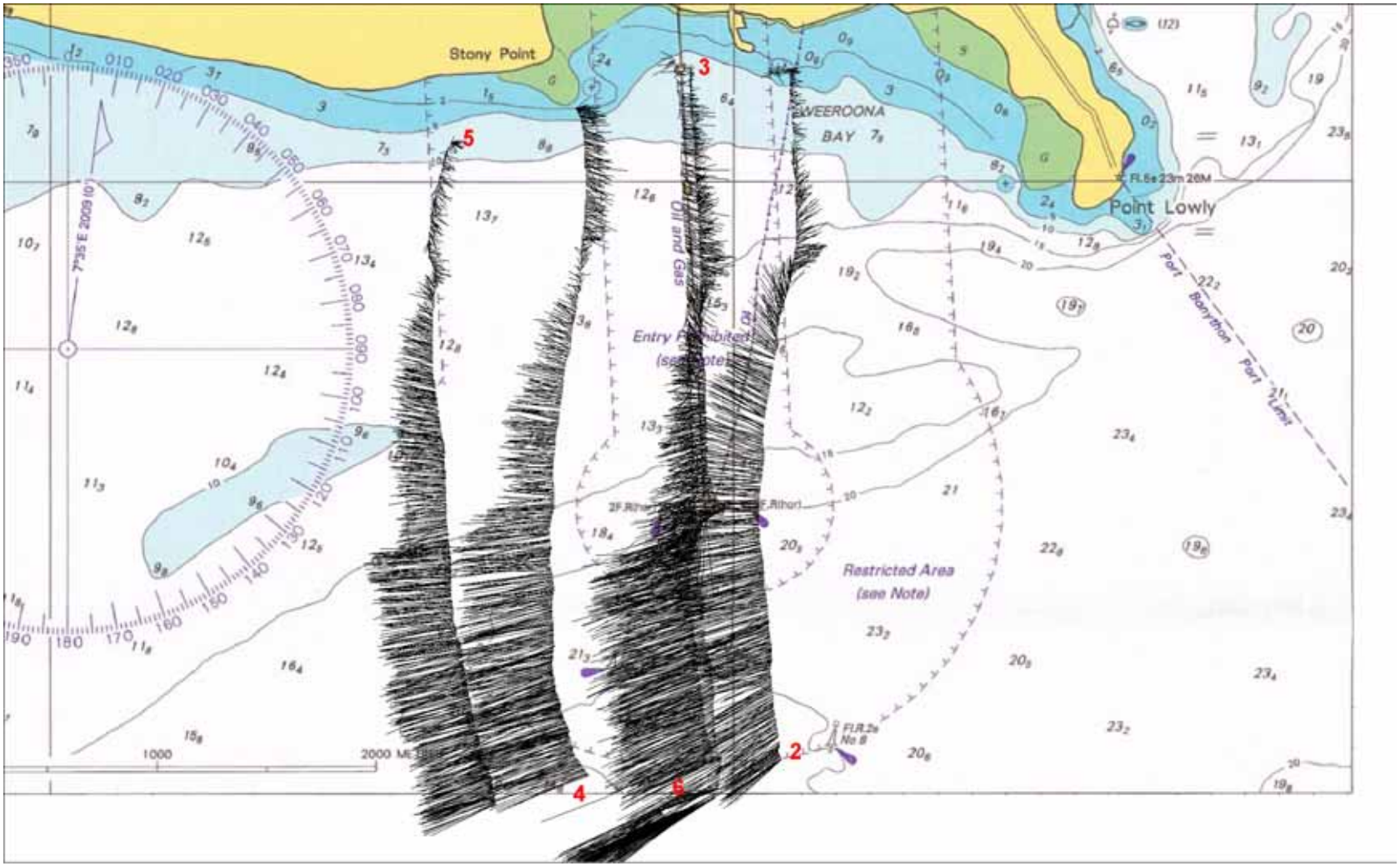

Figure 4-11 ADCP Profiling Data

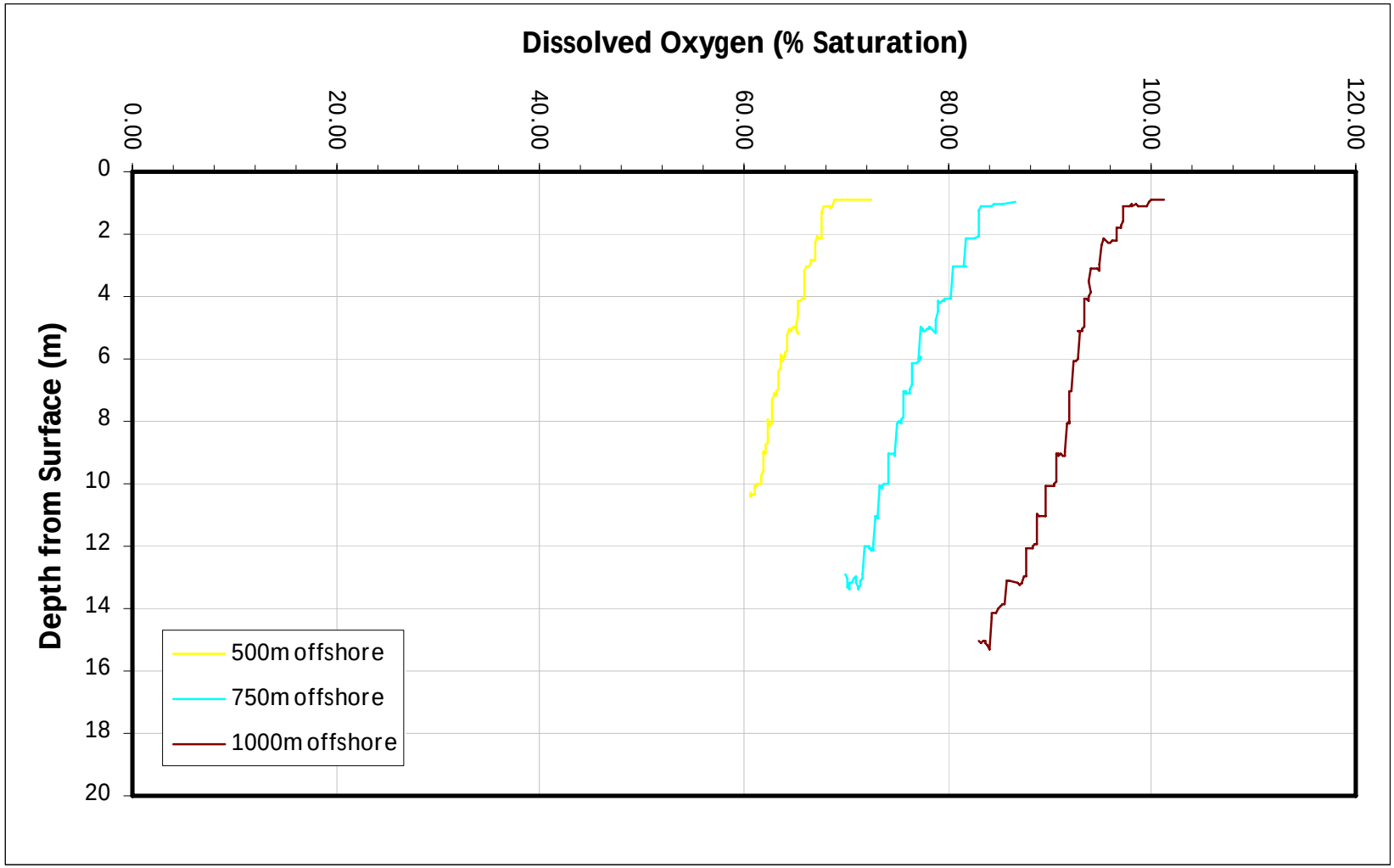

Figure 4-12 Sample of Recorded Dissolved Oxygen Profile Data

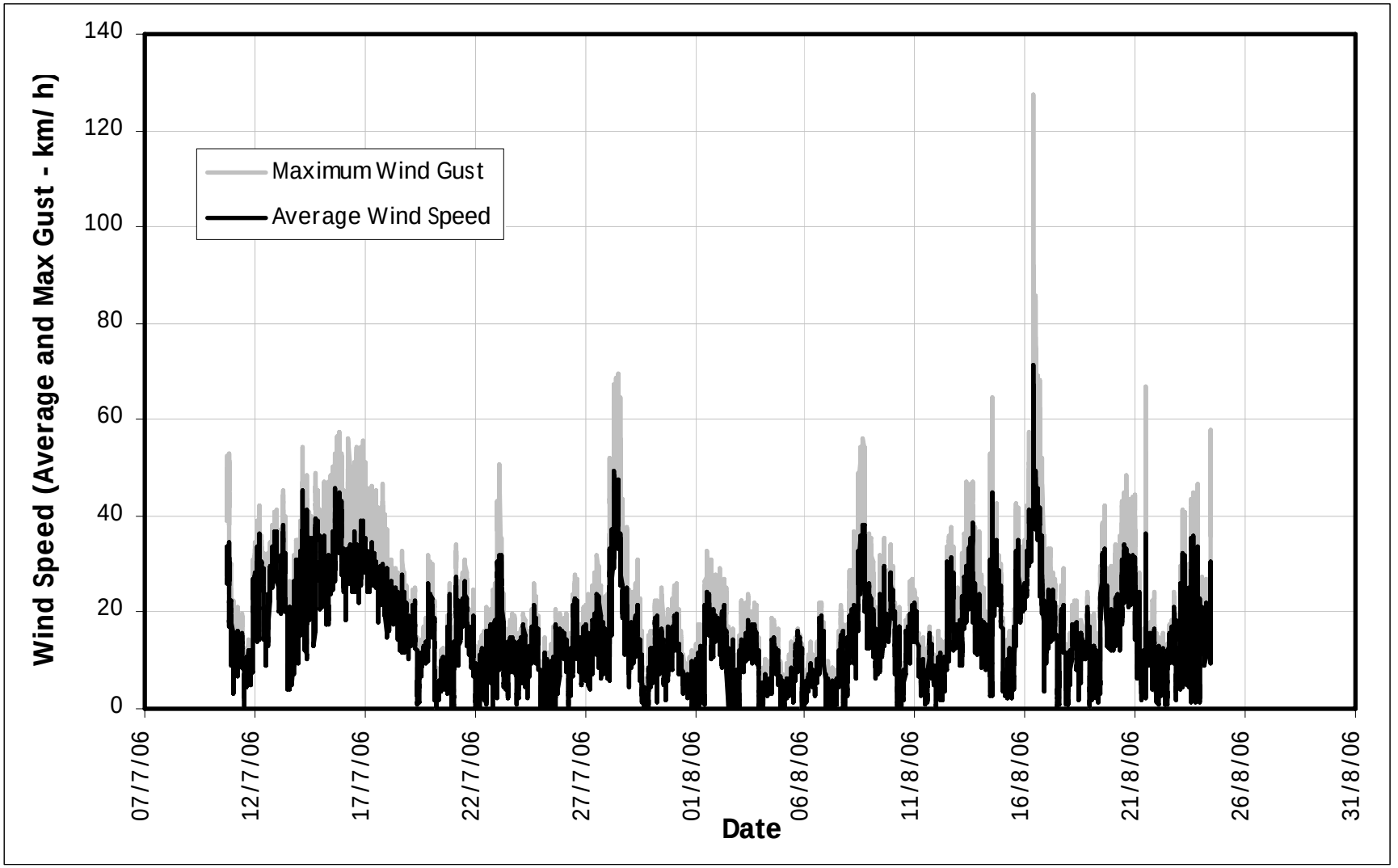

Figure 4-13 Recorded Wind Speed Data

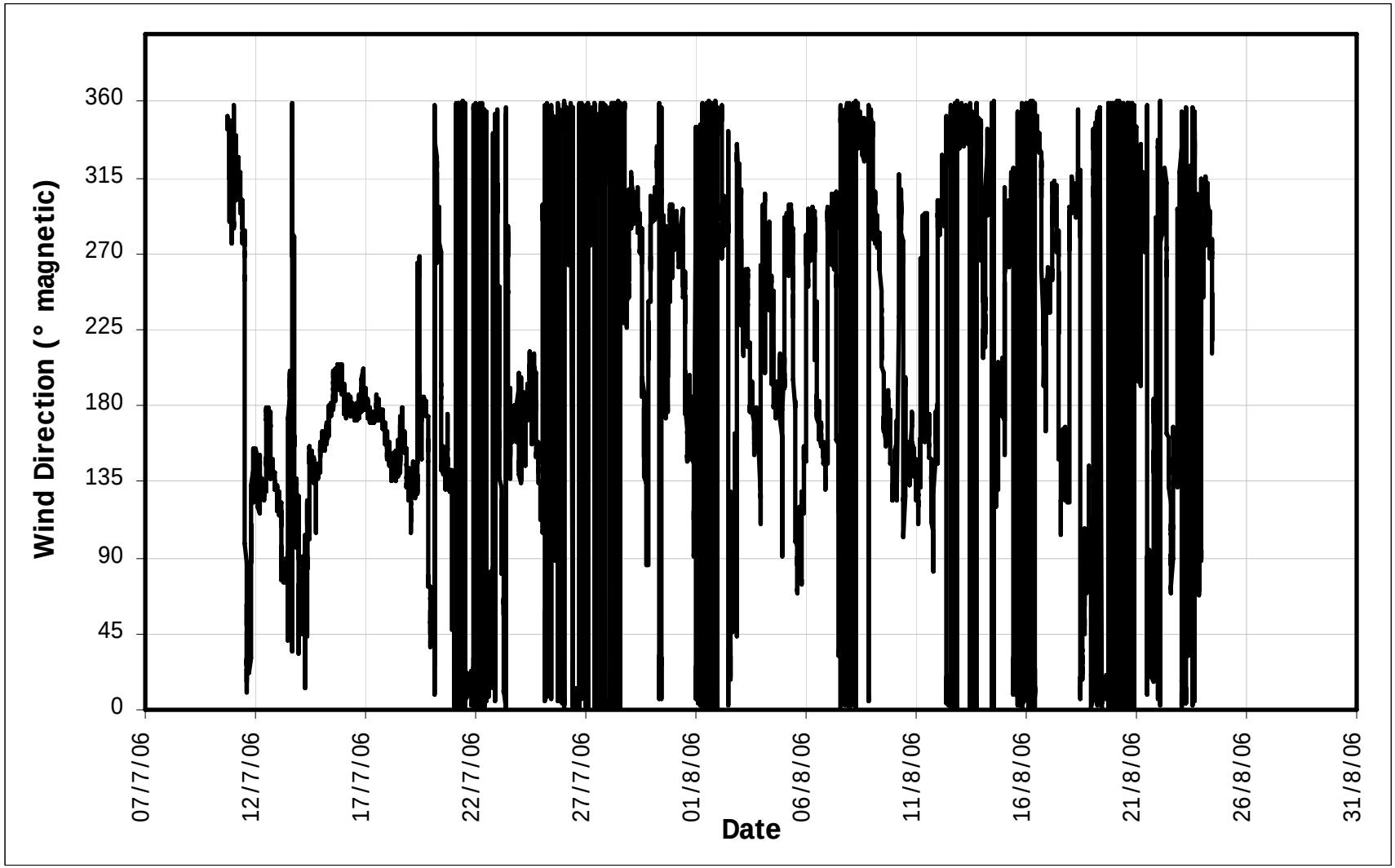

Figure 4-14 Recorded Wind Direction Data

5 MODEL DEVELOPMENT

5.1 Model Requirements

Based on the physical oceanography of Spencer Gulf summarised previously in this report, the requirements identified for a suitable numerical modelling system were:

- Three-dimensional: The modelling system must be able to simulate three-dimensional flow fields, as vertical stratification and horizontal gradients in both directions are important to the flushing regime.
- Temperature and salinity: The modelling system must be able to simulate both temperature and salinity.
- Surface thermodynamics: The salinity gradients in Spencer Gulf are the result of evaporative fluxes; therefore the modelling system must have a detailed surface thermodynamics module.
- Coriolis: This is the major determinant of large-scale convective flow patterns, and so is required to determine the long-term flushing characteristics of the Gulf.
- Tidal forcing: At the open boundary.
- Vertical mixing model: The modelling system selected must be able to simulate the effects of turbulence and mixing due to evaporative cooling, bottom friction, and wind stirring.

For this study, we have used the three-dimensional model ELCOM (Estuary, Lake and Coastal Ocean Model), developed by the Centre for Water Research, University of Western Australia (Hodges *et al.,* 2000). This model has been applied to more than 50 systems worldwide, including similar systems to Spencer Gulf such as the Venice Lagoon, the Adriatic Sea, the Caribbean Sea and Lake Maracaibo (Venezuela). ELCOM is also being used as part of the Adelaide Coastal Waters Study. Summary details of ELCOM are provided in Appendix A.

It is noted that the general approach to this modelling has been to run a control case and compare outfall simulations to the control case, with the simulation of five-year and annual to sub-annual periods in the far and mid-field models, respectively.

5.2 Set-up of coarse grid 3D hydrodynamic model

5.2.1 Bathymetry

A coarse grid of 2000 m horizontal resolution was generated from the DEM data discussed previously. This grid resolution was adopted such that adequate spatial representation of the study area was provided and also so that model runtimes were not excessively long.

The grid was rotated 36 degrees anticlockwise (pivoted at the northern end of the model domain) to align the open ocean boundary in the south with orthogonal grid co-ordinates. Figure 5-1 illustrates the rotated coarse grid bathymetry. The vertical grid scale ranged from 2m thick cells from the sea surface to 38 m below the surface, 4m thick cells from 38 to 50 m below the surface, and a bottom cell that was 10.14 m thick. The grid contained 6165 surface cells and a total of 101848 wet cells. The bathymetry data was referenced to Australian Height Datum (AHD). It is noted that ELCOM has

variable cell heights at the bottom during grid construction and at the free surface during simulation, so that shallow areas are sufficiently resolved as needed.

More specifically, water levels are computed by allowing the free surface to be defined at any height in the grid. Thicknesses of the bottom cells are defined during grid construction and determined by the local bathymetry. Therefore, volume is always conserved. Heating and cooling of partially filled cells above the bottom occurs over small model time-steps and generates baroclinicity that drives local convective flow, preventing extensive periods of heating/cooling in stagnant water. In the rare case of a shallow isolated cell undergoing heating and cooling for an extensive period, the temperature and salinity of the cell are limited to within user defined boundaries of 0 to 40 degrees Celsius and 0 to 70 psu, respectively, to avoid computational errors.

5.2.2 Initial conditions and set-up

Far-field ELCOM simulations were run for 5 years from Julian day 225 in 2000 (12/8/2000) to Julian day 225 in 2005 (13/8/2005) using a time-step of 2700 seconds, with a total number of timesteps of 58000. Notwithstanding this, it is noted that ELCOM sub-timesteps the advection and momentum routines to ensure Courant Numbers remain below 1. We note that the time step was a selected on the basis of model stability and computational efficiency requirements. Initial conditions were uniform in the vertical but horizontal salinity and temperature gradients were introduced using 25 surface samples collected in August 1982 (Nunes 1985), when the temperature field was approximately homogeneous and vertical stratification least likely. The initial temperature and salinity fields are shown in Figure 5-2 and Figure 5-3.

In depth-averaged models the Chezy-Manning bottom stress formulation is often applied to account for the dissipation in the entire water column, and used as a method of calibrating depth-averaged coastal models to reproduce tidal data. In the current 3D simulations of Spencer Gulf, detailed field data for calibrating bottom friction coefficients was not available and the formulation of a boundary model is unclear. In these simulations bottom and side-wall drag were defined using a constant drag coefficient of 2×10^{-3}, typically of sandy sediments.

5.2.3 Tidal forcing

Synthetic tides generated (using iostide) for sites at Whalers Bay, Wedge Island, Pondalawie Bay and Taylors Landing (Figure 5-4) were used to force the southern ocean boundary by splitting the boundary into four lengths, one for each tidal station. A large suite of constituents were used in this analysis including: M2, S2, K1, O1, SA, SSA, O1, K2, Q1, MSF, N2, T2, L2, MM, MU2, 2N2, MF, MS4, S1, M4, NU2 and 2MS6. The key reason that these synthetic tides were used at the boundary is that data measurements in the area were disjointed and fragmented. As such, it was not possible to isolate a concurrent period of 'real' tidal data across the mouth of the Gulf suitable for model forcing. In order to capture the tidal phasing across the mouth, synthetics tides were used

In order to assess the accuracy of this approach, synthetic tides at Port Lincoln were compared with measurements. It was found that the synthetic tides where correctly predicting phases, but underpredictiing height. As such, the amplitudes of the dominant S_2 and M_2 components were increased by 18% after deconstructing the observed and synthesised tides to match the components determined from data collected at Port Lincoln. This ensured the amplitudes were consistent and allowed the predicted tidal phase shift (which compared well to the field data) to be introduced via

synthetic data as a continuous rather then stepped change along the east-west ocean boundary. The series was then reconstructed (from constituents) and compared to measured data over a similar series to ensure accuracy. The generated data was used to enable capture of the East-West tidal phase shift along the ocean boundary. Hourly resolution tide data was sufficient to capture the tidal oscillations.

The above tidal data had an hourly time-resolution for the duration of the simulation and are shown in Figure 5-5. The tidal heights were referenced to AHD. Temperature and salinity at the tidal boundary were set to the long-term monthly means published for Port Lincoln, and are shown in Table 5-1.

Table 5-1 Mean monthly temperature and salinity at Port Lincoln

Month	Jan	Feb	Mar	Apr	May	Jun	Jul	Aug	Sep	Oct	Nov	Dec
Temp(^{0}C)	18.2	18.5	18.9	18.2	17.3	16.1	15.5	14.8	14.1	14.4	15.0	16.8
Salinity (g/L)	35.6	35.6	35.7	35.7	35.9	35.7	35.6	35.8	35.3	35.5	35.3	35.6

5.2.4 Meteorological forcing

Meteorological forcing data were compiled using the best available data for the simulation duration. Air temperature, relative humidity, wind speed and wind direction data were used from Port Augusta Aerodrome, Whyalla Aerodrome, Moonta, Minlaton Aerodrome and Stenhouse Bay, all with a time-resolution of 1 hour. The forcing was broken up over the surface boundary as shown in Figure 5-6 and the forcing data are shown in Figure 5-7 to Figure 5-11. Only wind speed and direction data were available from Moonta, so values of air temperature and relative humidity collected from Whyalla were assumed over this section of the surface. Half-hourly shortwave and longwave radiation data available from Adelaide was increased by 16% from the southern most surface section near the ocean boundary to the upper section near Port Augusta to approximate the typical radiation change over the extent of the gulf as shown in satellite imagery of the daily solar exposure (BOM). Simple estimates based on latitude suggest that shortwave radiation increases by less than 1% from the south to the north of the Gulf, and therefore the gradients are predominantly due to cloud bands that move over the southern region on the gulf. Figure 5-12 illustrates the shortwave and longwave radiation used to force ELCOM.

It is noted that the most complete sub-daily radiation time-series (longwave and shortwave) came from Adelaide and was used to generate a baseline time-series. The time-series was then adjusted to account for a ~16% increase in radiation from South to North that is evident in the data available from surrounding stations and in solar radiation maps published by BOM. The increase was distributed over the five surface sub-domains.

ELCOM uses the iterative procedure of Hicks (1975) to determine the surface exchange coefficients at each model time-step, thus taking into account air column stability and water roughness.

It is noted that there may be discontinuities at the regional boundaries of the surface meteorological forcing sub-domains, however forcing gradients from North to South are broken up using meteorological data available from 5 stations, so that discontinuities between regions remain small.

ELCOM determines evaporation from meteorological forcing data and simulated surface temperature. This is an important process in Spencer Gulf and its inclusion enabled ELCOM to capture seasonal salinity fluctuations. The effects of wind are included in the surface heat flux calculations. In addition,

the explicit surface mixed layer routine employed by ELCOM will maintain sharp gradients in a coarse vertical grid but this does not mean its advantages are lost when using a finer grid. In fact, performance will improve.

5.2.5 Other forcing data

A power station outfall at Port Augusta and salt lake inflow from north of Port Augusta were both included in the far and mid-field simulations. The salt lake discharge was set to 0.15 m^3 s^{-1} at a salinity of 70 psu (Bye and Hardison, 1991) and introduced at the top of the domain at a constant rate over the duration of the simulations. The power station discharge was included at 22m^3/s at ambient salinity (BHP, 2006) and a temperature increase of 2 degrees Celsius was applied. This is lower than the discharge temperature difference to account for cooling of the flow between the power station discharge point and the edge of the model domain.

Brine composition was found to vary depending on the ambient salinity at the intake location. A time-series was constructed using ambient salinity concentrations predicted by a control case simulation performed over the period of interest. An outfall salinity time-series was then constructed using the ambient salinity time-series and altering the salinity (multiplied by 1.8) to account an increase introduced by the desalination plant. Temperature was treated in the same fashion. BHP has also explicitly described the seasonal variation of the outfall brine quality during a subsequent annual ELCOM simulation reported elsewhere.

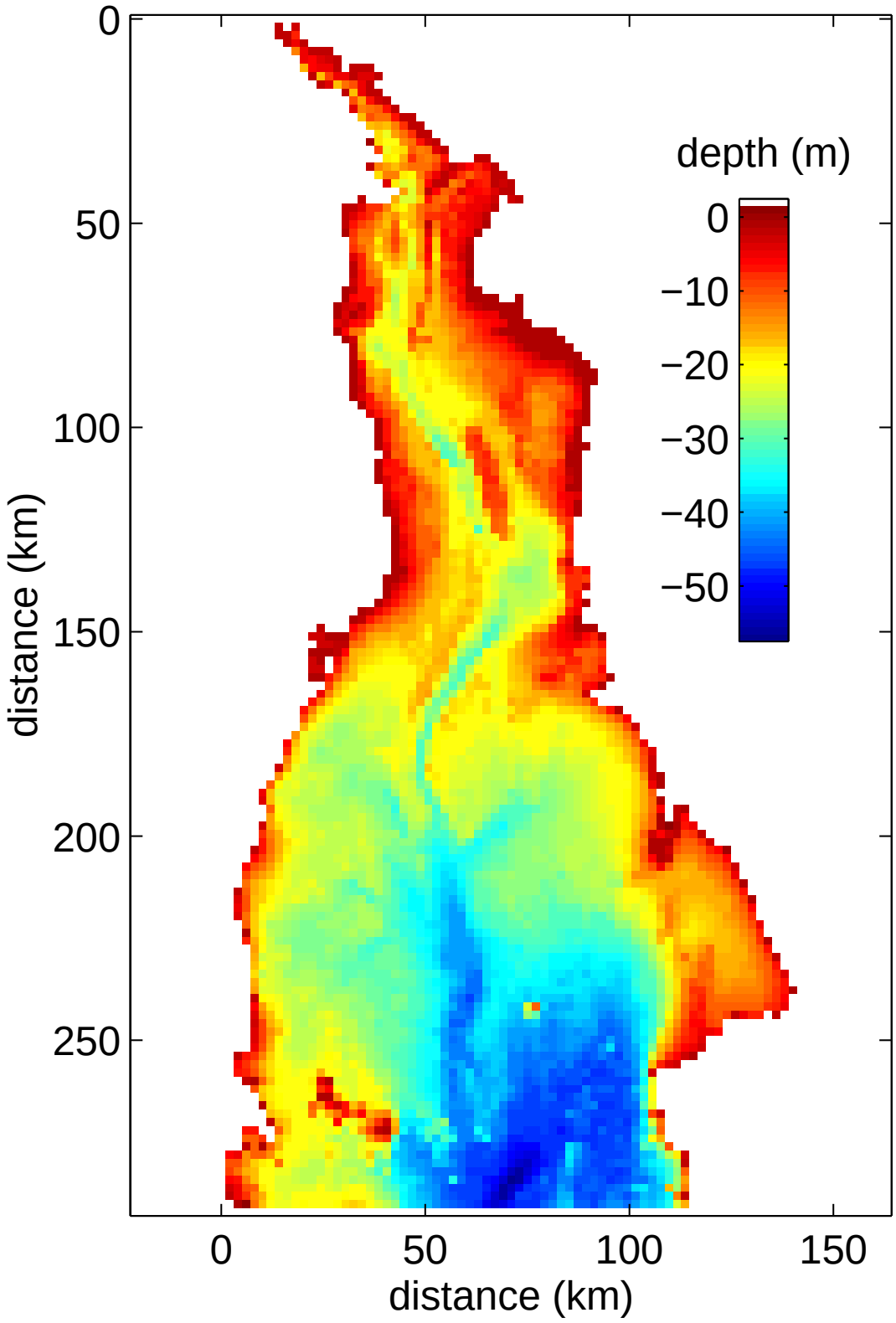

Figure 5-1 Coarse bathymetry grid rotated 36 degrees anticlockwise pivoted at northern end of model domain

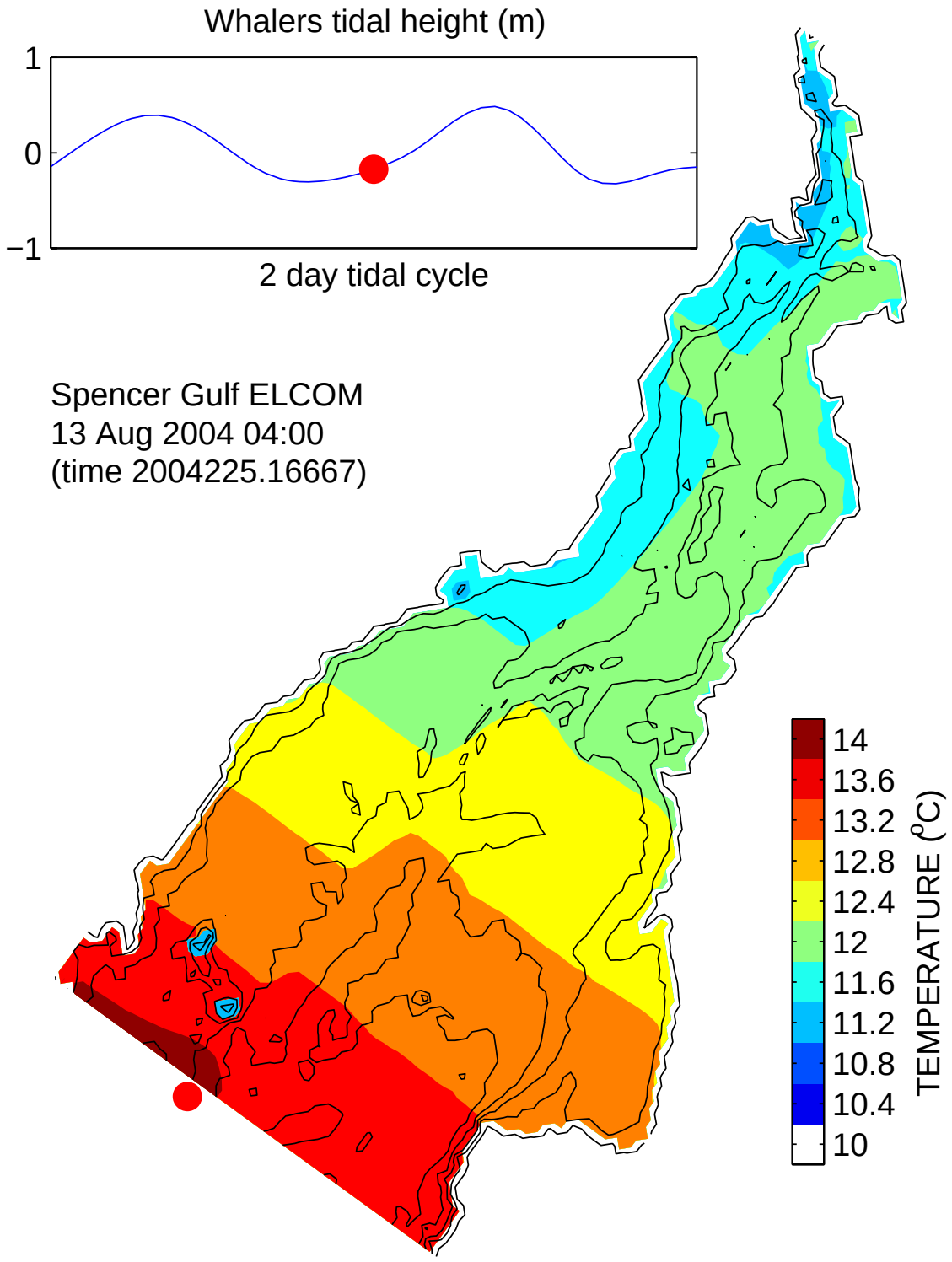

Figure 5-2 Initial horizontal temperature field for coarse grid simulations

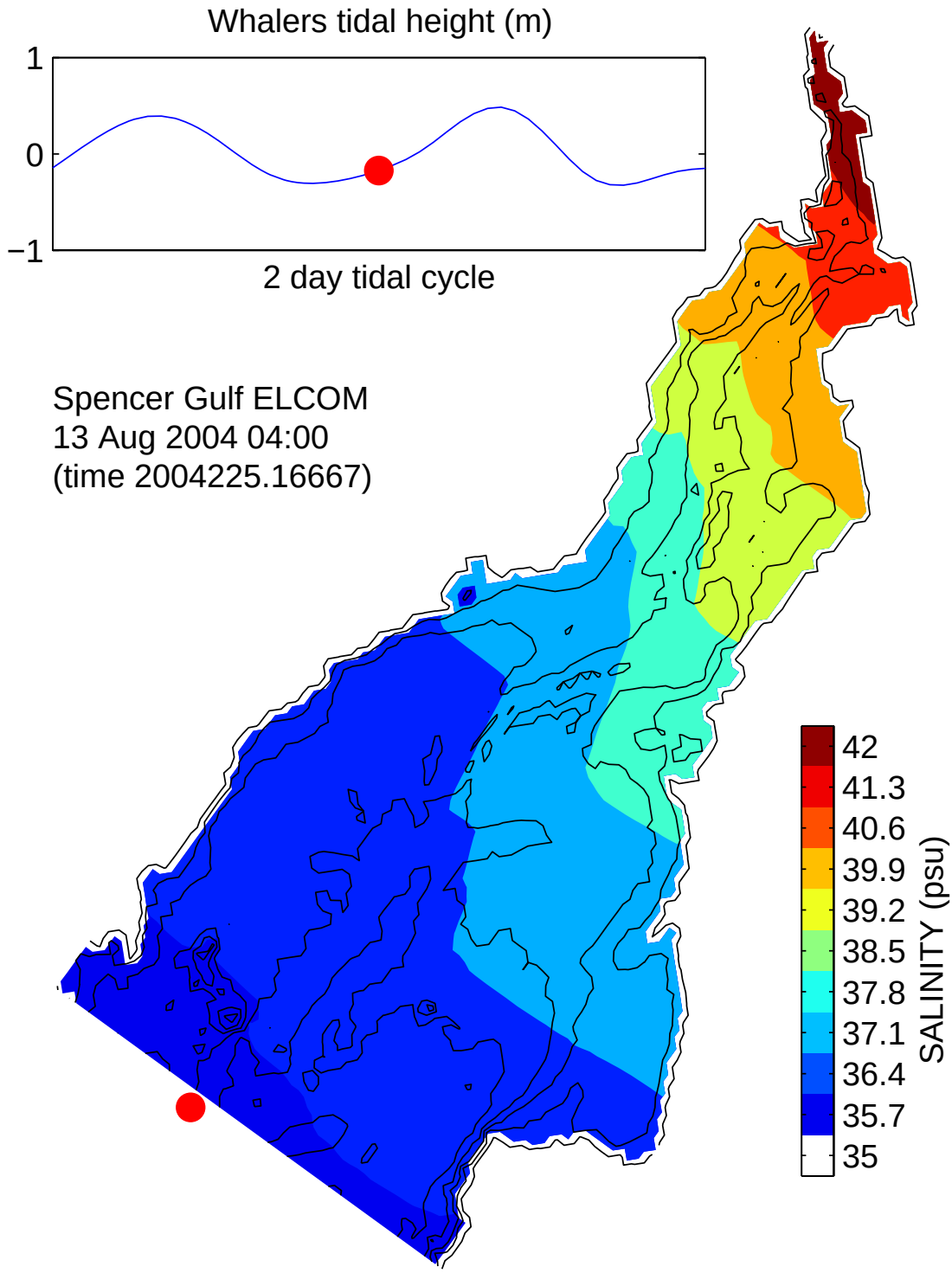

Figure 5-3 Initial horizontal salinity field for coarse grid simulations

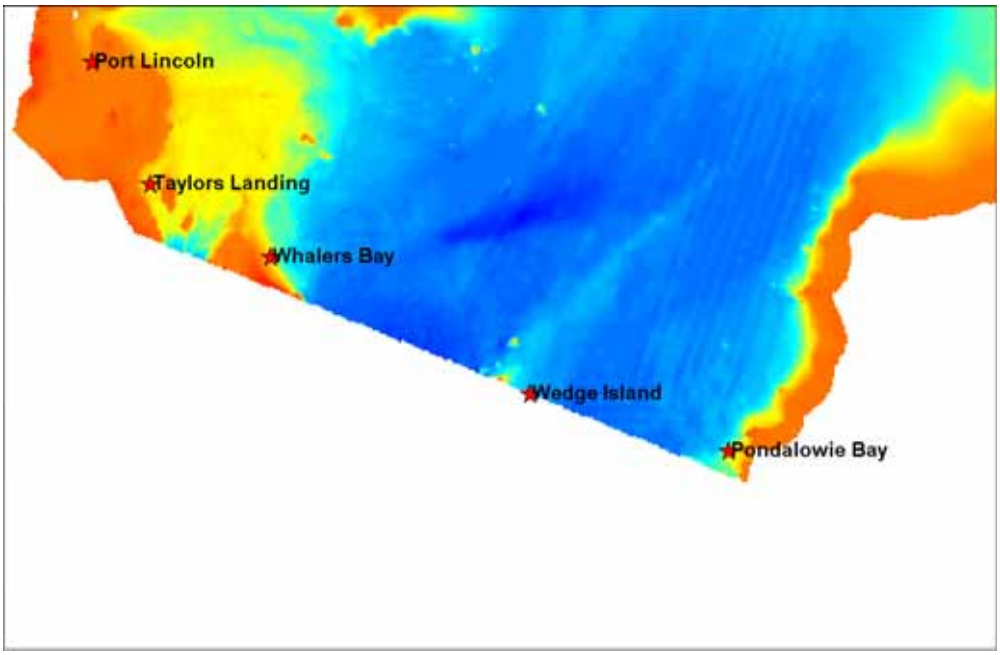

Figure 5-4 Tidal gauge locations at the ocean boundary of Spencer Gulf.

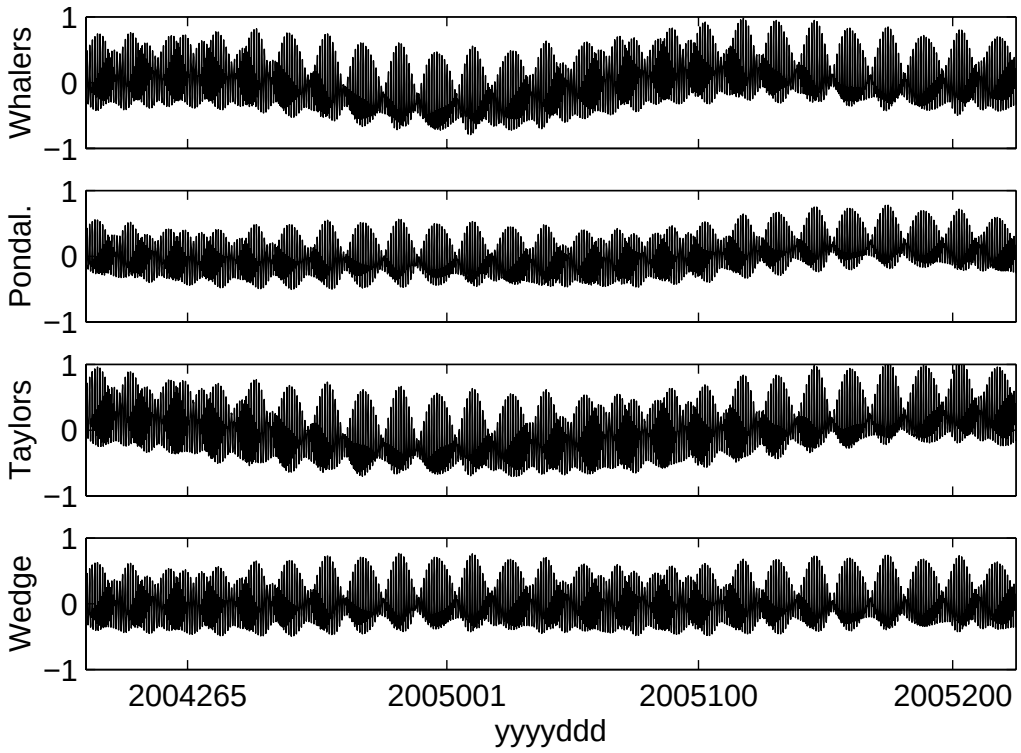

Figure 5-5 Tidal heights (mAHD) for the synthetically generated tides at Whalers Bay, Pondalawie Bay, Taylors Landing and Wedge Island.

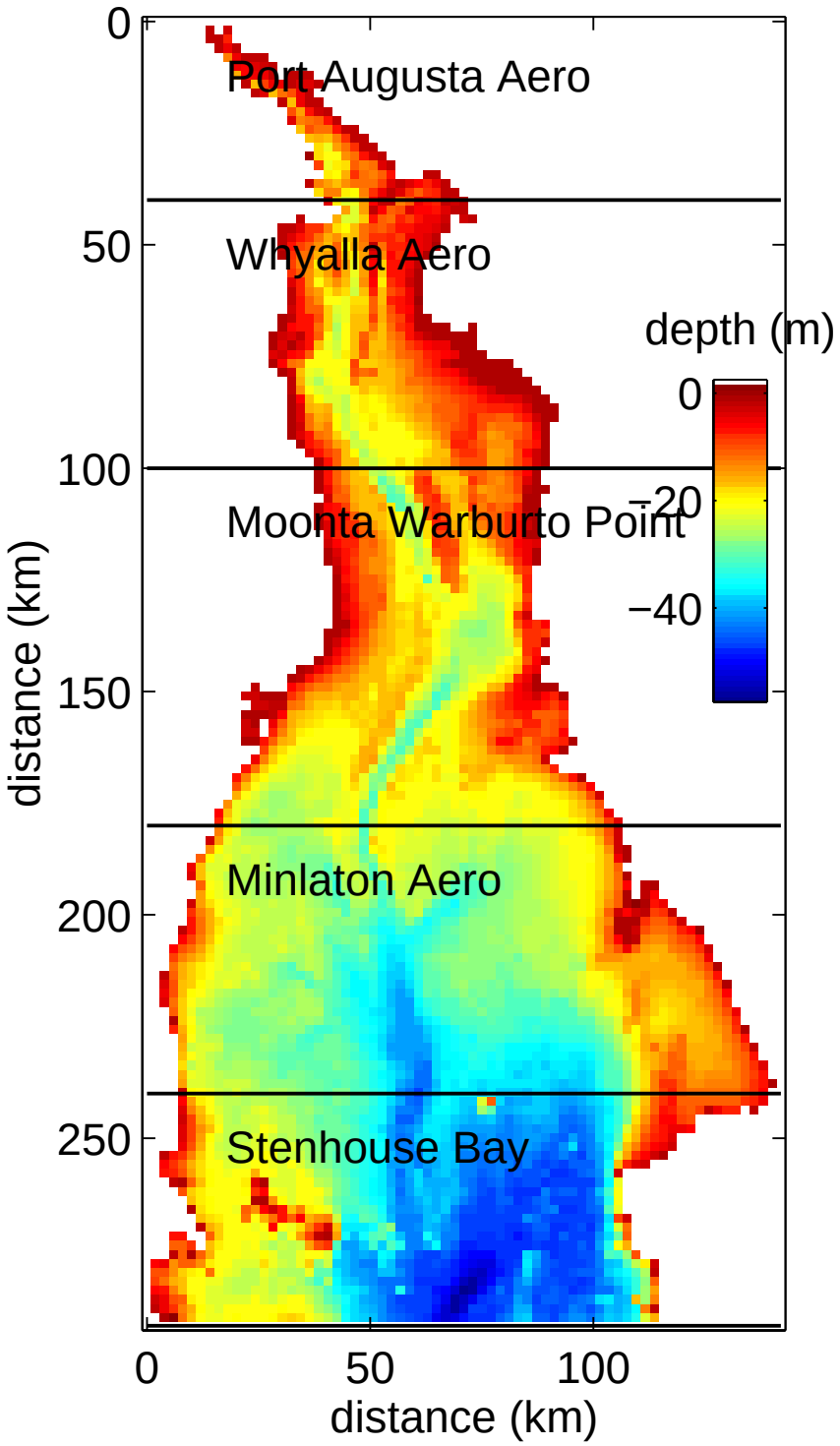

Figure 5-6 Forcing regions for air temperature, relative humidity, wind speed and wind direction at the surface boundary

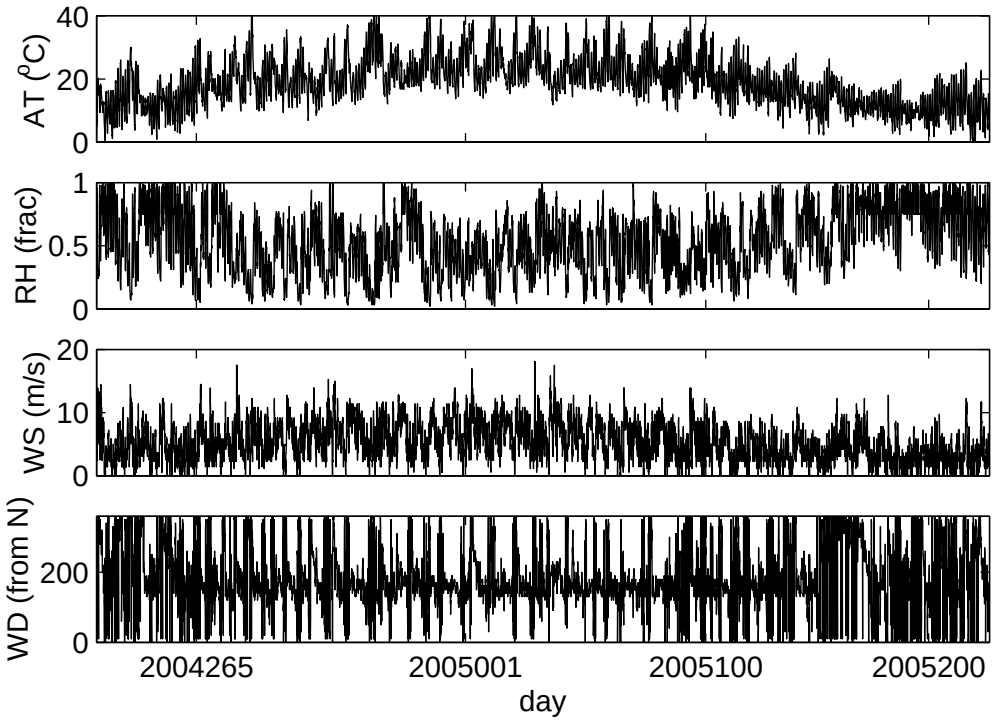

Figure 5-7 Port Augusta meteorological data: air temperature (AT), relative humidity (RH), wind speed (WS) and wind direction (WD).

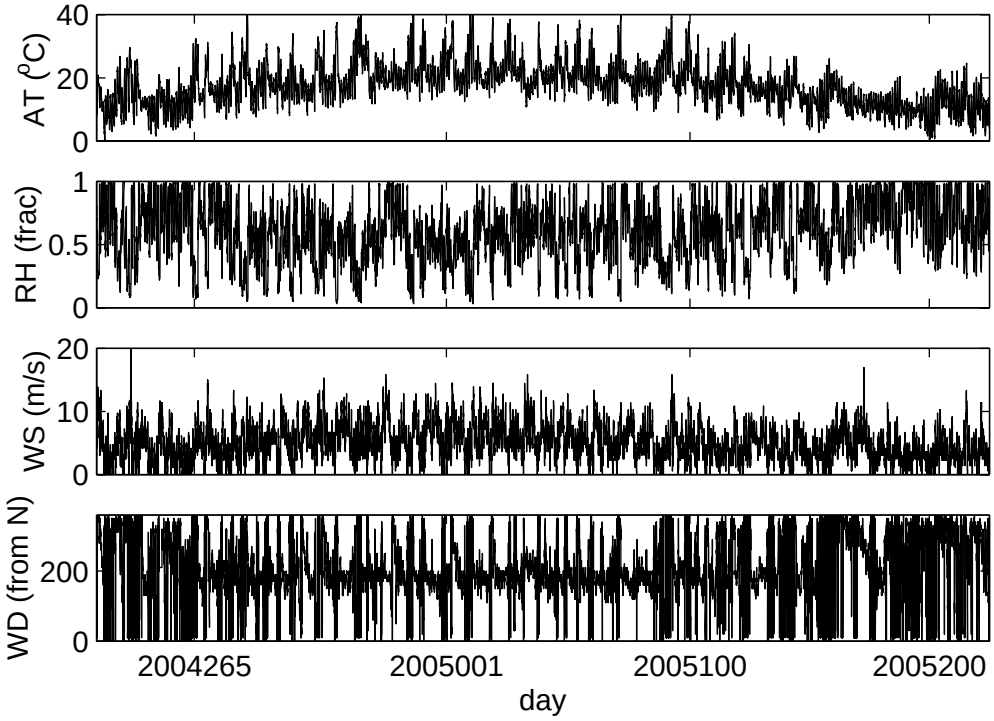

Figure 5-8 Whyalla Aerodrome meteorological data: air temperature (AT), relative humidity (RH), wind speed (WS) and wind direction (WD).

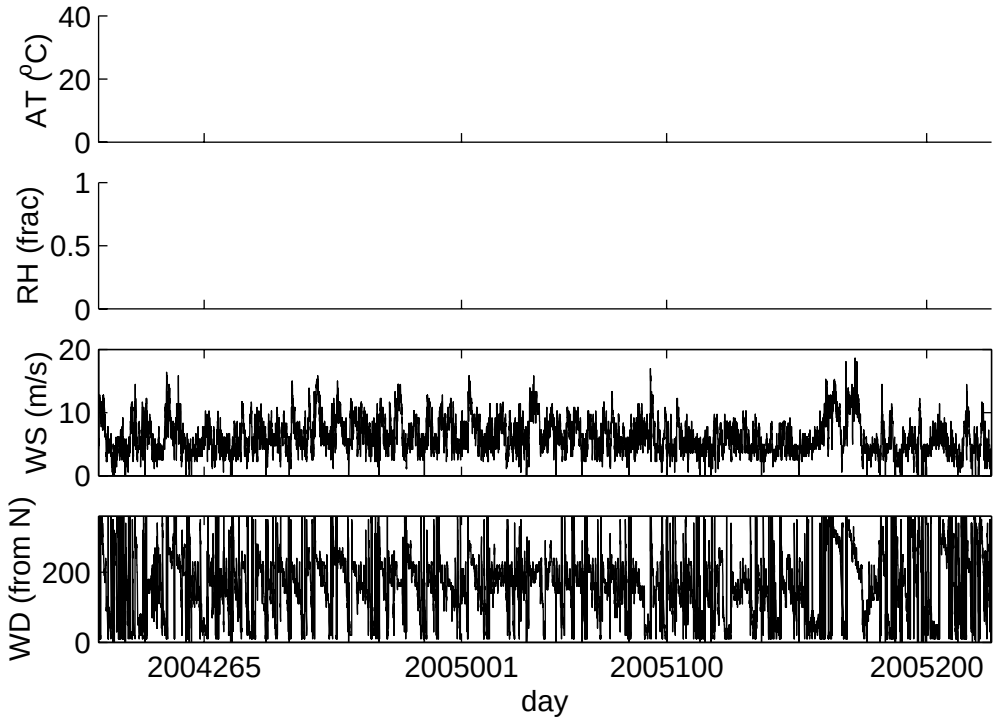

Figure 5-9 Moonta meteorological data: wind speed (WS) and wind direction (WD).

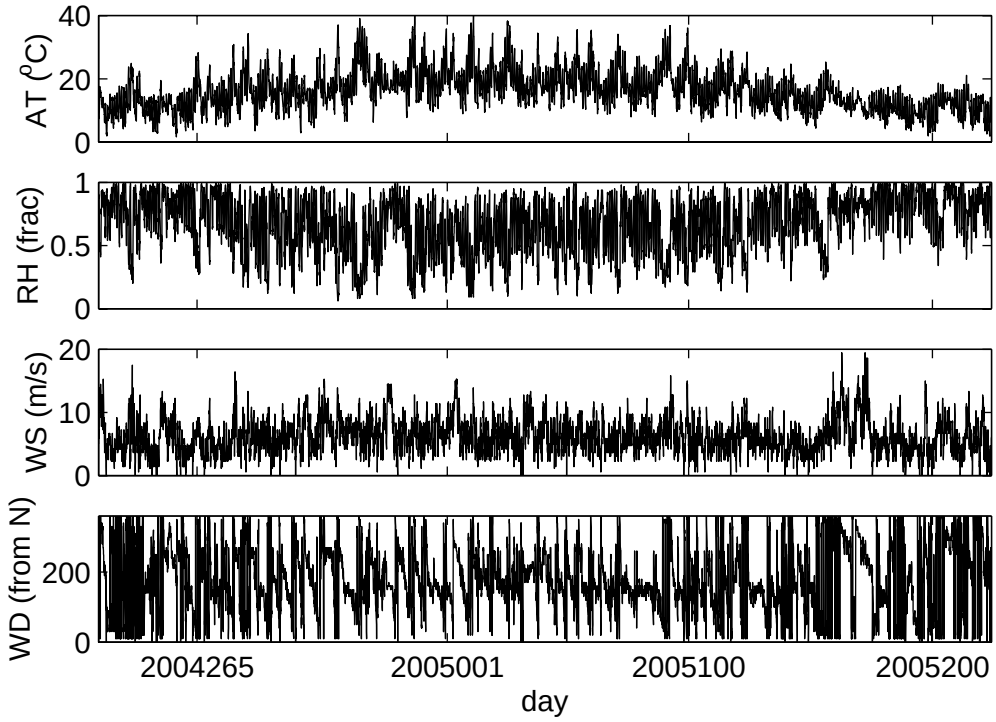

Figure 5-10 Minlaton Aerodrome meteorological data: air temperature (AT), relative humidity (RH), wind speed (WS) and wind direction (WD).

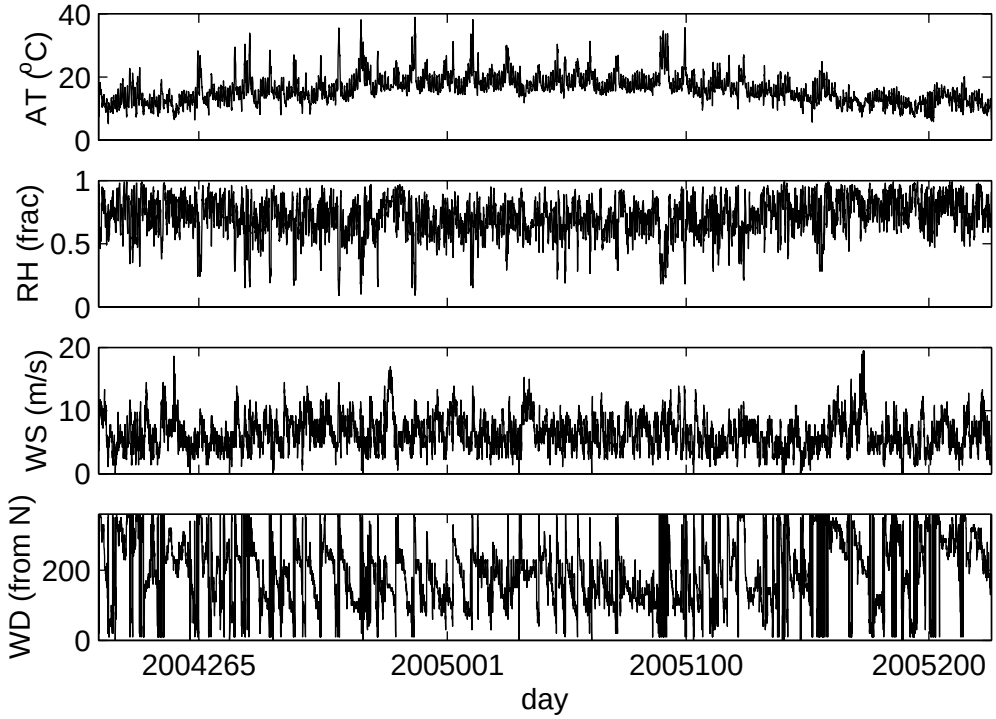

Figure 5-11 Stenhouse Bay meteorological data: air temperature (AT), relative humidity (RH), wind speed (WS) and wind direction (WD).

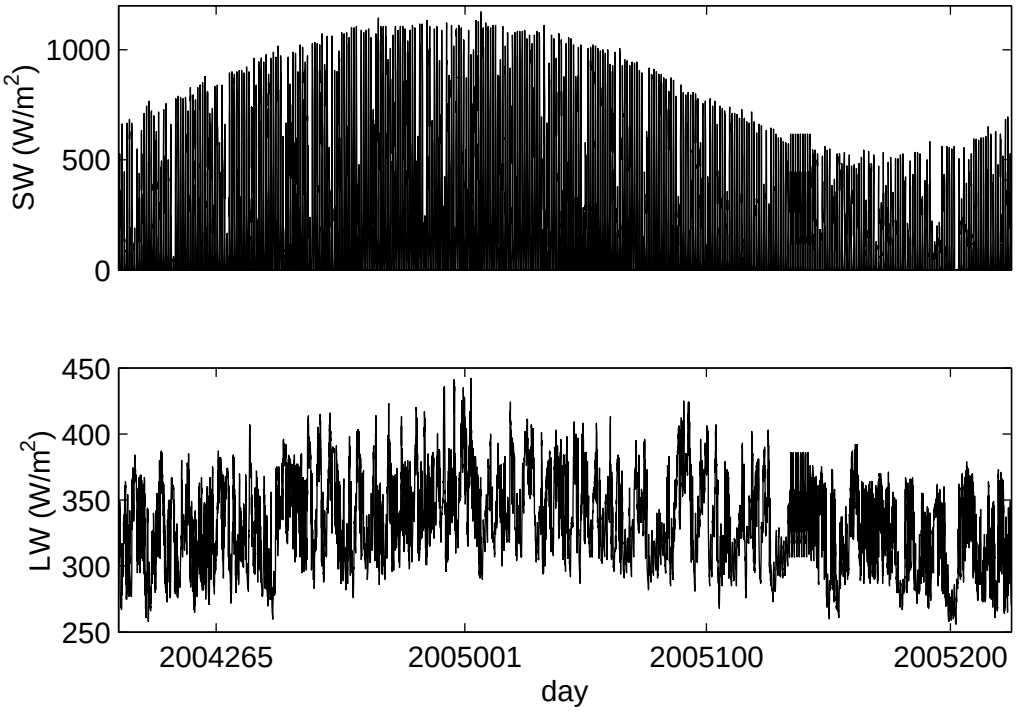

Figure 5-12 Shortwave (SW) and longwave (LW) radiation collected in Adelaide

5.3 ELCOM Results

5.3.1 Tidal Amplification

Modelled tidal amplification from the south to the north of the Gulf was compared with observed tidal amplification as a means to assess the barotropic performance of ELCOM, which is associated with frictional losses within the model. Within ELCOM, bed friction is constant with a drag coefficient of 2 x 10^{-3}. It is noted that additional 'friction loss' is introduced when the bottom becomes stepped and the side bathymetry more complex, such as in the northern extent of Spencer Gulf. The free-surface algorithm in ELCOM accounts for funnelling and shoaling and allows for periodic wetting and drying of model cells in response to tidal oscillations.

Figure 5-13 and Figure 5-14 illustrate modelled and observed tidal water level time series at Port Lincoln, Whyalla and Port Augusta for several day periods of respectively spring and neap tides. The measured tidal data was supplied by Flinders Port Corporation, and is at five-minute intervals. No filtering of this data has been performed following receipt by our team. The field data is 'as observed' so includes the constituents used to generate tidal boundaries (listed above). These figures show that the model is reliably reproducing tidal water levels and tidal phasing within the Spencer Gulf region. Observed tidal data over 2005 at Port Augusta is currently unavailable.

We note that, unlike the case for long-term salinity simulations (see discussion in Section 5.3.2 below), modelled and observed water level data apply to a common time (i.e. we are not comparing observed and modelled data from different time periods which have 'similar' tidal characteristics).

In general, it is noted that without accurate and concurrent tidal measurements across the expanse of the ocean boundary there will be error introduced at the boundaries that will manifest as larger differences between observation and simulations in the northern regions of the Gulf. In addition, the course and stepped structure of the grid will lead to a loss of momentum that slows tidal propagation. However, the long simulation times ensure that the range of observed tidal oscillations are covered in the simulation period. At resolutions high enough to resolve the finer features in the domain that effect tidal propagation, the model becomes impractically slow, and without highly accurate tidal forcing (as mentioned above) adds little value to the study.

Additional discussion and model interrogation regarding this matter is presented in Appendix B.

5.3.2 Horizontal salinity gradient

Given the timeframe of this study, and the fact that extensive consecutive boundary and forcing (e.g., solar radiation and meteorological) data sets were not available, the approach which was taken to demonstrate that the far field ELCOM model is reproducing salinity accumulation and long-term water movement patterns in Spencer Gulf was as follows:

- The extensive data said on temperature and salinity levels in the upper reaches of Spencer Gulf (effectively north of Wallaroo), collected by Dr Rick Nunes-Vaz (Nunes 1985) was adopted as the model comparison data set. These data comprised 14 surveys of salinity and temperature at a number of sites (see Figure 5-15 for example) in the upper Gulf over a period of time extending from July 1982 to January 1985. As such, the data set mostly encompasses 1983 and 1984 (11 of the 14 surveys), which represent average rainfall used in the region (see Figure 5-16).

- ELCOM modelling was conducted for a five-year period from 2000 to 2005. The final two years of this model simulation were then adopted for comparison with the 1983 and 1984 data set of Nunes Vaz. While there is a considerable time period between the model comparison data and simulation periods, there have been no major changes to the Gulf (e.g. new discharges etc), and as such comparison between the two data sets should be practical.

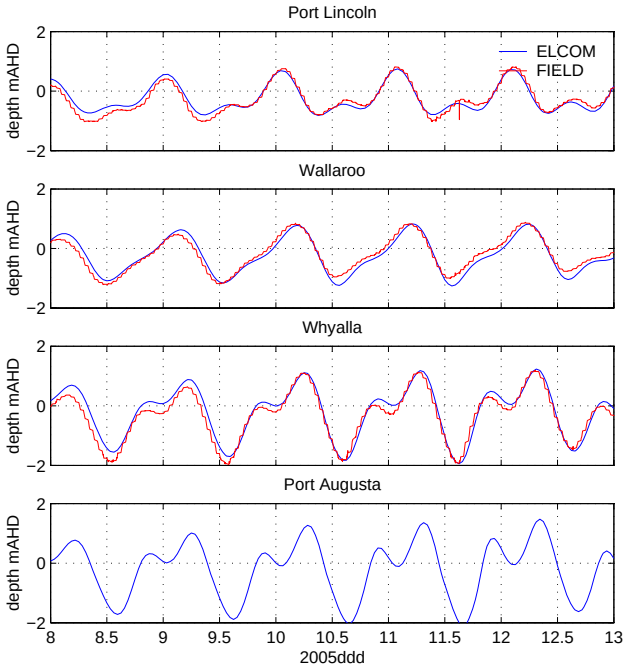

Figure 5-13 Modelled and Observed Tidal Water Levels - Spring Tides

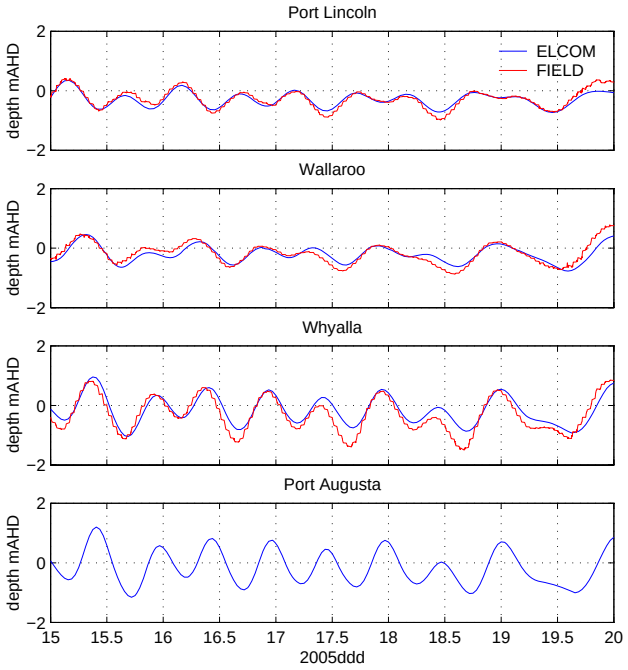

Figure 5-14 Modelled and Observed Tidal Water Levels - Neap Tides

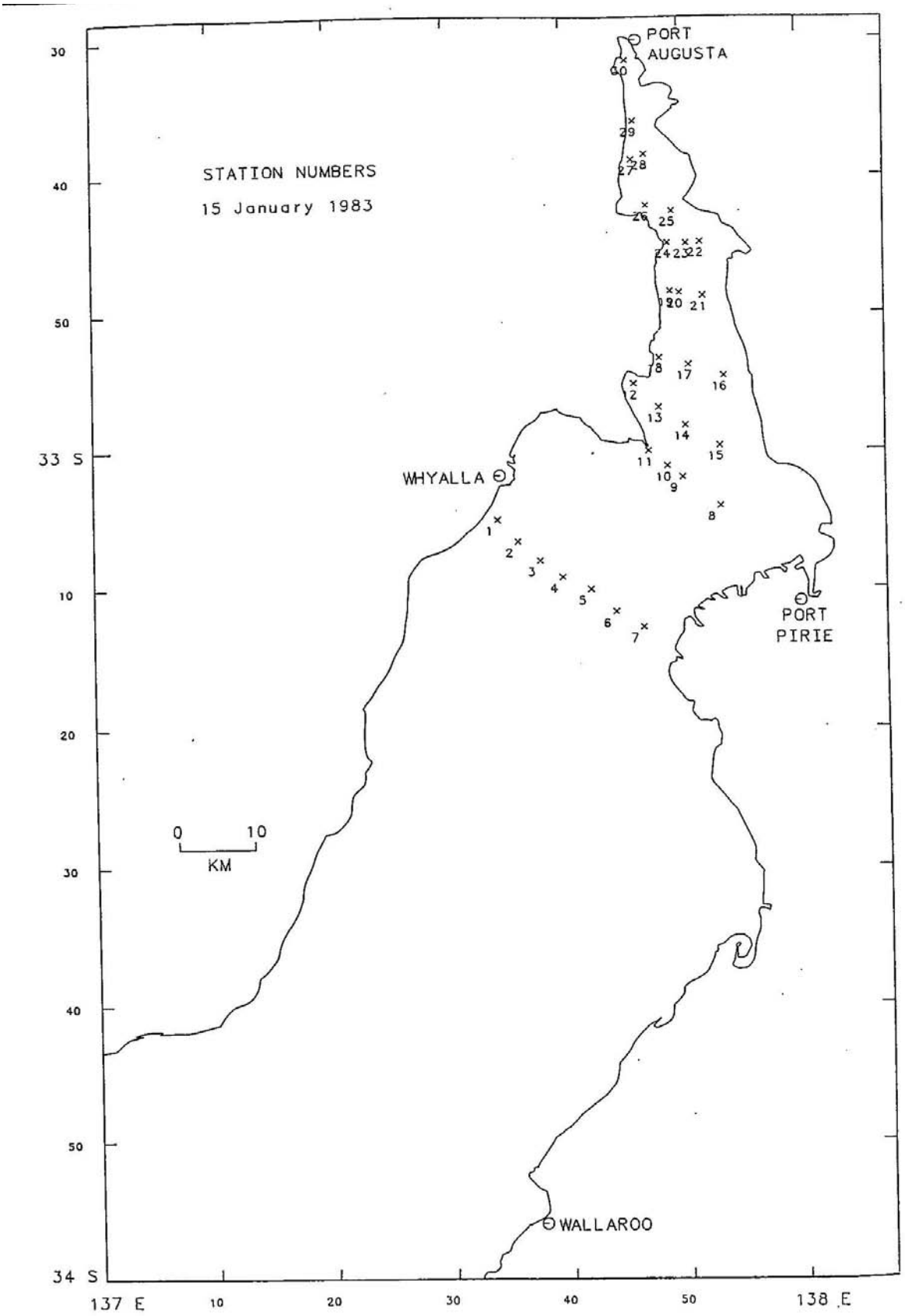

Figure 5-15 Example Nunes Vaz Data Collection Locations

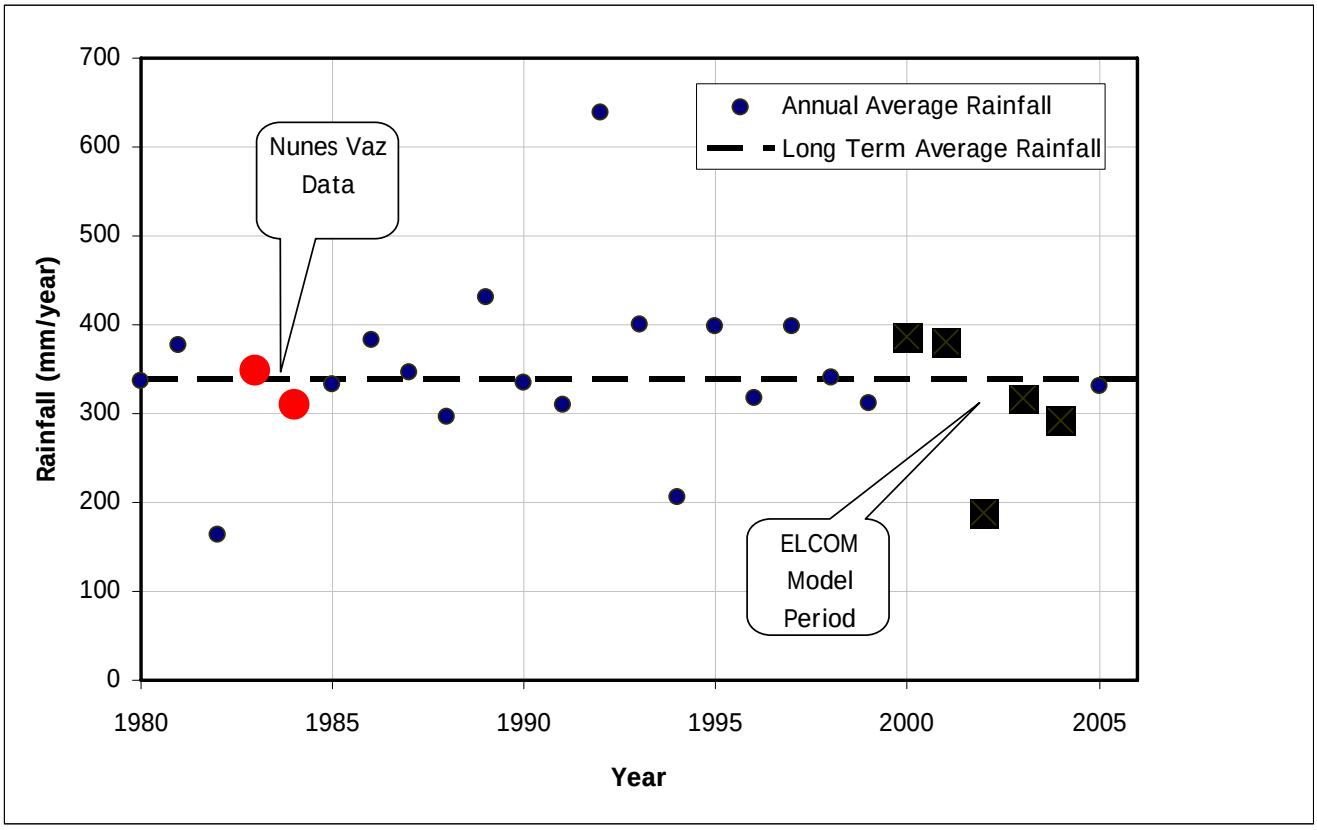

Figure 5-16 Historical Annual Rainfall Data - Port Augusta

- Time series ELCOM model results were then extracted from four (4) sites in the upper reaches of Spencer Gulf, respectively at mid Channel locations at Wallaroo, Port Bonython, Yatala Harbour and Port Augusta. These data are compared with the data of Nunes Vaz in Figure 5-17 to Figure 5-20. A box and whiskers plot illustrating model/data comparison at each site is also presented in Figure 5-21.
- Plan view comparisons were also made between late summer (March 1984) and late winter/early spring (October 1984) data of Nunes Vaz and ELCOM model predictions, specifically to ensure that the model is reproducing the recognised density/Coriolis driven salinity gyre in the upper Spencer Gulf region. These comparisons are presented in Figure 5-22 to Figure 5-25. Whilst there are some minor structural differences between the modelled and measured data sets, the seasonal assembly and dismantling behaviours of the salinity discharge from the Northern Gulf are well replicated.

It is noted that the only tidal current data available for calibration of these models within the study timeframe is that collected as part of the dedicated program undertaken at Port Bonython by the study team in 2006 (see later sections). As such, no tidal current data is available to compare with the predictions of the far field model. Even if it were, however, it is unlikely that small scale field measurements would be meaningfully comparable to predictions of a model using a 2km grid cell.

Additional discussion and model interrogation regarding this matter is presented in Appendix B.

5.3.3 Large scale gyre

The large scale baroclinic gyre measured by Nunes-Vaz is best illustrated by long-term tracking of an inert tracer released in the north of the gulf. The tracer is released with the brine outfall and therefore its distribution reflects that of the brine discharge, and as such is subject to Coriolis effects. The tracer does not contribute to density. Figure 5-26 shows the fate of a tracer released at Pt Bonython from the beginning of the simulation in August 2000 to August 2004. The tracer is released constantly at the end of the jetty near Point Lowly with a flow rate of 3.15 $m^3 s^{-1}$. The tracer plume shows the Coriolis-driven large-scale gyre confines outflowing water (dyed by tracer) to the eastern shores of the gulf and inflowing water (no tracer signal) to the western shore. The previously presented salinity distributions (Figure 5-22 to Figure 5-25) also show a clear response to the large-scale gyre, however the tracer signal provides a better illustration because it has no initial distribution favouring the long-term pattern of its final distribution.

It is noted that the brine from the above discharge is numerically 'dyed' with a tracer with a concentration of 1 and therefore the fate and dilution of the tracer is directly representative of the advection and mixing imposed on the brine. The brine (as traced by the tracer) is subjected to baroclinicity and its motion captures baroclinic advection. It is a numerical method only (not a real world dye) and is used to highlight the behaviour of an introduced fluid without having any influence on its behaviour.

Additional discussion and model interrogation regarding this matter is presented in Appendix B.

5.3.4 Vertical stratification

There have been reports of stratification being an issue of concern in the upper reaches of Spencer Gulf. In this regard, our models were interrogated and such inspection showed that vertical stratification is weak throughout the simulations. Figure 5-27 and Figure 5-28 show the modelled salinity and temperature timeseries offshore in the channel adjacent to Yarraville Shoal where the potential energy anomaly was shown to be at its greatest (Nunes 1985), presumably driven by the tidal straining as more saline water generated by evaporation in the north moves beneath incoming tidal flood waters. The results illustrate that over seasonal cycles, the modelled difference between salinity near the surface and salinity at a 40m deep site reaches a maximum of approximately 1 psu during autumn. The modelled temperature record suggests that temperature stratification is also negligible.

We recognise that under extraordinary conditions (e.g., mid summer, low winds, dodge tides) that more noticeable stratification may develop.

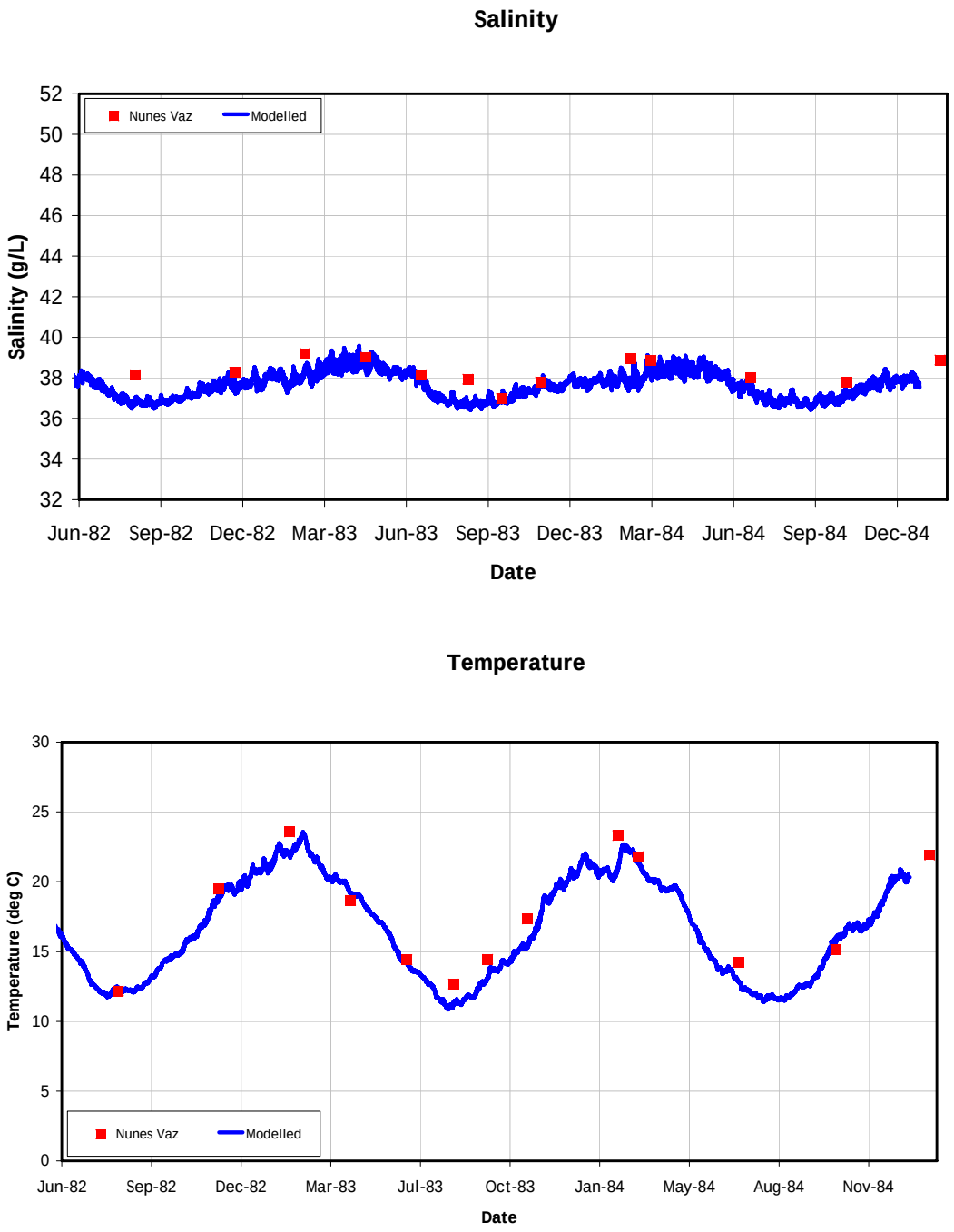

Figure 5-17 Time Series Far Field ELCOM Model Calibration - Wallaroo

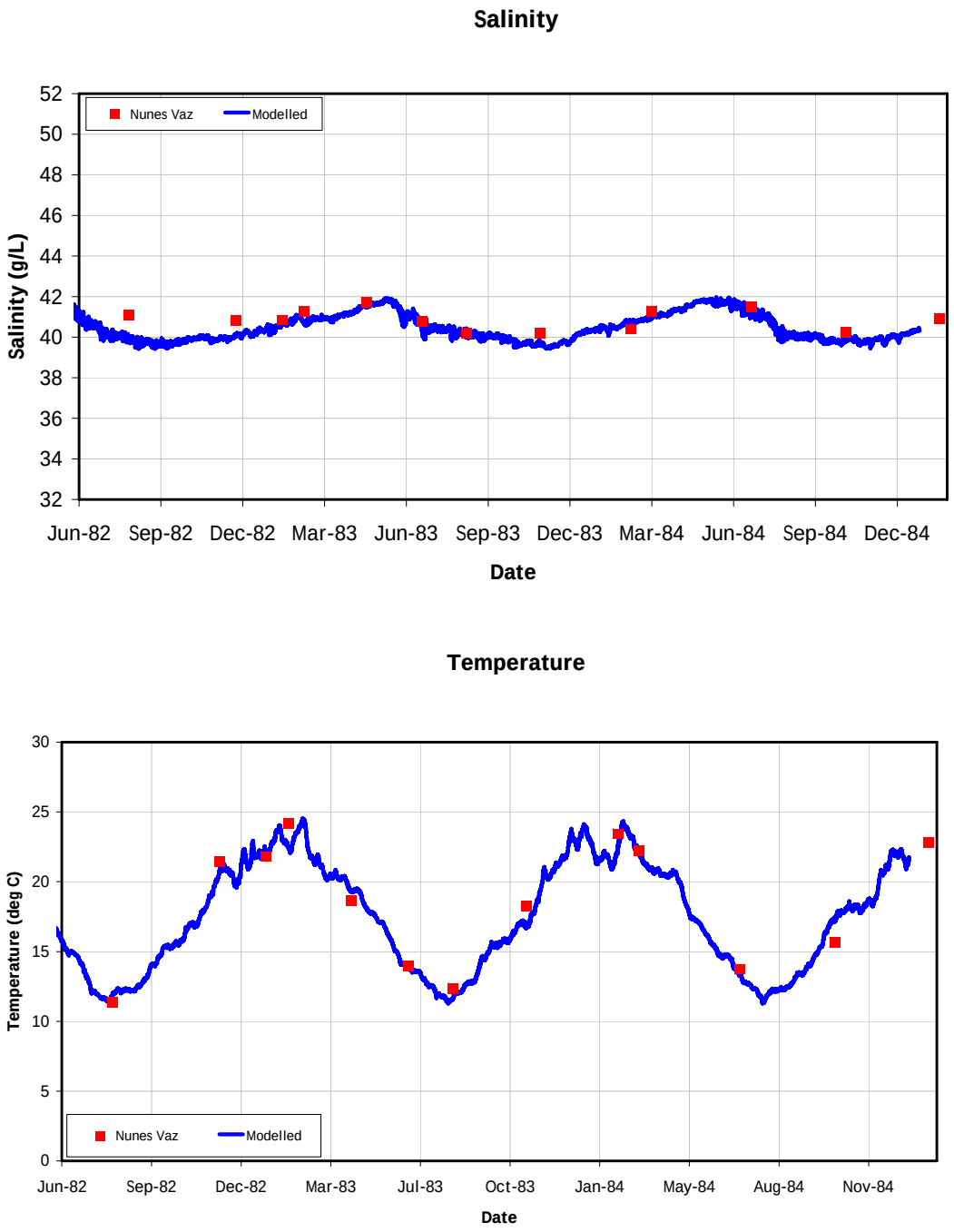

Figure 5-18 Time Series Far Field ELCOM Model Calibration - Port Bonython

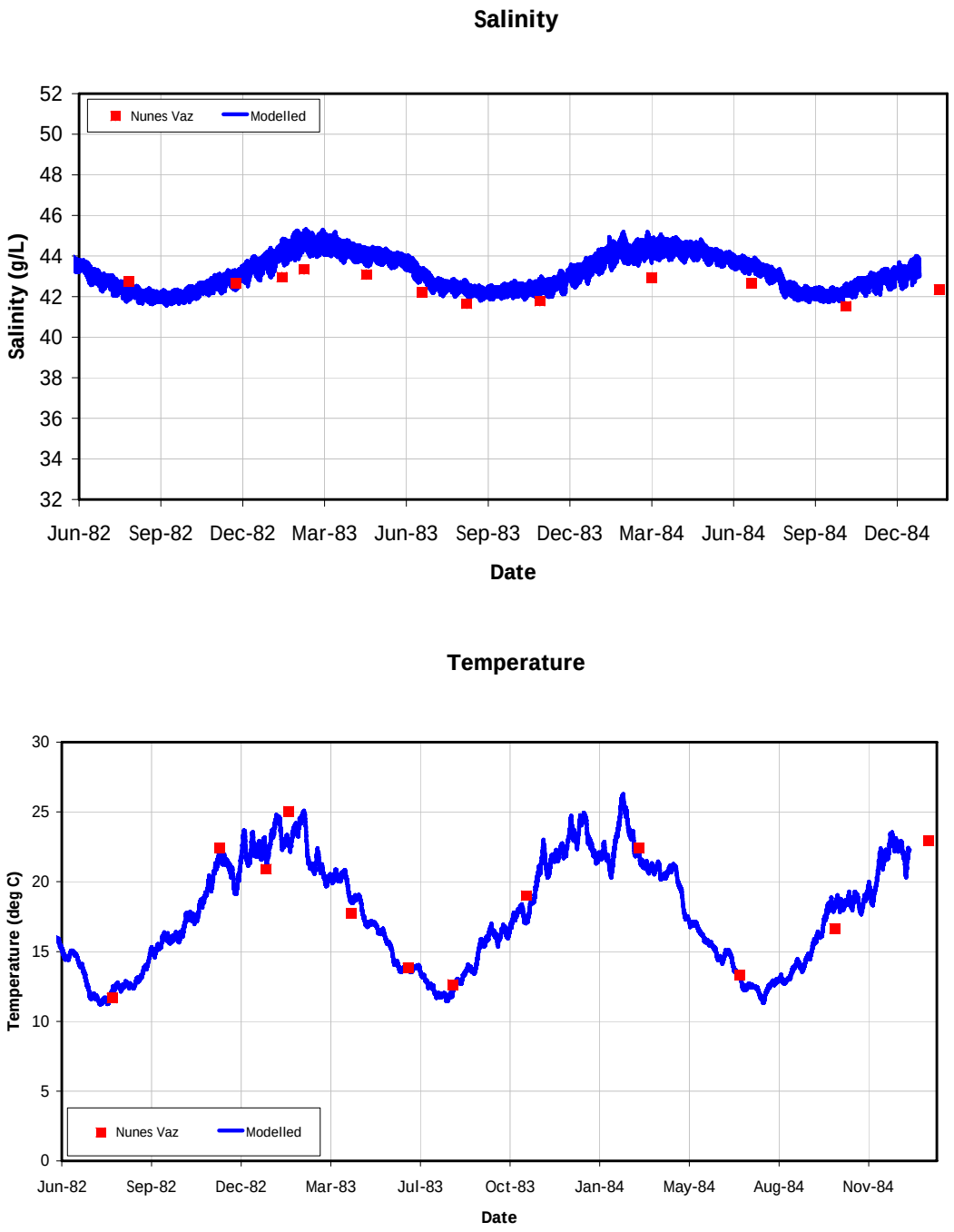

Figure 5-19 Time Series Far Field ELCOM Model Calibration - Yatala Harbour

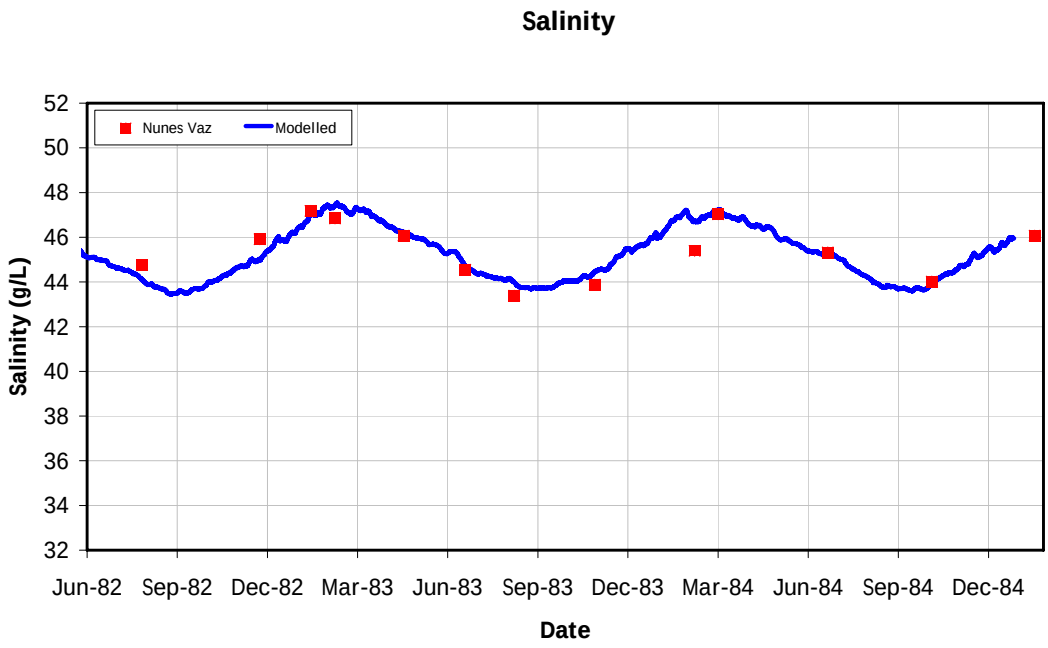

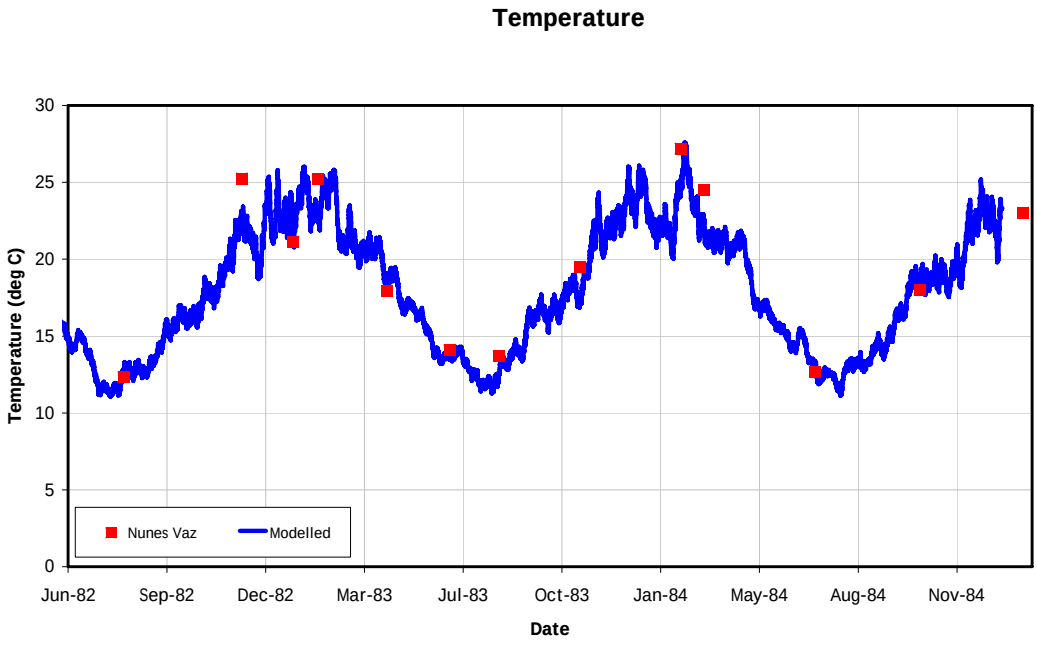

Figure 5-20 Time Series Far Field ELCOM Model Calibration - Port Augusta

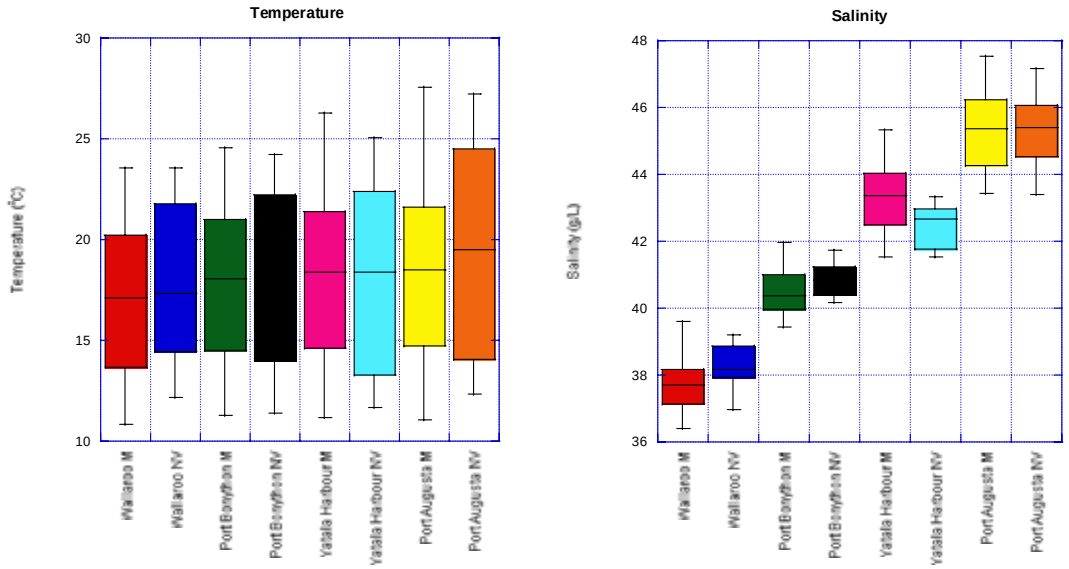

Figure 5-21 Box and Whiskers Analysis of Far Field ELCOM Model Calibration

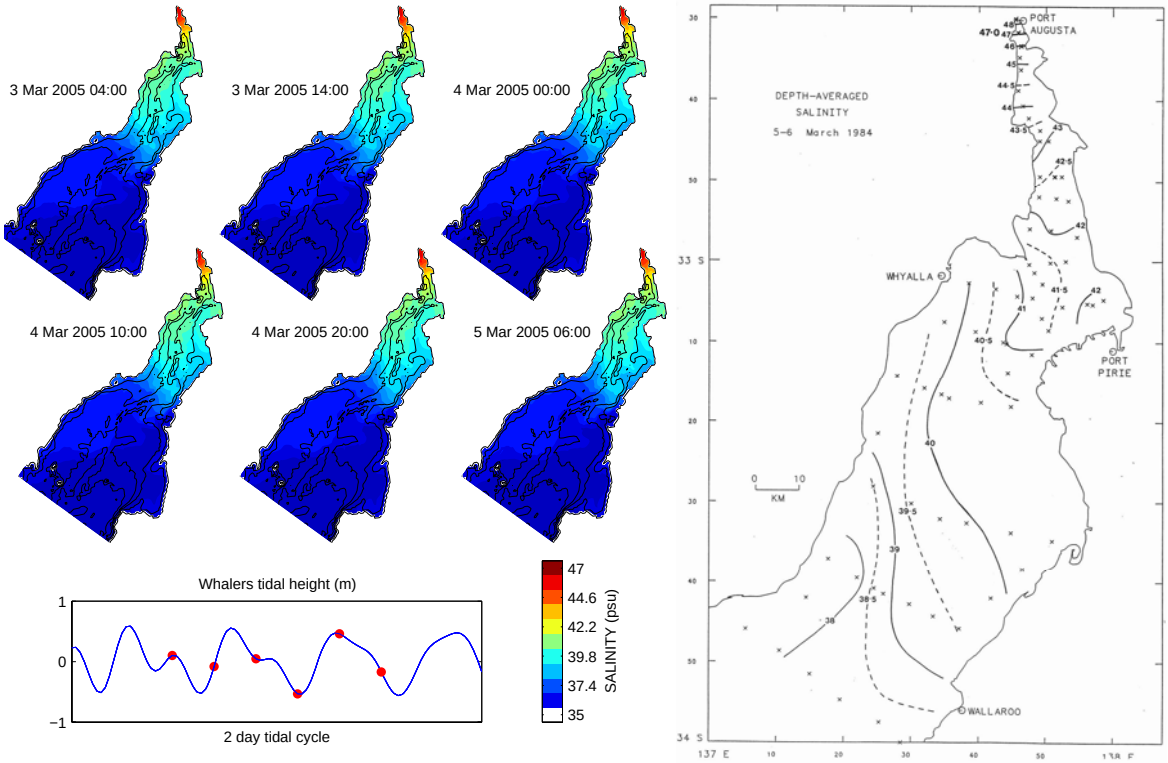

Figure 5-22 Far Field ELCOM – Nunes Vaz Salinity Comparison - Late Summer

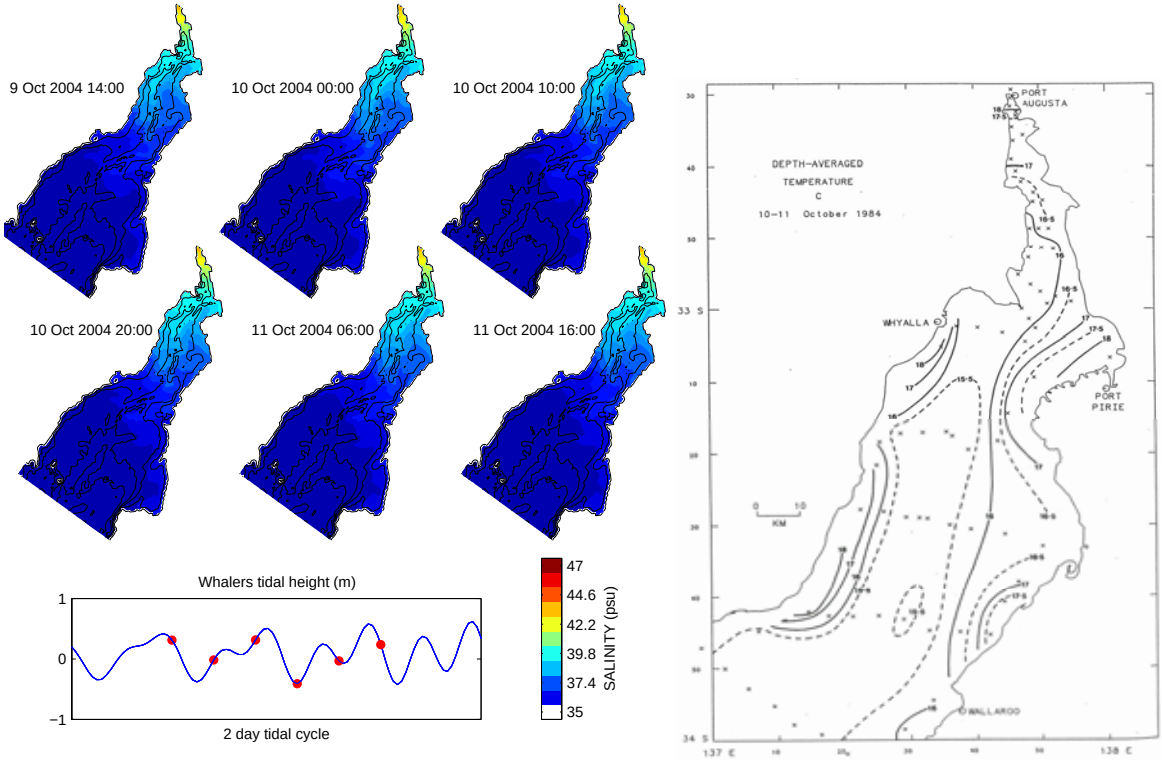

Figure 5-23 Far Field ELCOM – Nunes Vaz Salinity Comparison - Late Winter/Early Spring

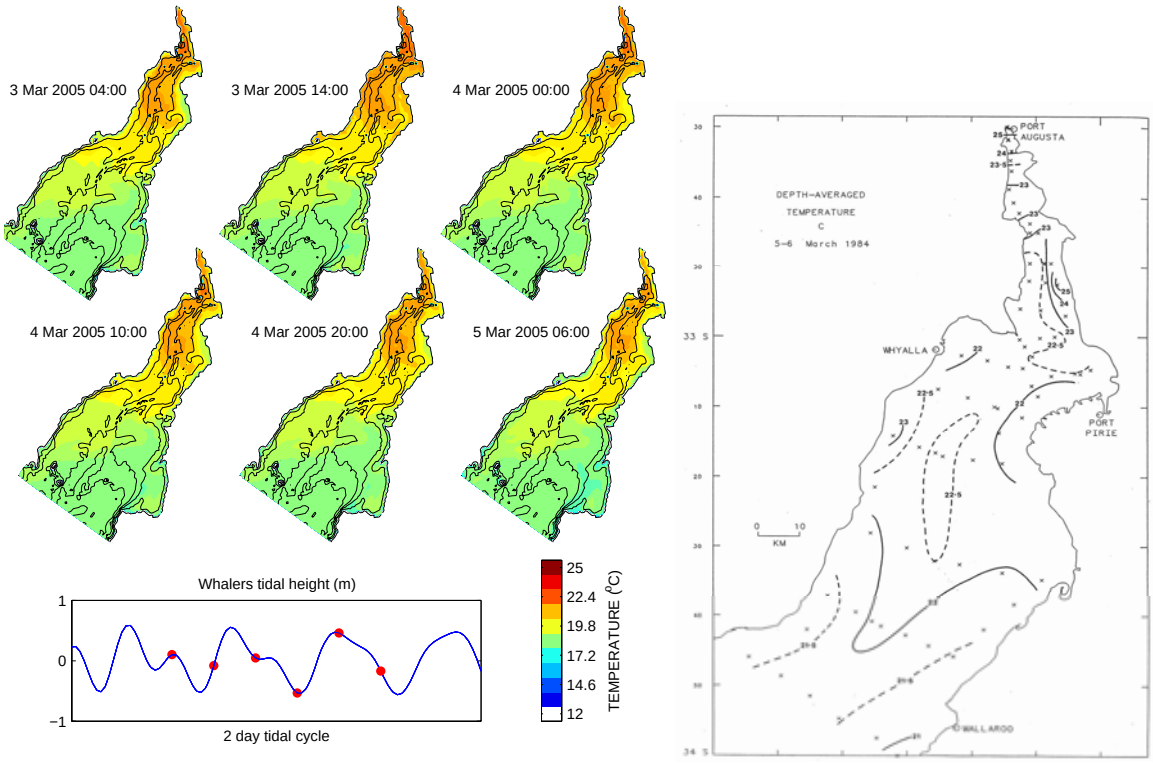

Figure 5-24 Far Field ELCOM – Nunes Vaz Temperature Comparison - Late Summer

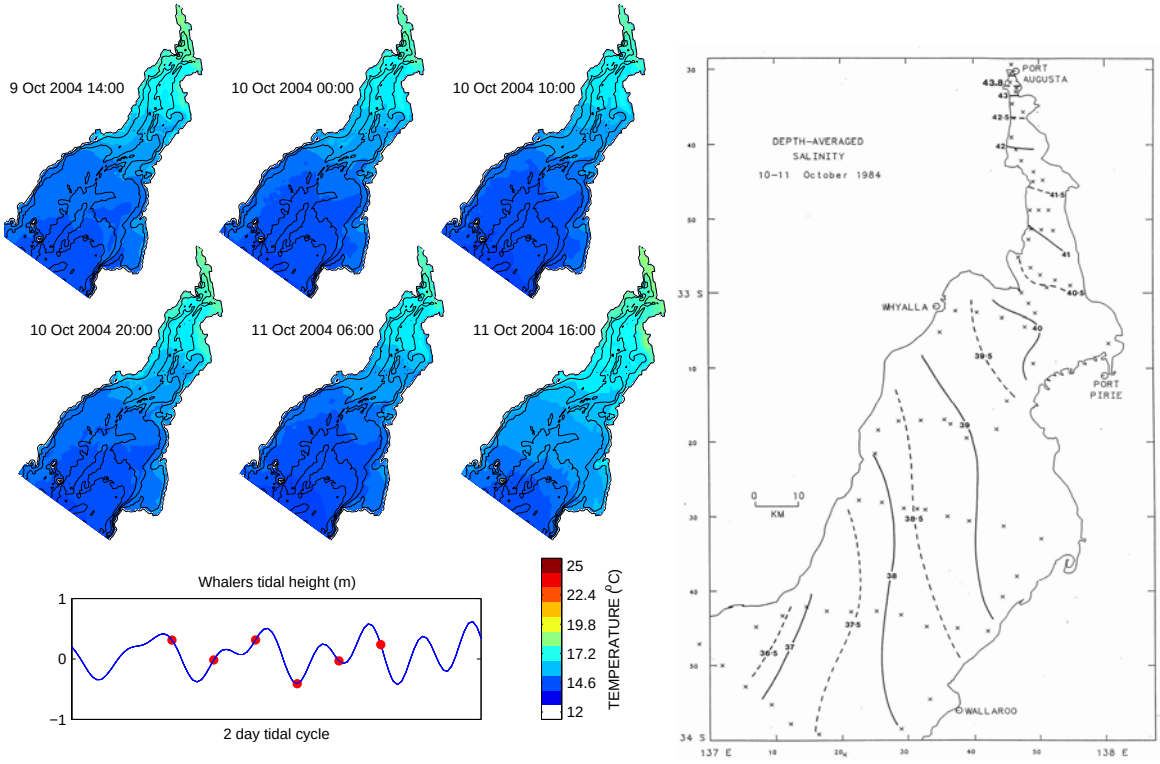

Figure 5-25 Far Field ELCOM – Nunes Vaz Temperature Comparison - Late Winter/Early Spring

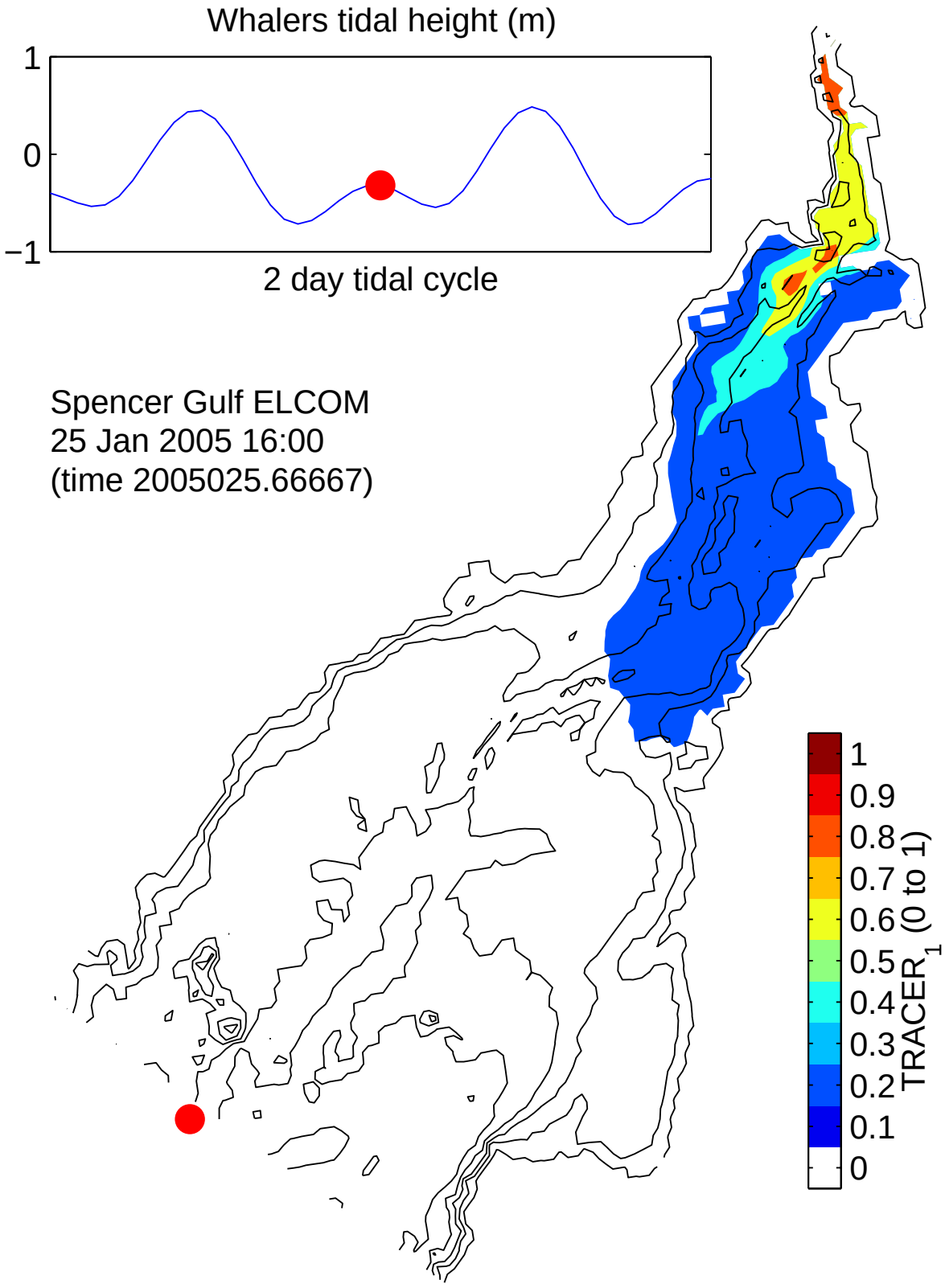

Figure 5-26 North-South tracer distribution after 4 years of simulation.

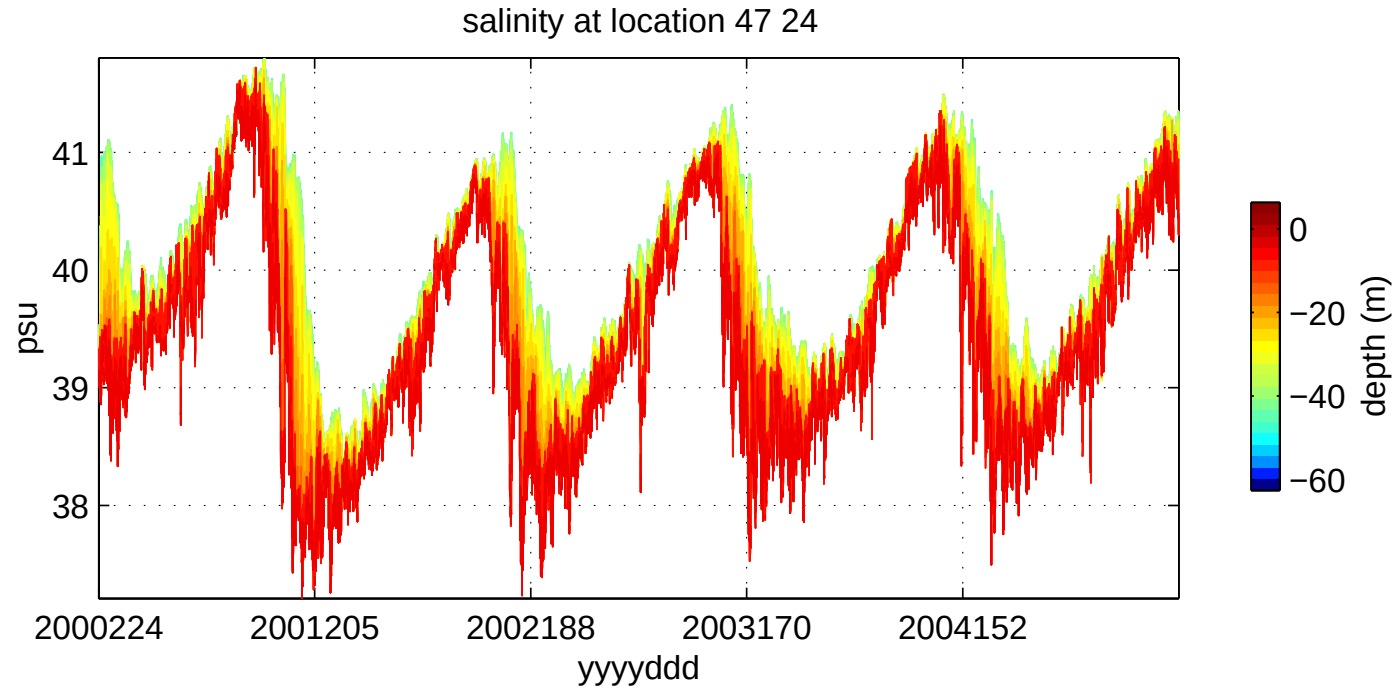

Figure 5-27 Salinity timeseries near Yarraville Shoal for 5 year ELCOM simulation

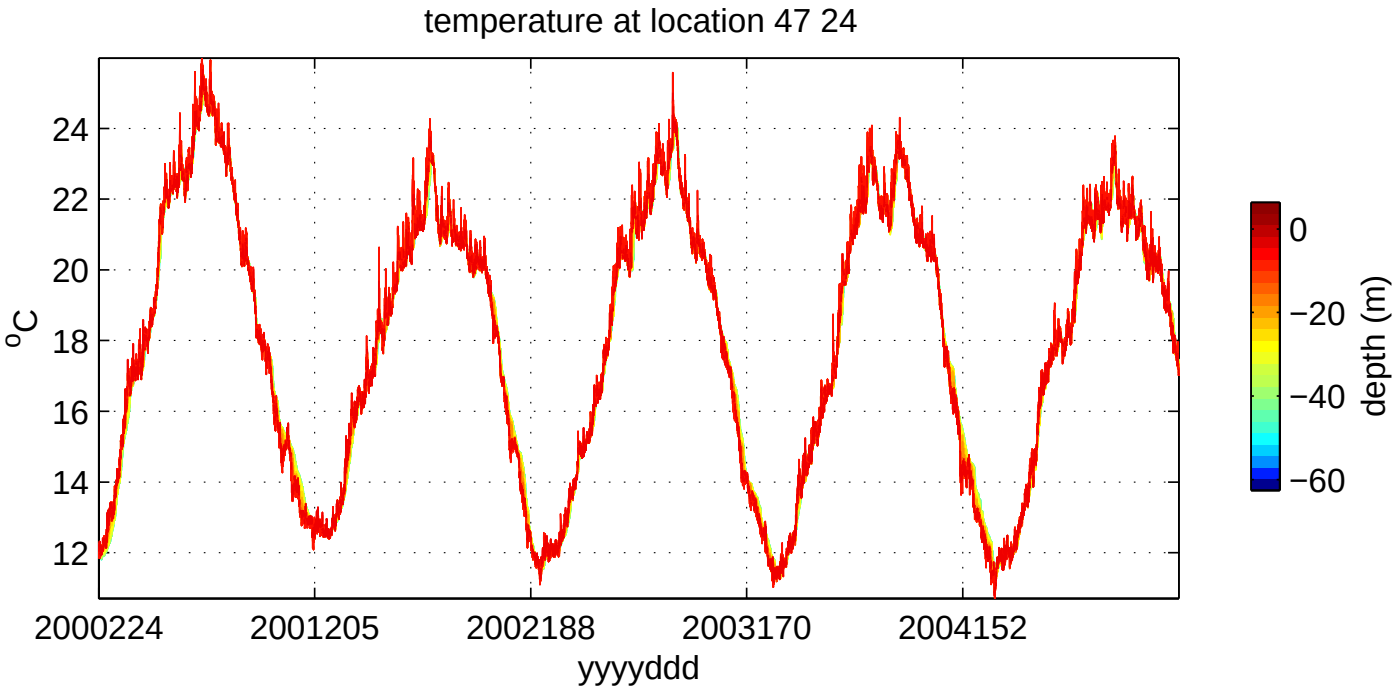

Figure 5-28 Temperature timeseries near Yarraville Shoal for 5 year ELCOM simulation

5.4 Nested Mid Field Model of Pt Bonython

5.4.1 Bathymetry

A subsection of the detailed Spencer Gulf DEM data was used to generate a 200 x 200 m bathymetry that was also rotated 36 degrees anticlockwise (with the pivot point at the northern extent of the model domain) to align the tidal boundaries with the grid. The vertical cell size was 2 m over the top 24 m and 5 m for the deepest cell (at the far southern boundary).The mid field model bathymetry stretches from Whyalla north, and is illustrated in Figure 5-29. Again, the adoption of the 200m grid was based on model stability (noting ELCOM's substepping capability to ensure Courant numbers less than 1) and computational considerations, together with a desire to have sufficient spatial detail in this region.

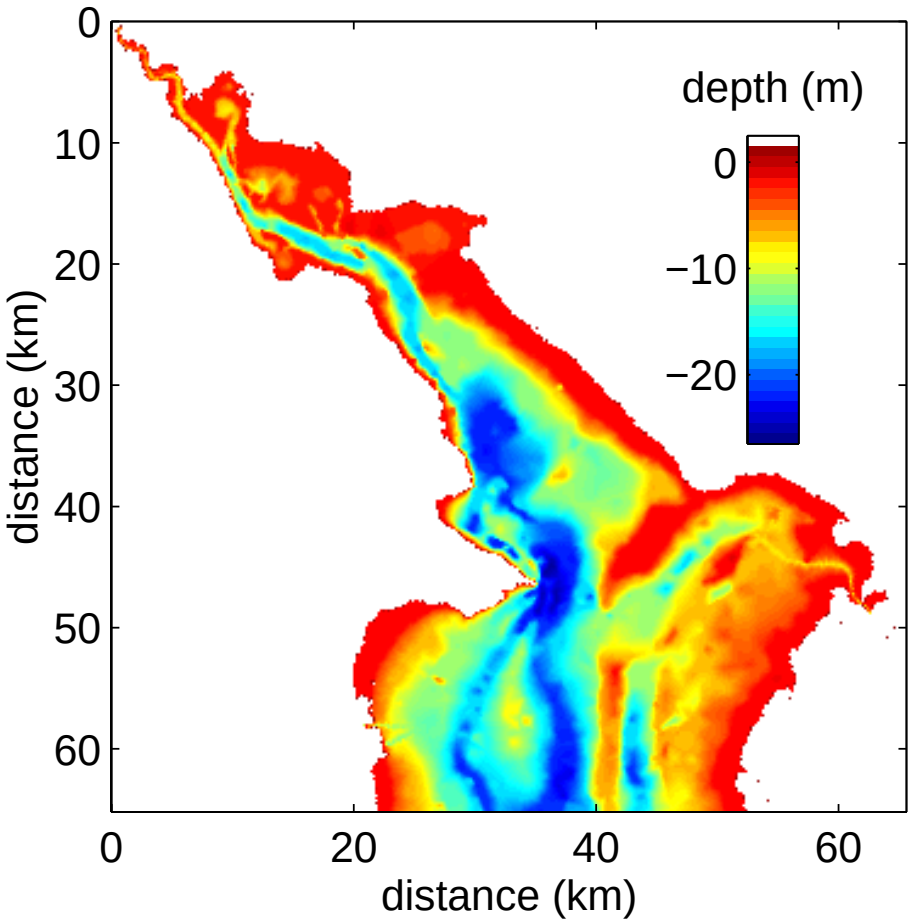

Figure 5-29 Nested 200 x 200 m mid field model bathymetry.

5.4.2 Initial Conditions and Set-up

The initial temperature and salinity conditions for the mid field model were sub-sampled from the coarse grid simulation and linearly interpolated to fill the smaller grid. The mid field model was started from dynamic rest with a water level consistent with the mean level computed by the coarse grid model at the location of the southern boundary of the mid field model at the time of initialisation. ELCOM simulations using the mid field grid were run using a model time-step of 2700 seconds.

ELCOM has an in-built linear interpolation to determine forcing at each time-step if the data resolution is coarser than the time-step

5.4.3 Tidal and Meteorological data

Temperature and salinity profiles and water height at the open boundary of the mid field model were extracted from the coarse-grid model output with a resolution of 1200 seconds. The E-W difference in forcing was introduced by using data from all the cells in the coarse grid model that are geographically coincident with the southern boundary of the mid field model. Air temperature, relative humidity and wind speed were defined using the Whyalla Aerodrome data over the entire surface of the model and appropriate radiation data was used.

It is noted that the meteorological data from Port Augusta and Whyalla is similar (eg ~ 0.4 m/s difference in mean wind speed, < 2^{o}C in mean air temp). Only Whyalla was used for the mid-field simulations due to its proximity to the proposed outfall locations, better data resolution, and, more importantly, to avoid imposing a surface domain boundary with possible discontinuities across the 200 m cell spacing. The far-field model was focussed on long-term build up of lateral salinity gradients and seasonal changes and therefore the meteorological sub-domains were required to reproduce the observed North-South gradients. However, the mid-field model was run over far shorter time-periods.

5.4.4 Simulated Eddy Structure

ADCP transect results showing the eddy structure on the southern bank of Point Lowly during an ebbing tide are presented in Figure 5-30. In order to provide an initial comparison with the mid field model results, the mid field model was interrogated for a similar tidal period, the results of which are shown in Figure 5-31. Qualitatively, the figure shows that ELCOM reproduced the eddy structure during an ebbing tide, with comparable velocities and directions.

In order to progress this analysis in a more quantitative fashion, a detailed comparison of the mid field model results and the boat mounted ADCP measurements was undertaken. To do so, the measured tidal and wind forcing data (collected by the study team in July and August 2006 when the ADCP transects were made) was inserted into the midfield model using a forcing and initial conditions (including momentum spin up) series from a previous year (2001). A similar point of a similar tide in 2001 to that measured was chosen as the 'changeover point;' between the previous year's forcing and the measurements made by this study team in 2006. This ensured the transition was as smooth as possible. This changeover point was set to be several days prior to the actual ADCP measurements to allow for any effects of the discontinuity to dissipate. It is noted that this approach was agreed to with the external reviewers of this study.

The above comparison is shown in Figure 5-32 to Figure 5-34. These are the last three ADCP transects. The first three, whilst valuable for qualitative analysis, were subject to uncertainties in the field data collection technique, with unknown potential for time mismatching between DGPS and ADCP instruments. These uncertainties were later identified and corrected mid way through the sampling program. Due to these analysis difficulties, the first three transects have not been presented. ADCO measurements are shown in black, and ELCOM predictions in green. The length of the vectors represents velocity magnitude as per the scale vector.

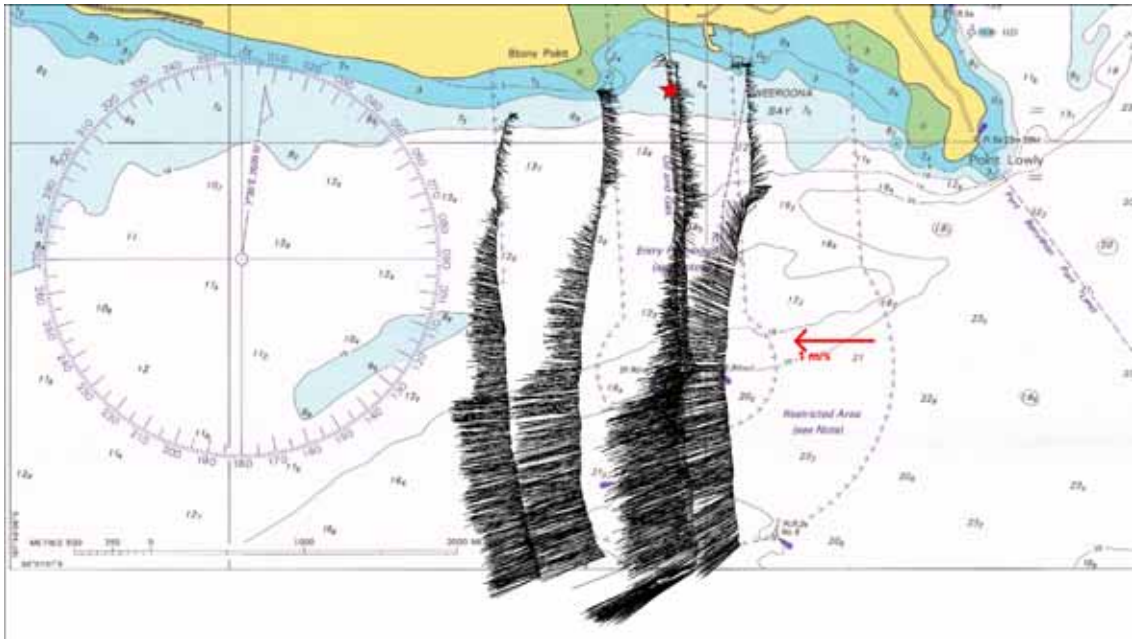

Figure 5-30 Measured surface velocities from ACDP transects during an ebbing tide.

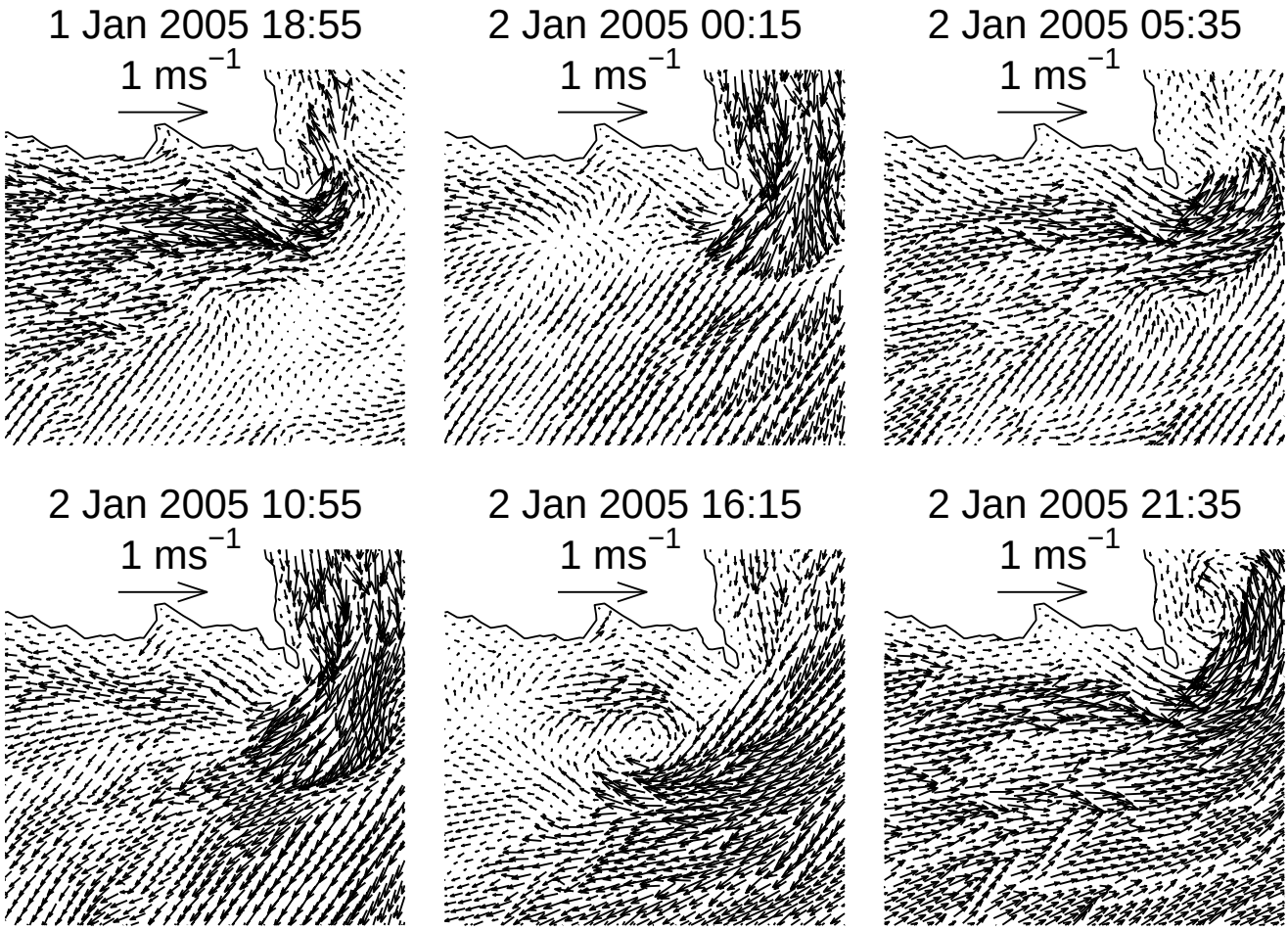

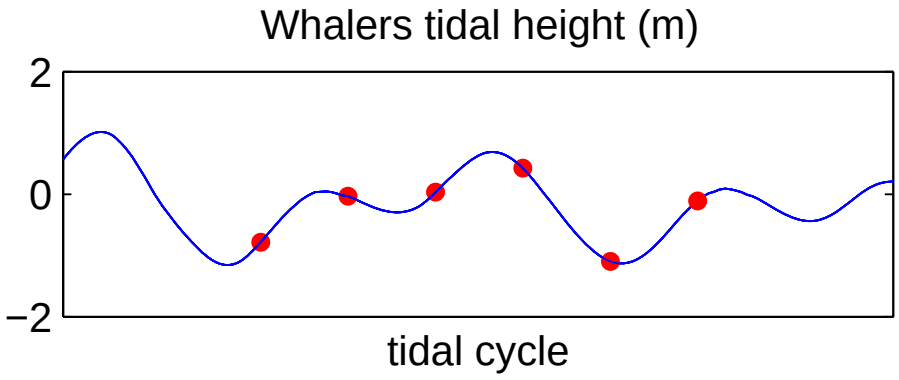

Figure 5-31 Modelled velocities 1 m below the surface. Eddy structure on the south side of Pt Bonython is shown during the ebbing tide

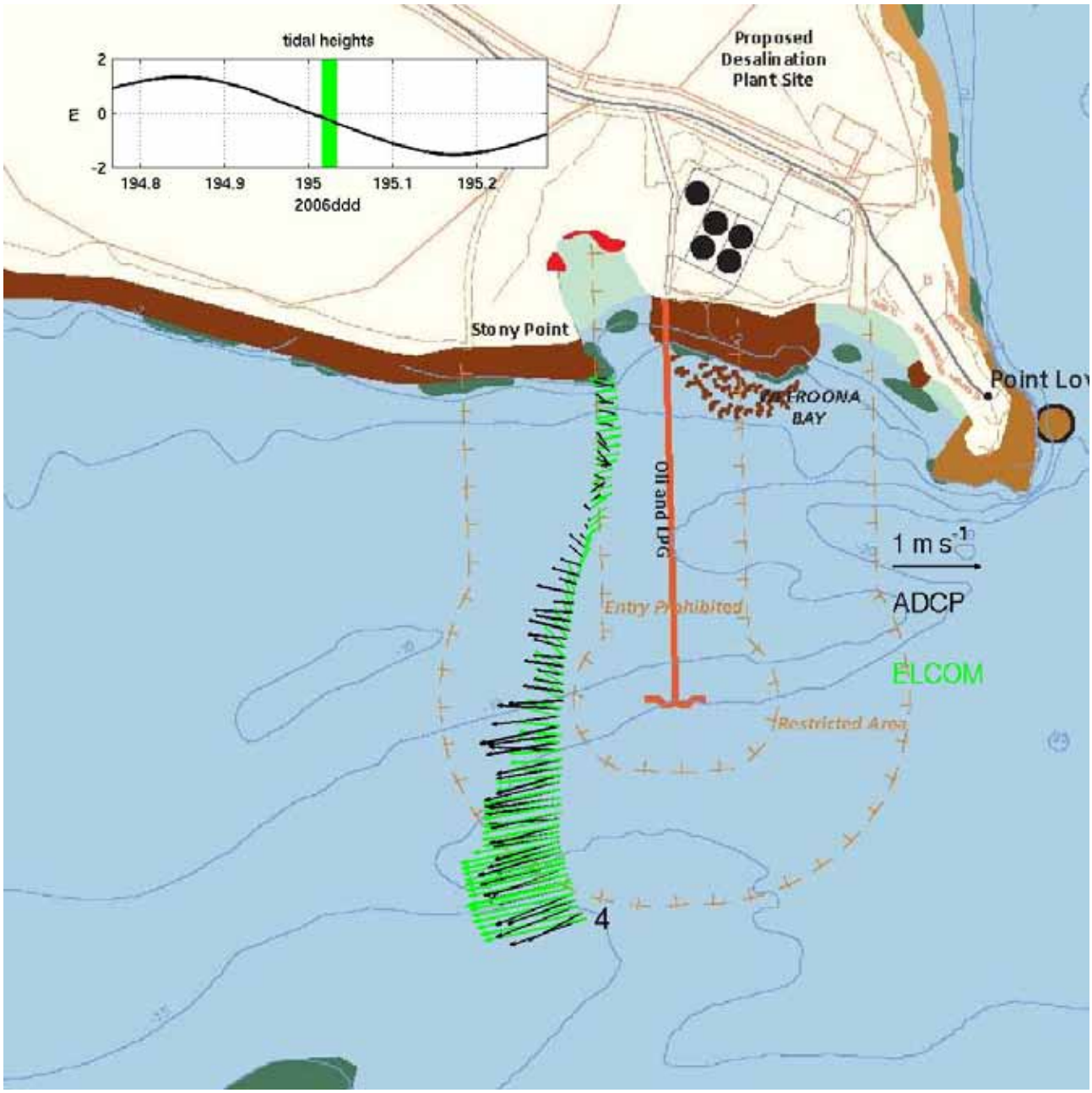

Figure 5-32 Mid Field and ADCP Comparison: Section 4

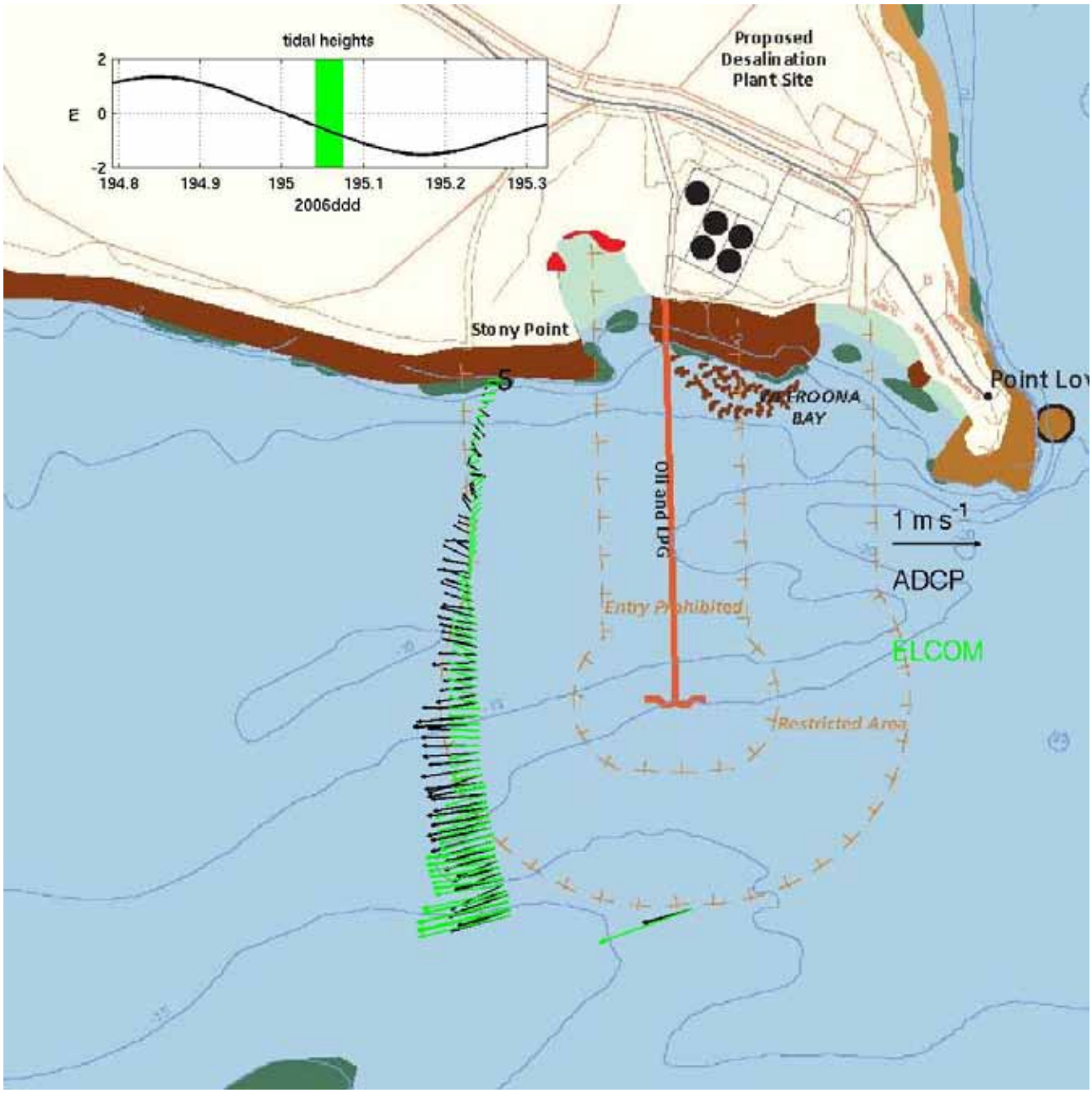

Figure 5-33 Mid Field and ADCP Comparison: Section 5

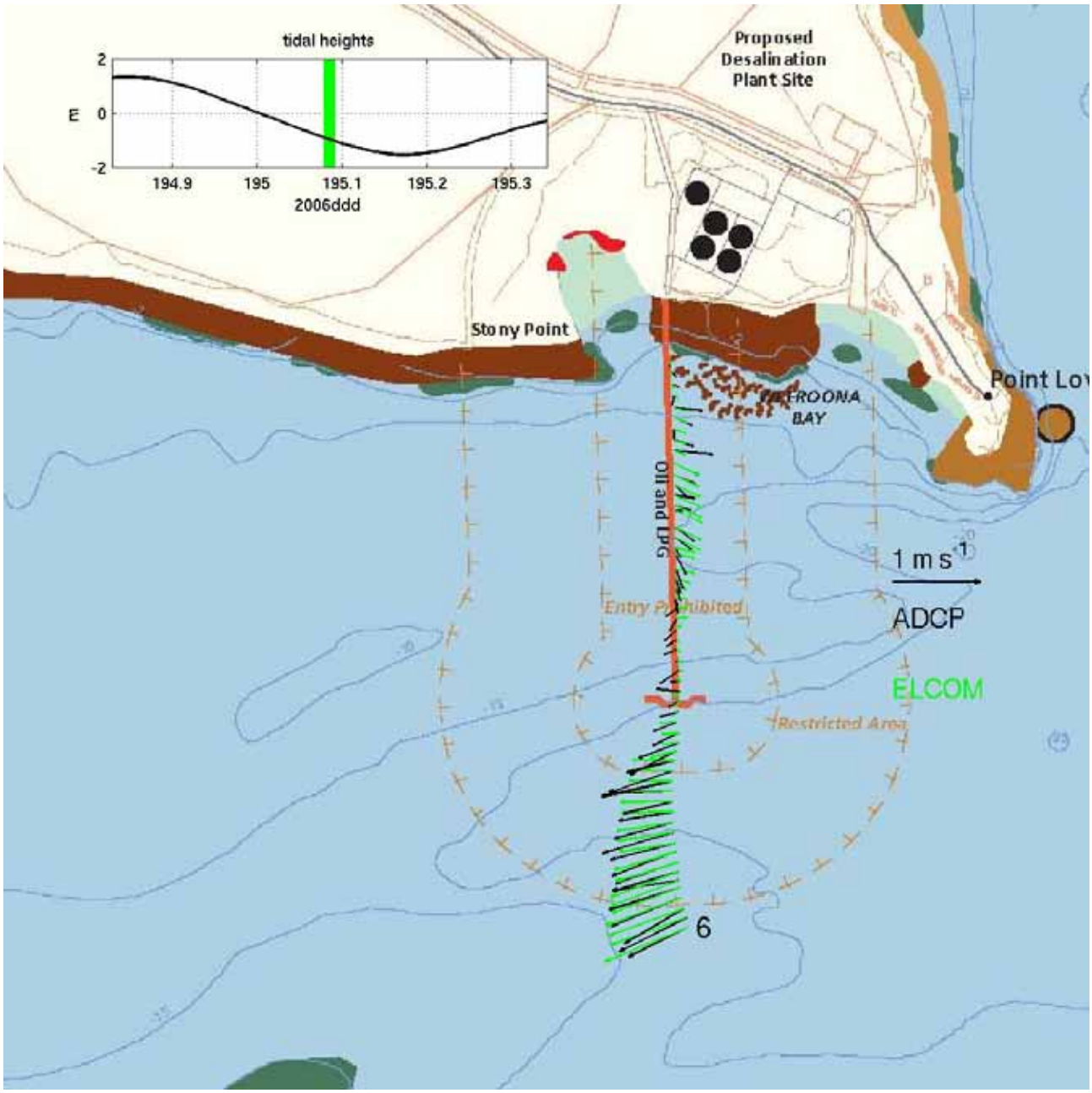

Figure 5-34 Mid Field and ADCP Comparison: Section 6

In general, ELCOM shows an excellent reproduction of the ADCP data.

5.4.5 Simulated Velocity Data

Figure 5-35 compares bottom mounted ADCP current speed recordings with model predictions for a spring tide period, while Figure 5-36 provides a similar comparison for a neap tide. Figure 5-37 and Figure 5-38 subsequently compare observed and predicted current direction data, respectively for a spring and neap tide. Finally, to illustrate the accuracy of the modelling, we have prepared comparisons of depth averaged field data/model results for a several day spring to neap tide period, as illustrated in Figure 53-9. It is stressed that these all the above comparisons are qualitative only as the model was not run over the same time period that field data was collected, so differences in detail are to be expected, with major trends being comparable.

These figures highlight how accurately the midfield model is reproducing local current patterns, as summarised below:

- the magnitude of observed and predicted current speeds match closely;
- the magnitude of observed and predicted current directions match closely;
- the vertical patterns of variation in observed and predicted current speeds and directions match closely; and
- the pattern of current direction change as the model transitions from flood to ebb tide (and vice versa) closely matches the observed data set.

5.4.6 Coupled Plume model

Preliminary simulations of plume dispersion were conducted using the mid field ELCOM model by introducing a saline discharge at the end of the existing wharf, with an associated inert tracer. Intakes were also included in all scenario simulations and both the intake and outfall occur at the base of the deepest cell in the specified location. Based on preliminary information regarding the character of the SWRO plant, the outfall was introduced at 3.14 m^3s^{-1}, with a salinity of 74.6 g/L and a temperature of 1^oC higher than the simulated ambient temperature. Figure 5-40 illustrates the outfall plume over the mid-field domain after 2 days of simulation time. Figure 5-41 shows behaviour of the tracer plume near the outfall location over the same period. In both cases the tracer was discharged with a concentration of unity, and as such dilutions of more than 1000 times are predicted for locations a kilometre or more distant from the outfall.

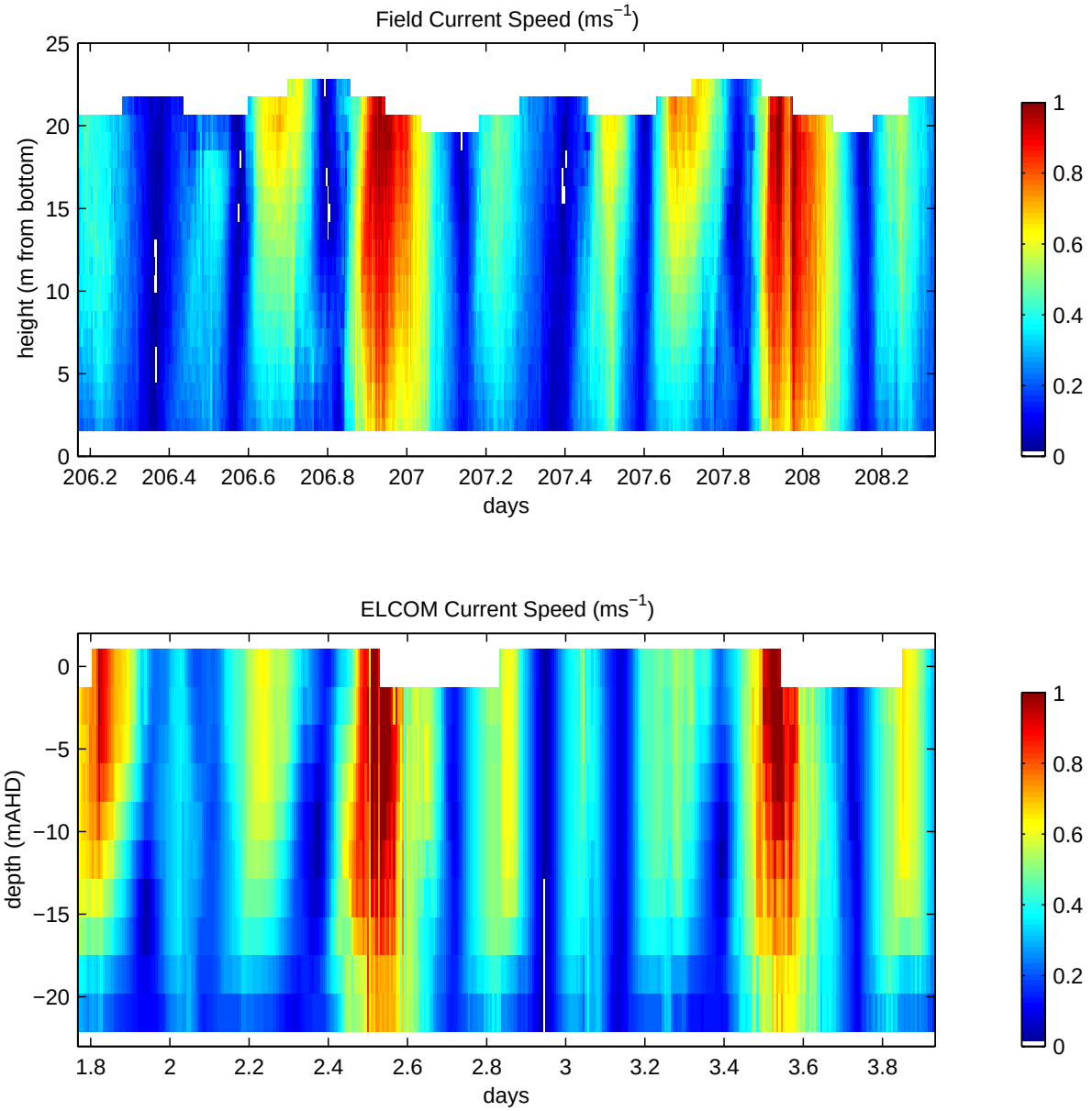

Figure 5-35 Spring Tide Midfield ELCOM Model Current Speed Calibration

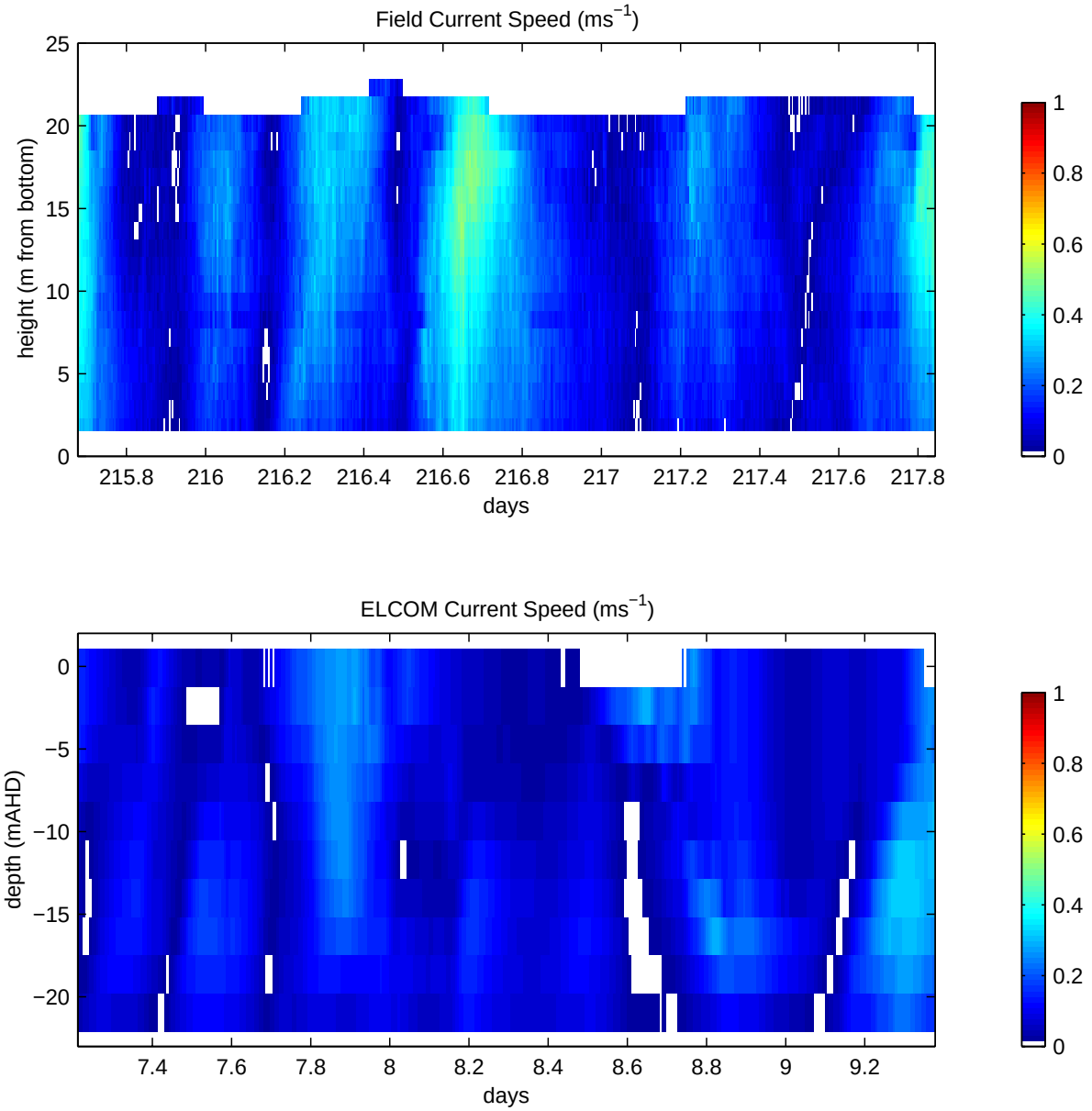

Figure 5-36 Neap Tide Midfield ELCOM Model Current Speed Calibration

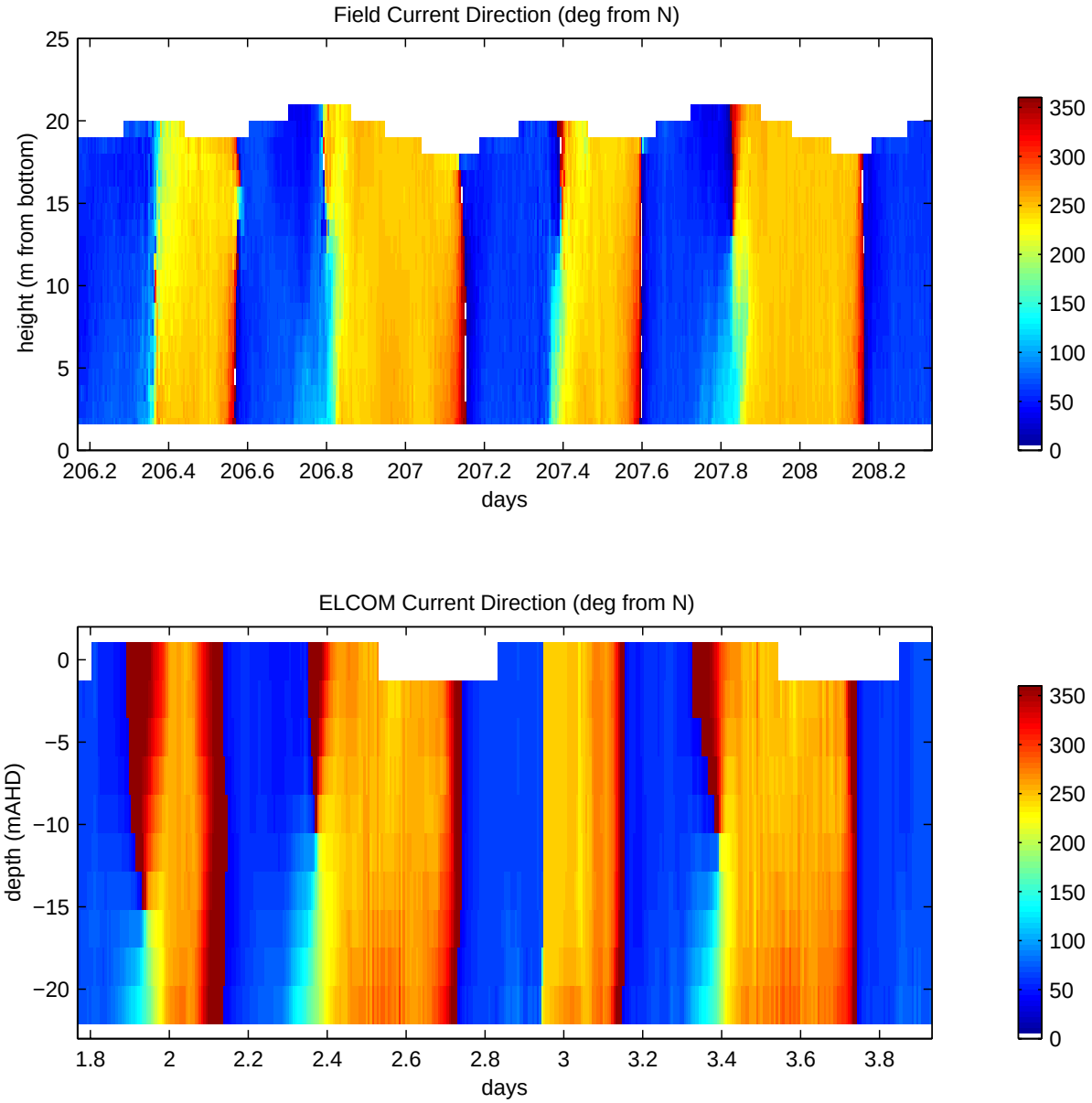

Figure 5-37 Spring Tide Midfield ELCOM Model Current Direction Calibration

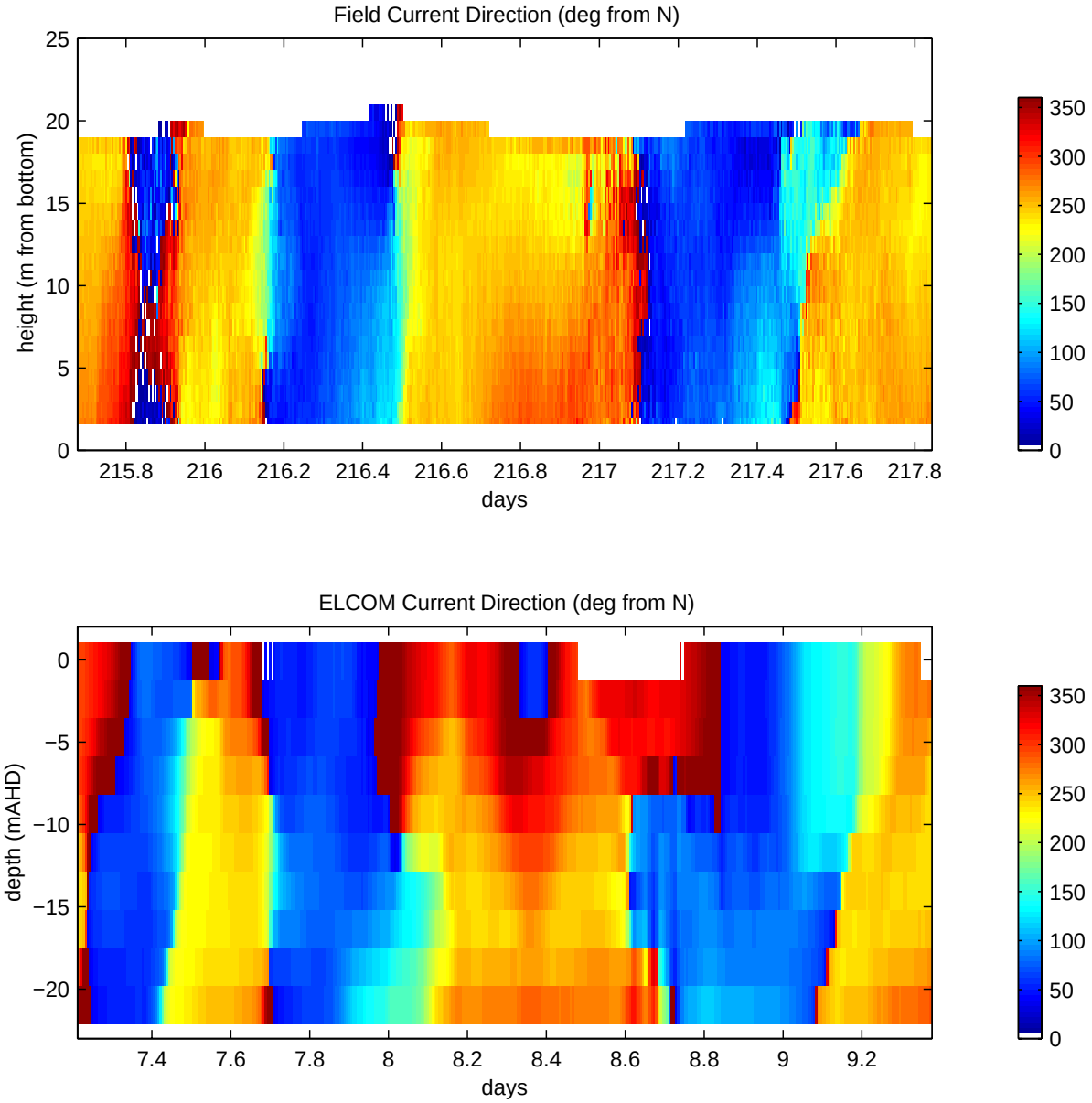

Figure 5-38 Neap Tide Midfield ELCOM Model Current Direction Calibration

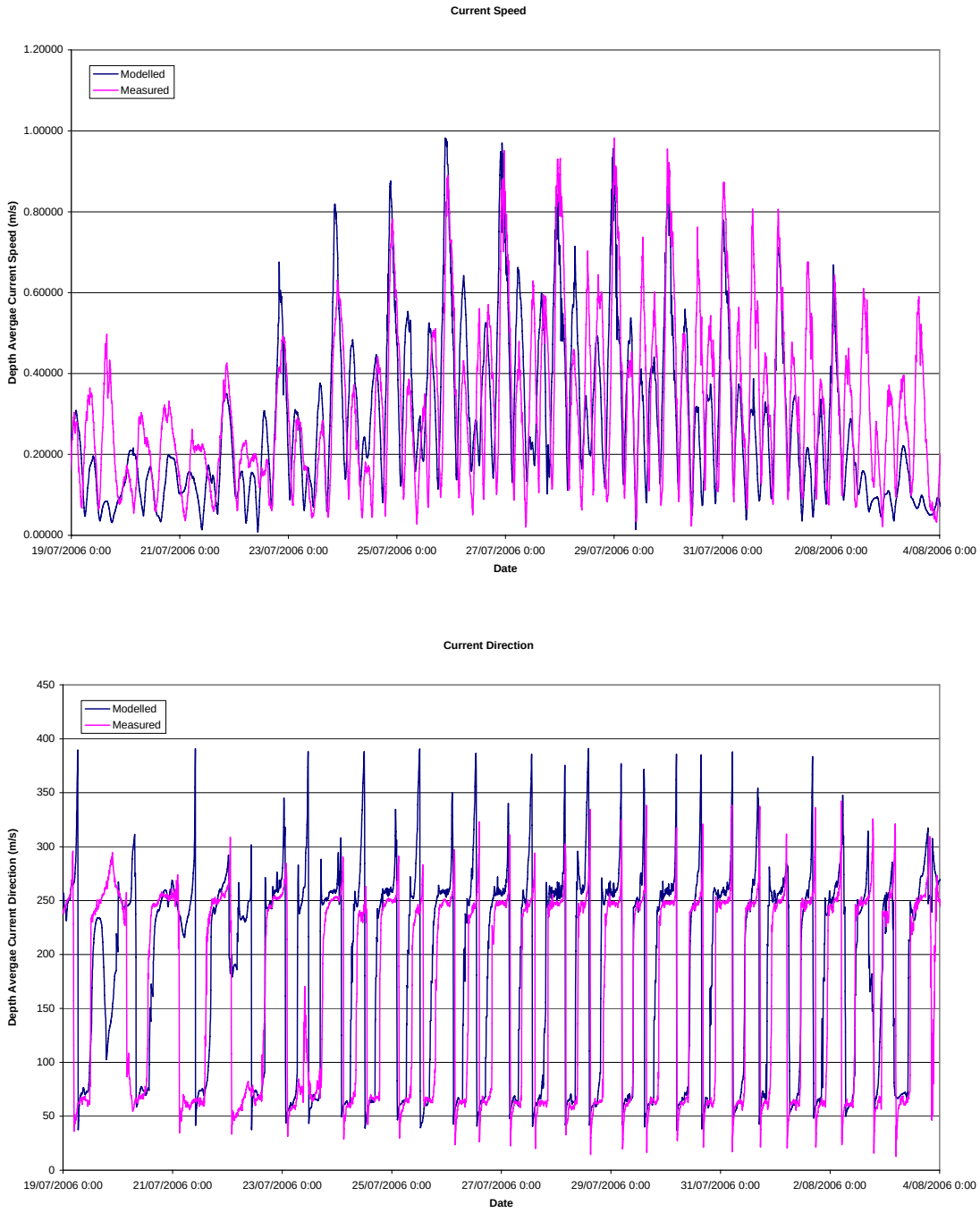

Figure 5-39 Depth Averaged Midfield ELCOM Model Current Calibration

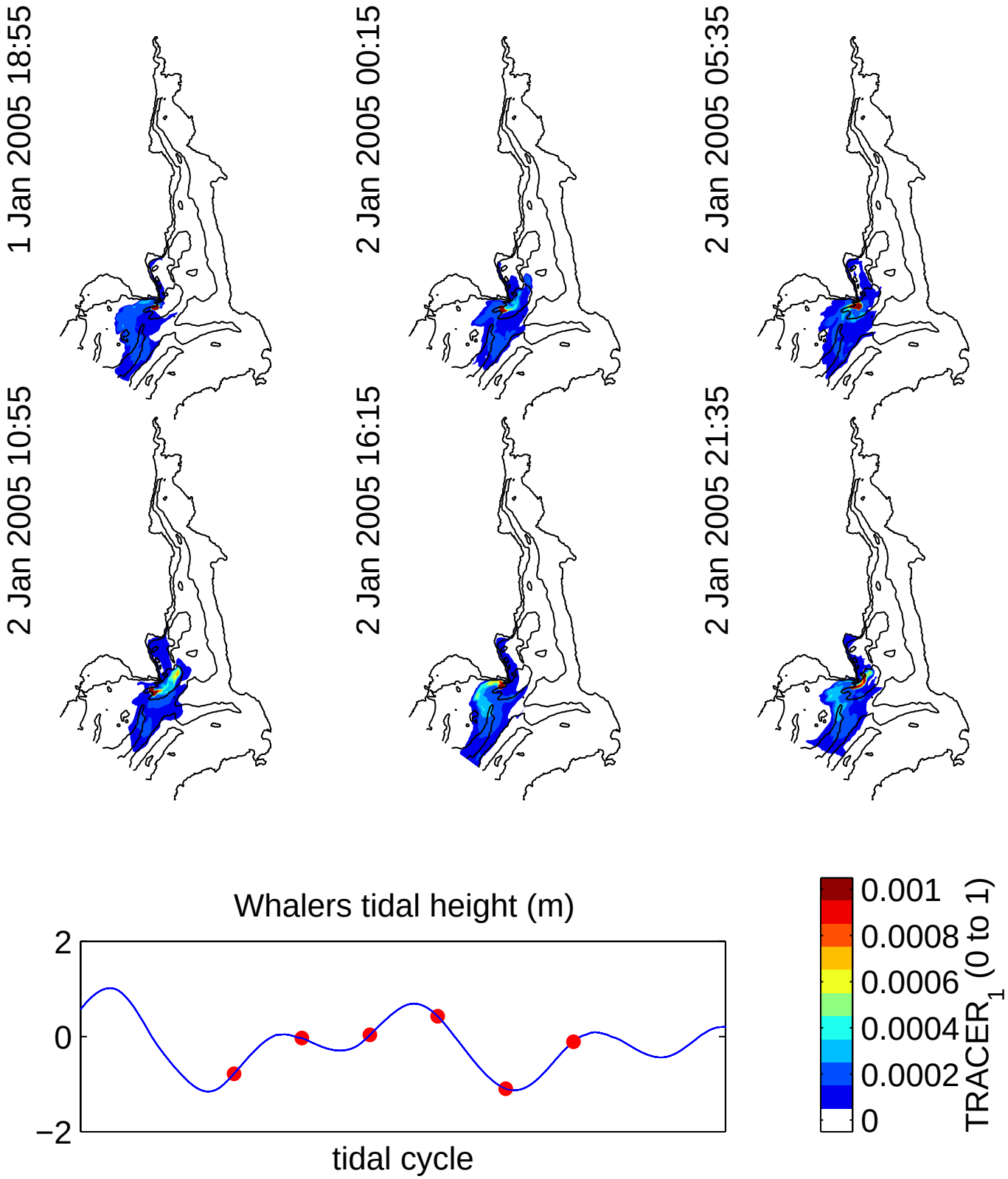

Figure 5-40 Tracer plume from desalination outfall over mid field grid model

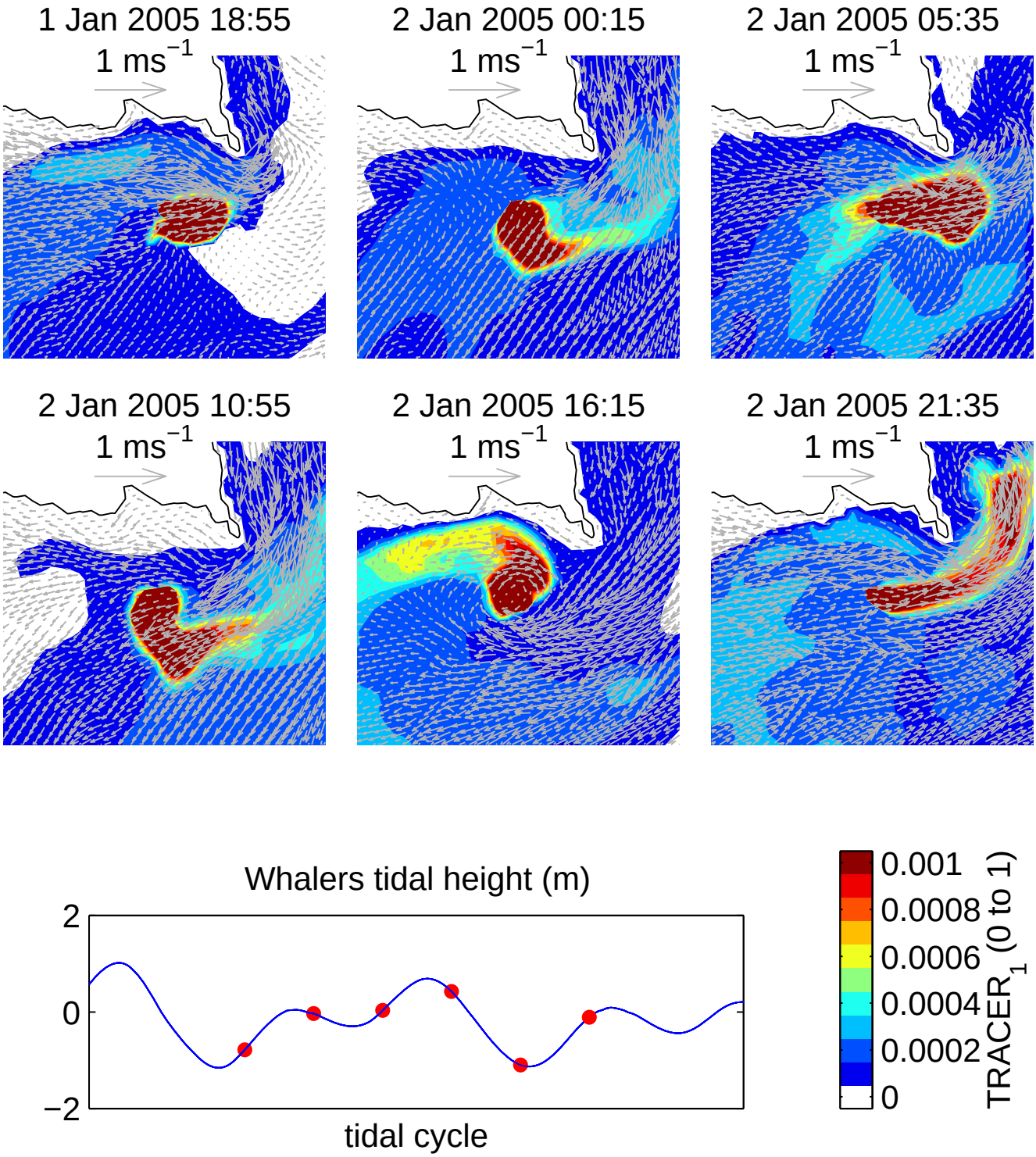

Figure 5-41 Tracer concentration and velocity structure showing the outfall release and eddy structure in the mid field grid model

Further to the above, the brine discharge will occur though a diffuser that will cause the brine to form a plume of greater than 2 m height and the behaviour of the plume in the local flow will be determined by the near-field model. Hence, the ELCOM simulations are conservative in that the plume is injected directly into the bottom cell and only diluted by the initial input into the full cell volume. Any further dilution is in response to the ambient flow. As an example, near field simulations reported in subsequent documents have found that (at median ambient velocities) hydrodynamic centreline dilutions of up to 50 can be obtained within 25 metres of the outfall.

Dissolved oxygen is not modelled by ELCOM alone, but can be modelled using the ecological model CAEDYM that links with ELCOM. Modelling DO is, however, likely to be of limited use as ambient currents generally prevent extensive long term pooling (see subsequent reporting) and preliminary data provided by BHP and Arup suggest that the effluent may not be significantly oxygen depleted (subject to confirmation).

Additional discussion and model interrogation regarding this matter, and the comparison of far and mid field model predictions, is presented in Appendix B.

6 REFERENCES

BHP. 2006 Olympic Dam Development Pre-Feasibility Study, Infrastructure and Environment Study

Bye, J.A.T. and I.P. Harbison. 1991. Transfer of inland salts to the marine environment at the head of Spencer Gulf, South Australia. Palaeogeography, Palaeoclimatology, Palaeoecology, 84: 357-368.

Hicks, B.B. 1975 A procedure for the formulation of bulk transfer coefficients over water. 8:315-324. *Boundary Layer Meteorology* **8**, pp. 315-324.

Hodges, B.R., Imberger, J., Saggio, A. and Winters, K.B. (2000) Modelling basin-scale internal waves in a stratified lake. Limnology and Oceanography, 45(7): 1603-1620.

Laval, B., Imberger, J. and Findikakis, A.N. (2003) Mass transport between a semi-enclosed basin and the ocean: Maracaibo system. Journal of Geophysical Research (Oceans), 108 (C7): 3236.

Nunes, R.A. (1985). Catalogue of Data from a Systematic Programme of oceanographic Measurements in Northern Spencer Gulf from 1982 to 1985. School of Earth Sciences Flinders University of South Australia, Cruise Report No. 9.

Nunes, R.A., and G.W. Lennon. (1986). Physical property distributions and seasonal trends in Spencer Gulf, South Australia: an inverse estuary. Australian Journal of Marine and Freshwater Research. 37: 39-53.

Nunes Vaz, R.A., G.W. Lennon and D.G. Bowers. (1990). Physical behaviour of a large, negative or inverse estuary. Continental Shelf Research. 10(3): 277-304.

APPENDIX A: ELCOM DESCRIPTION

ELCOM (Estuary, Lake and Coastal Ocean Model) is a three-dimensional hydrodynamics model for estuaries, lakes and reservoirs, and is used to predict the variation of water temperature and salinity in space and time. ELCOM solves the unsteady Reynolds-averaged Navier - Stokes equations using a semi-implicit method similar to the momentum solution in the TRIM code with the addition of quadratic Euler - Lagrange discretization, scalar (eg. temperature) transport using a conservative flux-limited approach, and elimination of vertical diffusion terms in the governing equations. ELCOM does not assume a relationship between the vertical Reynolds stress terms and the resolved shear, but instead applies a mixing model to directly compute the vertical turbulent transport. Molecular diffusion in the vertical direction is neglected as turbulent transport and numerical diffusion are generally dominant. The free-surface evolution is governed by vertical integration of the continuity equation for incompressible flow in the water column applied to the kinematic boundary condition.

Heat exchange through the water's surface is governed by standard bulk transfer models found in the literature. The energy transfer across the free surface is separated into nonpenetrative components of long-wave radiation, sensible heat transfer, and evaporative heat loss, complemented by penetrative shortwave radiation. Nonpenetrative effects are introduced as sources of temperature in the surface-mixed layer, whereas penetrative effects are introduced as source terms in one or more grid layers on the basis of an exponential decay and an extinction coefficient (Beer's law).

ELCOM computes a model time step in a staged approach consisting of

- introduction of surface heating/ cooling in the surface layer
- mixing of scalar concentrations and momentum using a mixed-layer model
- introduction of wind energy as a momentum source in the wind-mixed layer
- solution of the free-surface evolution and velocity field
- horizontal diffusion of momentum
- advection of scalars, and
- horizontal diffusion of scalars.

The fundamental numerical scheme is adapted from the TRIM approach of Casulli and Cheng (1992) with modifications for accuracy, scalar conservation, numerical diffusion, and implementation of a mixed-layer turbulence closure. The solution grid uses rectangular Cartesian cells with fixed Δx and Δy (horizontal) grid spacing, whereas the vertical z spacing may vary as a function of z but is horizontally uniform. The grid stencil is the Arakawa C-grid: velocities are defined on cell faces with the free-surface height and scalar concentrations on cell centres. The free-surface height in each column of grid cells moves vertically through grid layers as required by the free-surface evolution equation. Replacement of the standard vertical turbulent diffusion equation with a mixed-layer model eliminates the tridiagonal matrix inversion for each horizontal velocity component and transported scalar required for each grid water column in the original TRIM scheme. This provides computational efficiency and allows sharper gradients to be maintained with coarse grid resolution.

Examples of ELCOM applications include the modelling of internal wave processes in stratified lakes (Hodges *et al*, 2000) and the modelling of exchange flow between a tidal strait and coastal lake (Laval *et al*, 2003).

APPENDIX B: ADDITIONAL CALIBRATION WORKS

BMT WBM

Memorandum

From:	Michael Barry	To:	James Brook
Date:	21 August 2008	CC:	Tony McAlister
Subject:	Additional Calibration Works		

Dear James

Following the initial issue of the Spencer Gulf model calibration report in 2006 and 2007 (latest version is R.B15583.004.02.Calibration.doc), we have undertaken additional works with the intent of further assessing the performance of the far field ELCOM model, and its relationship to the mid field model. Specifically, we have investigated the far field model's ability to reproduce:

- The well-known winter salt ejection mechanism;
- Field data collected in the 1980s; and
- Mid field model predictions.

This memorandum briefly describes and reports on these works. In addition, further details are provided on:

- The advection-dispersion scheme used in ELCOM;
- The role of turbulent horizontal diffusion in the model framework;
- The role of molecular diffusion in the model framework;
- The vertical mixing schematisation in ELCOM;
- The turbulent closure scheme in ELCOM;
- The ability of ELCOM to conserve tracer within the adopted advection-dispersion scheme;
- The nett circulations of the wider Gulf during each season; and
- Recent ADCP data collected at Point Lowly.

Winter Salt Ejection Mechanism

Over the last twenty years, considerable effort has been expended in investigating and understanding the global hydrodynamics of Spencer Gulf. This has primarily taken the form of collection and interpretation of monitoring data (e.g. Nunes 1985, Nunes and Lennon 1986, Nunes-Vaz Lennon and Bowers 1990, Bye and Harbison 1991). One key finding of these, and other studies, has been the identification of a salt ejection mechanism that operates within the Gulf.

In summary, it has been found that hypersaline waters develop in the upper reaches of the Gulf during summer and early autumn (due to high atmospheric evaporation rates) and that the density gradient created by these waters forces them southwards during autumn and early winter. The southwards migration of saline water manifests itself as an underflow (due to its density difference relative to less saline southern waters) and the underflow is pushed, via the operation of Coriolis efffects, towards the eastern boundary of the Gulf. This process thus accounts for an 'ejection' of salt from the Gulf on an annual timescale, with the ejected salt mass being replaced by incoming oceanic waters, albeit by a proportionately larger volume of the latter at a considerably lower salinity. This section investigates the ability of the far field model to reproduce this mechanism, and examines the potential impact of brine from the proposed desalination plant on its operation.

To this end, the far field model was run over 2003 (with the antecedent warmup period as before), and the presence of the seasonal ejection mechanism investigated. In order to do so, a series of east-west (in plan) vertical curtains were inserted into the model as extraction templates, with particular reference to extracting salinity. These curtains were inserted in addition to the existing surface and bottom sheets.

Figure 1 and Figure 2 present the resultant salinity contours from the base case at snapshots in late March and mid June 2003, respectively. Each figure has four panels on the left and two panels on the right hand side. From top to bottom, the left hand panels show the vertical curtain salinity contours at each east-west curtain, moving southwards along the Gulf. The two right hand panels show the bottom and surface salinities. All salinities are colour contoured to the same range, as given in the colour bar at the top of each figure. It is noted that the colour bar limits have been chosen so that the saline waters associated with the ejection mechanism operation are clear, and that this has resulted in visual 'truncation' of the higher salinities in the upper Gulf, for presentation purposes only. The actual simulated salinities in the upper Gulf region (i.e. in the vicinity of curtain 1) at the times of the snapshots below are greater than 40 g/L.

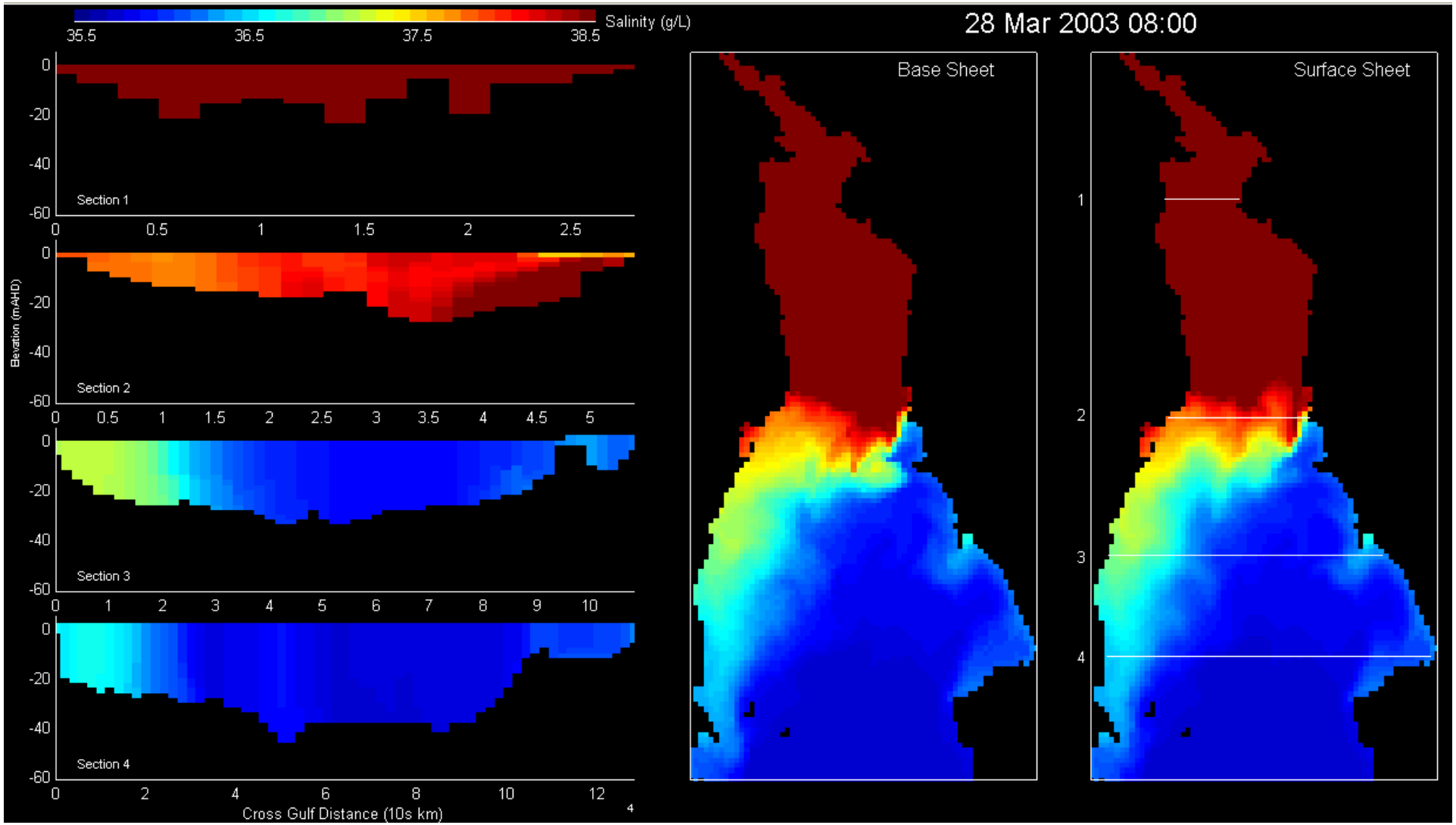

Figure 1 Base Case Salinity Contours – March 2003

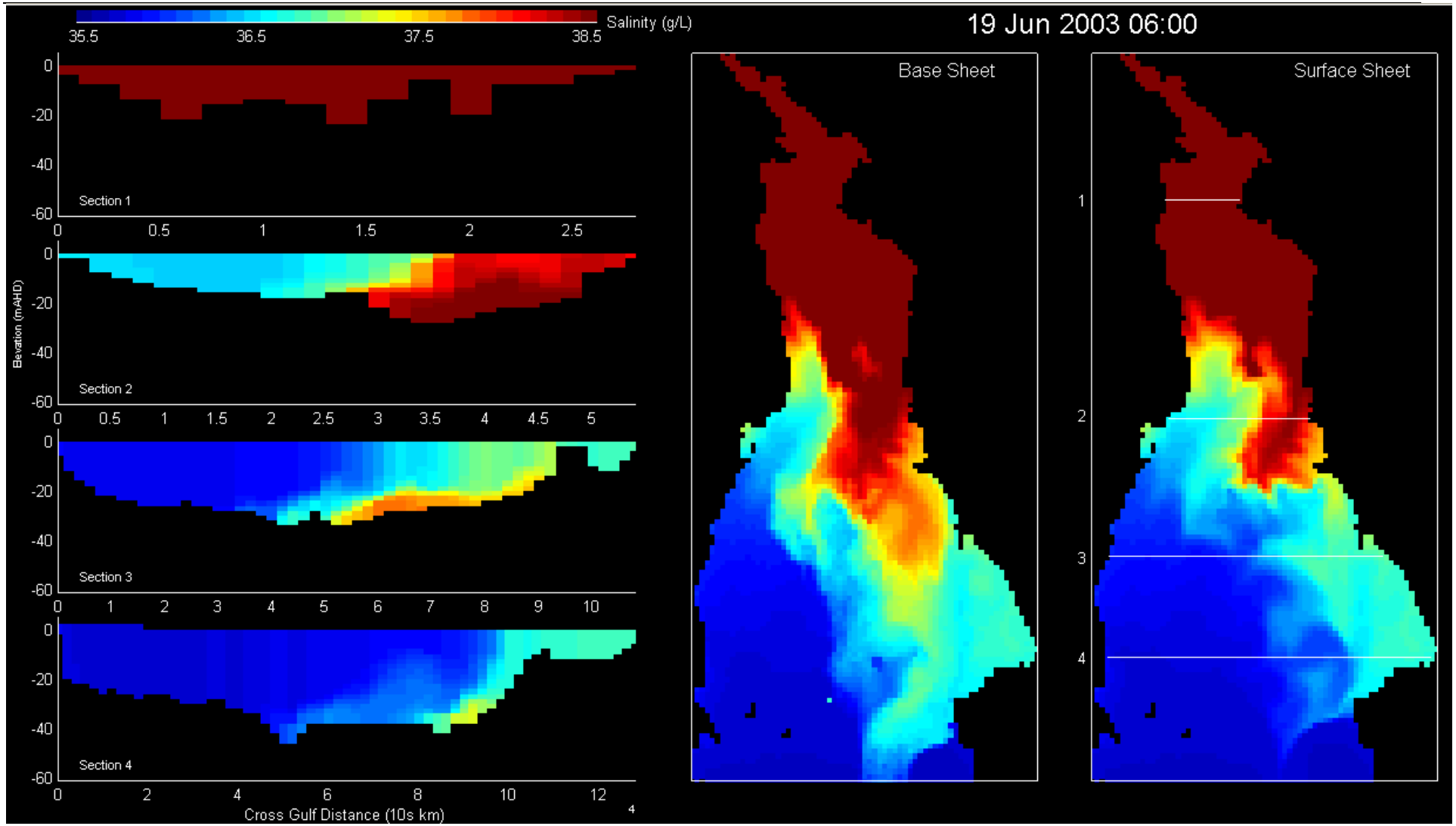

Figure 2 Brine Discharge Salinity Contours – June 2003

The figures demonstrate that the far field model is representing the set up and operation of the saline ejection process over late Autumn to early Winter. The southward migration, and eastward deflection under Coriolis, of the saline underflow is evident in the bottom sheet and curtains 2, 3 and 4 for the June figure. The operation of this mechanism is consistent with the salt balance analysis undertaken in the modelling assessment report, where salt is predicted to accumulate in the Gulf over summer and then leave the system over winter.

It is noted that the annual timescale of this ejection mechanism implies that the order of magnitude of flushing timescales for the upper Gulf should be similar, i.e. the ejection mechanism influences the retention time of upper Gulf waters to an extent that accumulation of waters in this region for multi-annual periods is unlikely. The retention time data presented in the modelling assessments report is consistent with this hypothesis.

Comparison with 1980s Field Data

Hydrodynamic and physical water quality data was collected over several episodes in the 1980s. Dr Rick Nunes-Vaz and his colleagues primarily undertook this work. Dr Nunes-Vaz has kindly made this data available for use in this study, primarily for comparison with model predictions. These data are separate, and additional to, those already provided by Dr Nunes-Vaz and used in the calibration study. Data has been provided for three locations:

- Beacon 5;
- Yarraville Shoals; and
- Myponie.

Dr D Provis of RK Steedman & Assoc and RPS Metocean Engineering kindly agreed to supply the Myponie data, and is acknowledged here. The location of the three sites is shown in Figure 3. The cell from which data was extracted from the far field model at Beacon 5 is also shown.

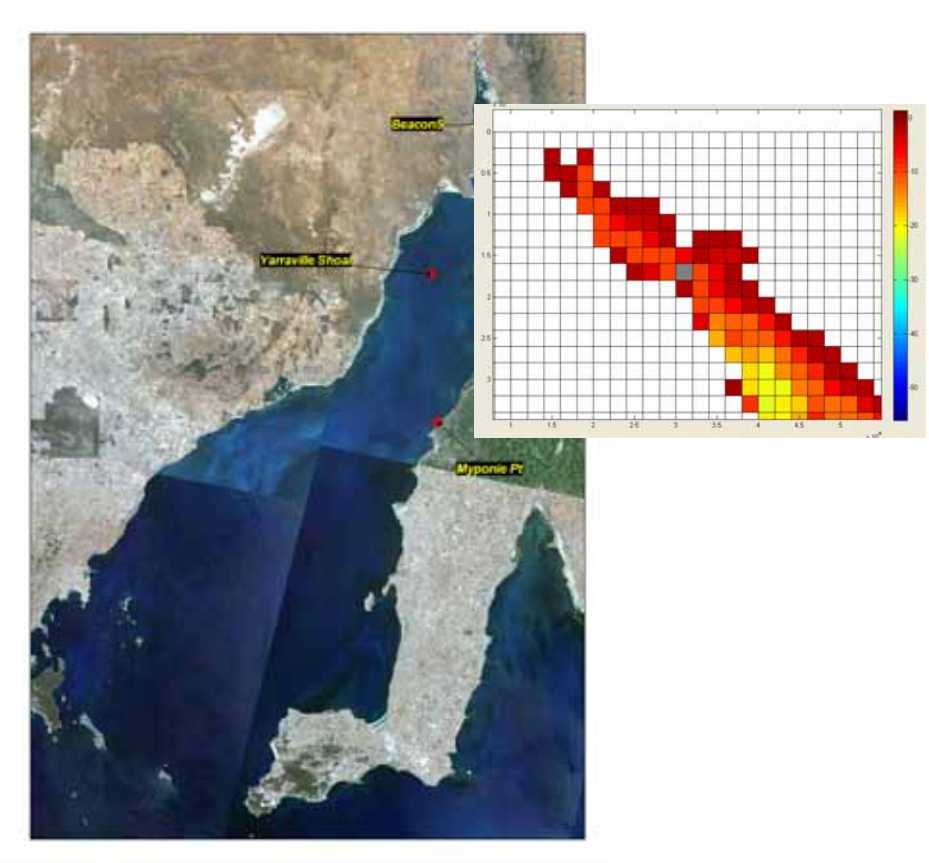

Figure 3 Field Data Locations

The model simulation and data collection periods do not temporally overlap, so a 'day of year' analysis was undertaken where data was plotted not against time, but against a day of year. This allowed collapse and comparison of the temporally divergent data sets, particularly with regards to their seasonality.

Data compared includes (where available, and for water column top and bottom signals):

- Tides
- Salinity
- Density
- Temperature

Some velocity magnitude and direction data was supplied for Beacon 5 however this has not been quality checked so is not presented here.

Comparisons are shown below. Blue and red are always measured and modelled data sets, respectively. It is noted that all red data points are not from a single year, but represent model predictions from three years overlain on the same 'day of year' axis. This approach has been taken to overcome the disparate time periods that the compared data sets cover – the model and measured data are not temporally coincident. By plotting all model data in this 'day of year' sense, the relationship between the measured and modelled data can be better estimated in terms of broad trends – the temporal bias associated with selecting a single model year to compare with the measured data is removed. One consequence of this approach, however, is that there is an apparently large variability in model predictions on a daily timescale (e.g. 2 g/L in salinity). This, however, is not the case: this variability is due to inter-annual salinity variations on a given 'day of year', rather than actual intra-day variations on a set date.

Beacon 5

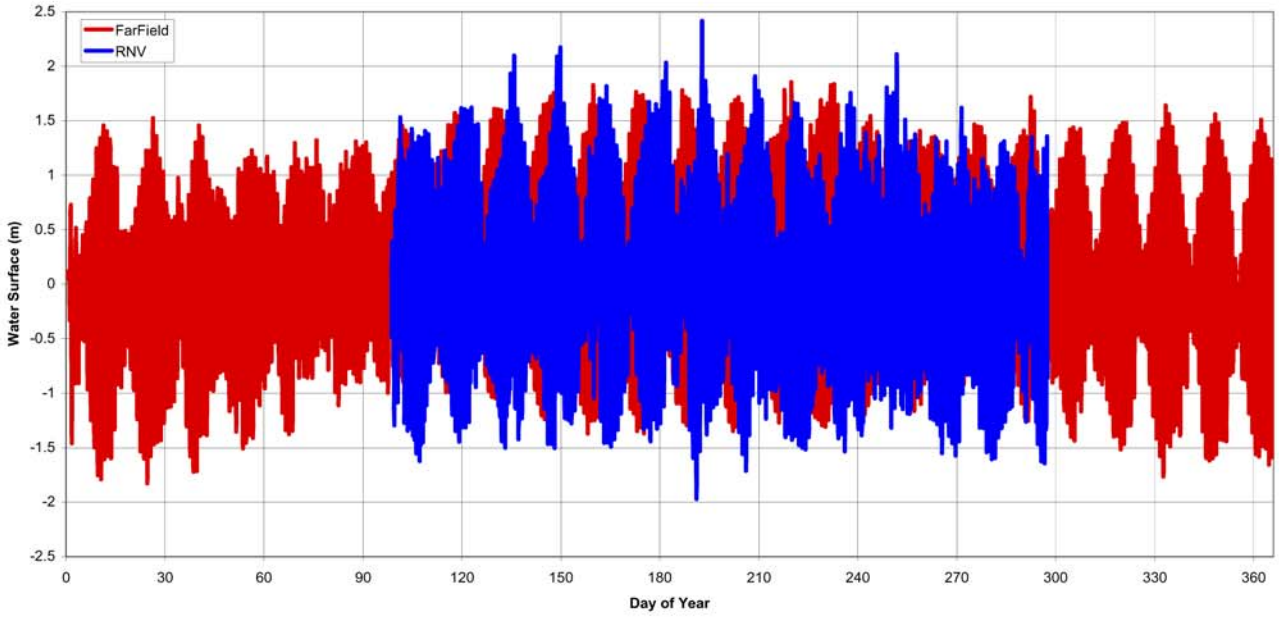

Figure 4 Water Surface Elevation

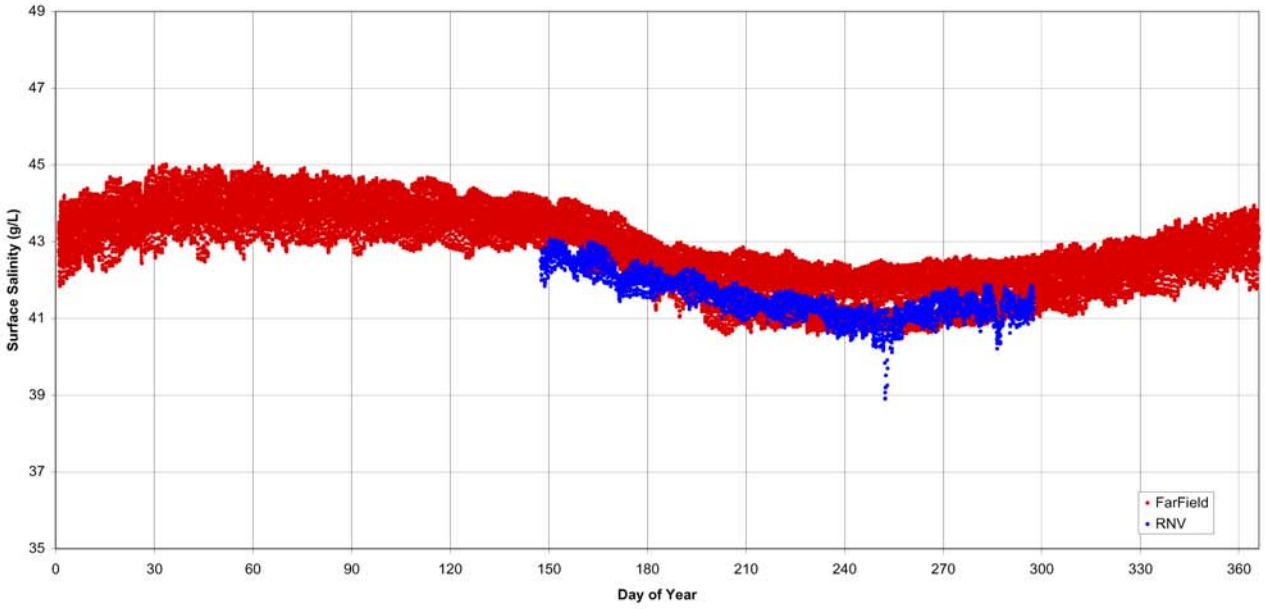

Figure 5 Surface Salinity

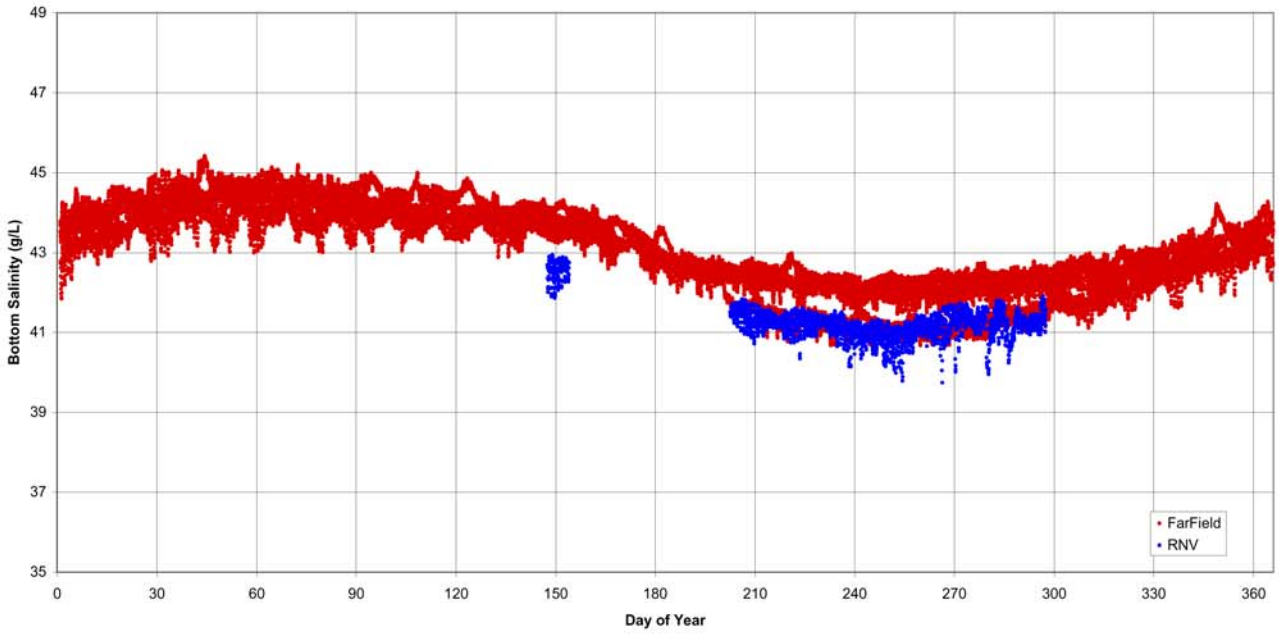

Figure 6 Bottom Salinity

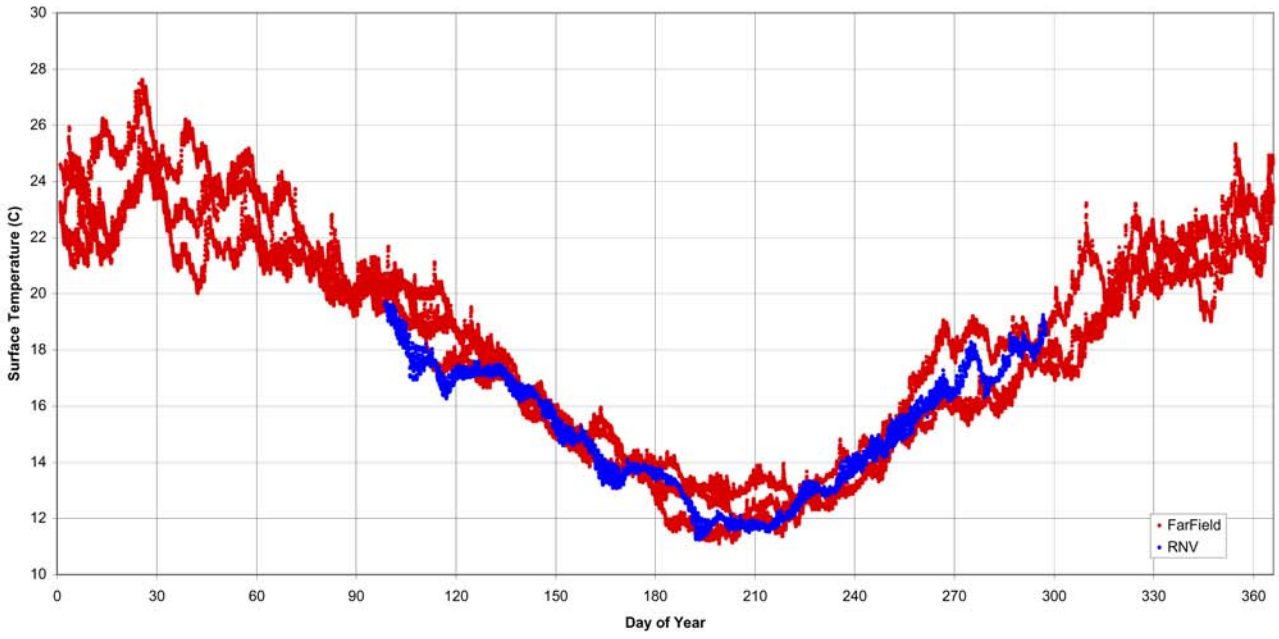

Figure 7 Surface Temperature

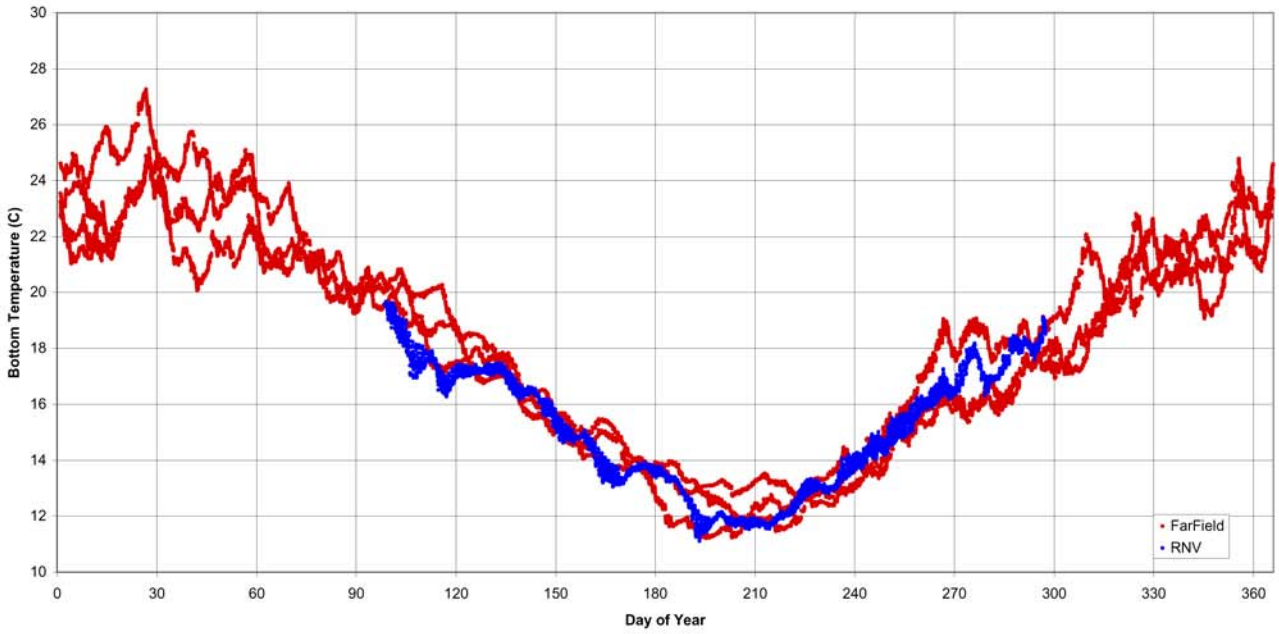

Figure 8 Bottom Temperature

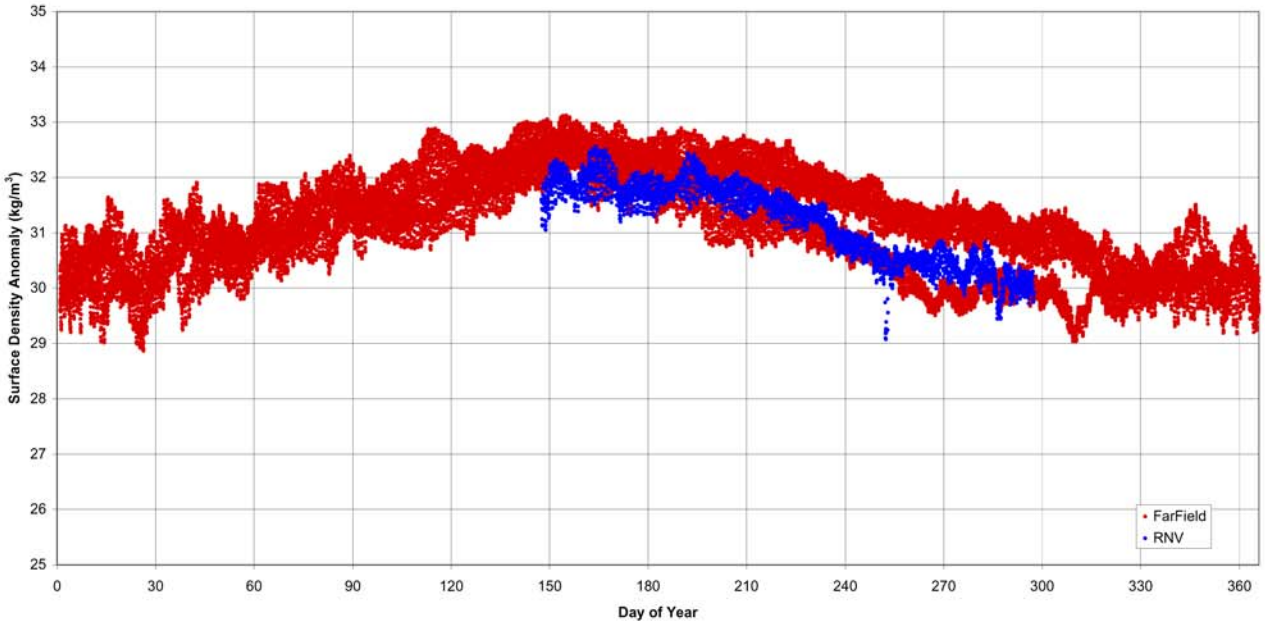

Figure 9 Surface Density

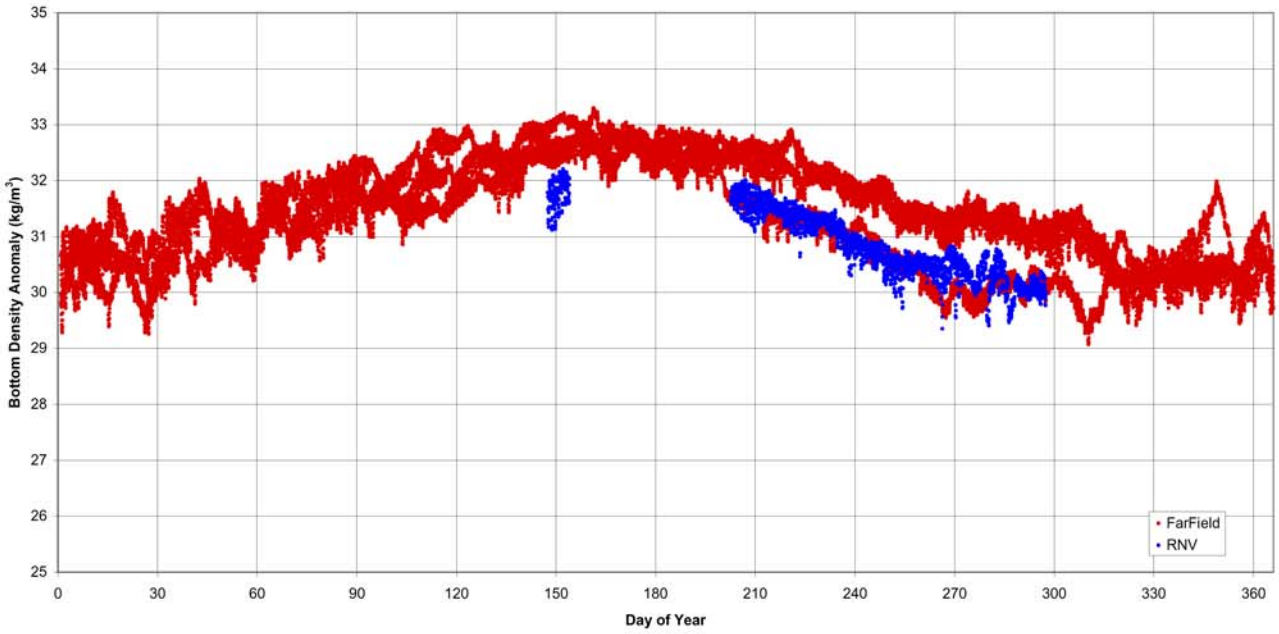

Figure 10 Bottom Density

The figures show that modelled and measured data sets are consistent.

Yarraville Shoal

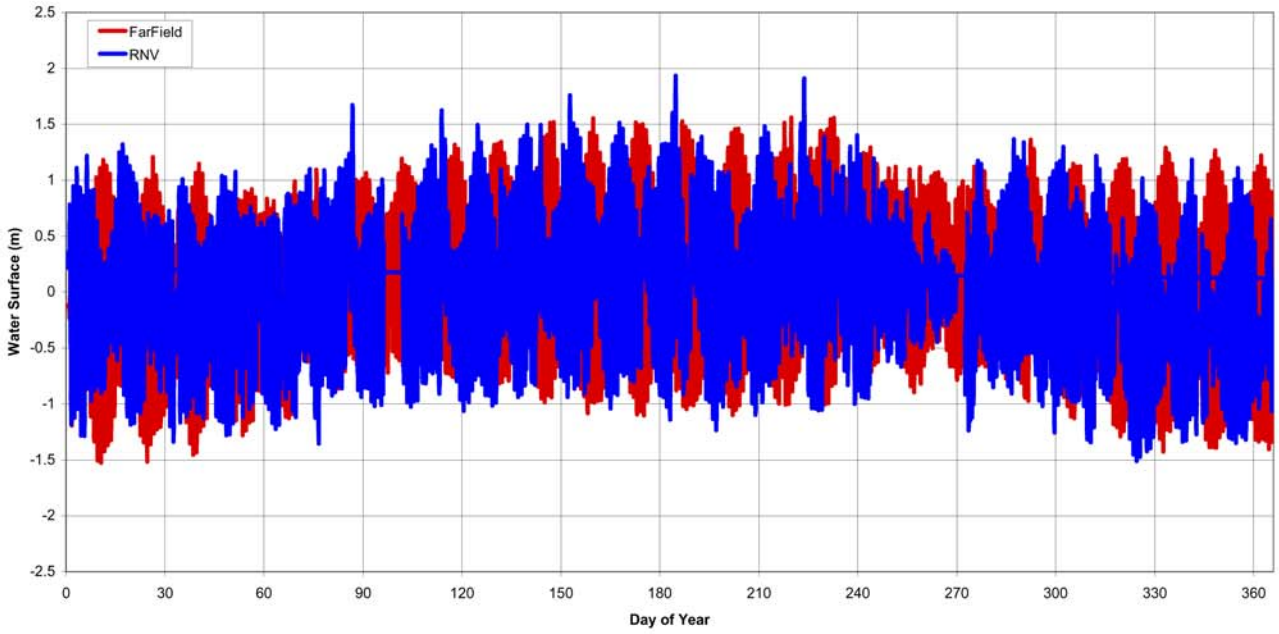

Figure 11 Water Surface Elevation

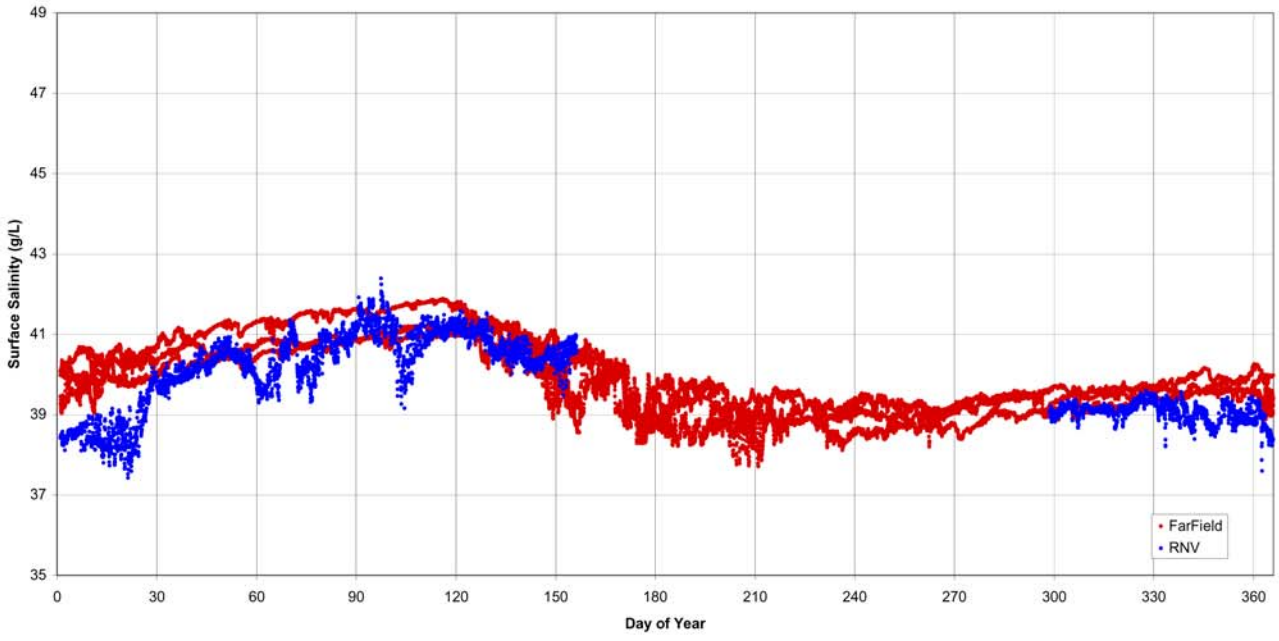

Figure 12 Surface Salinity

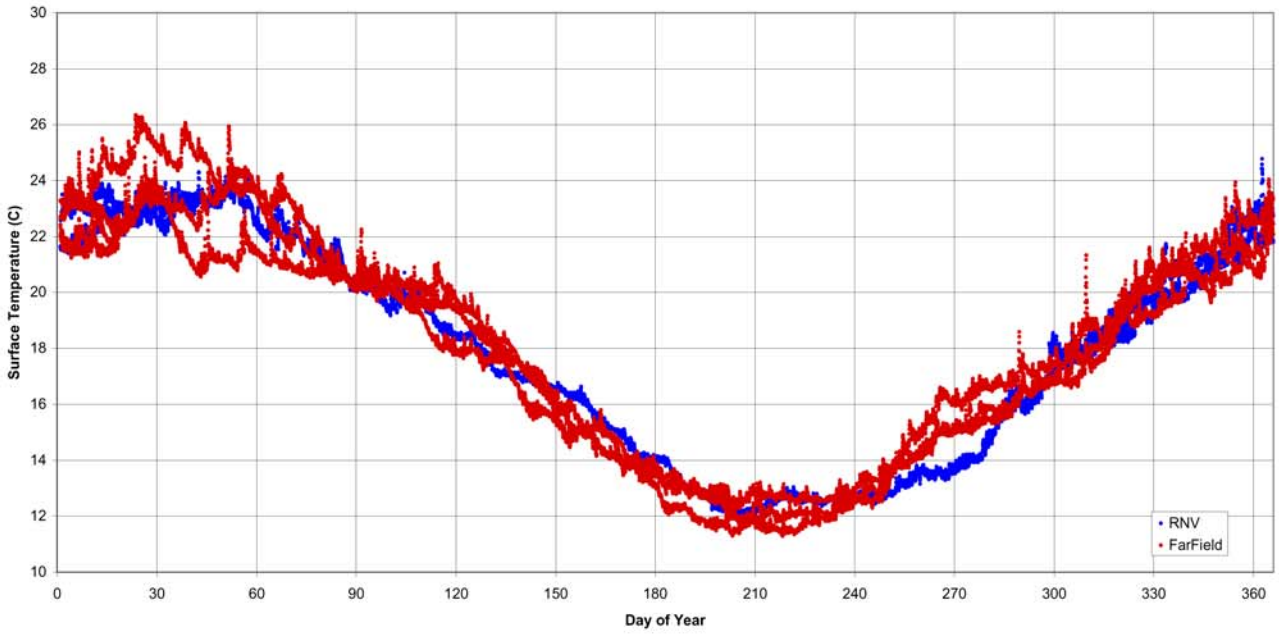

Figure 13 Surface Temperature

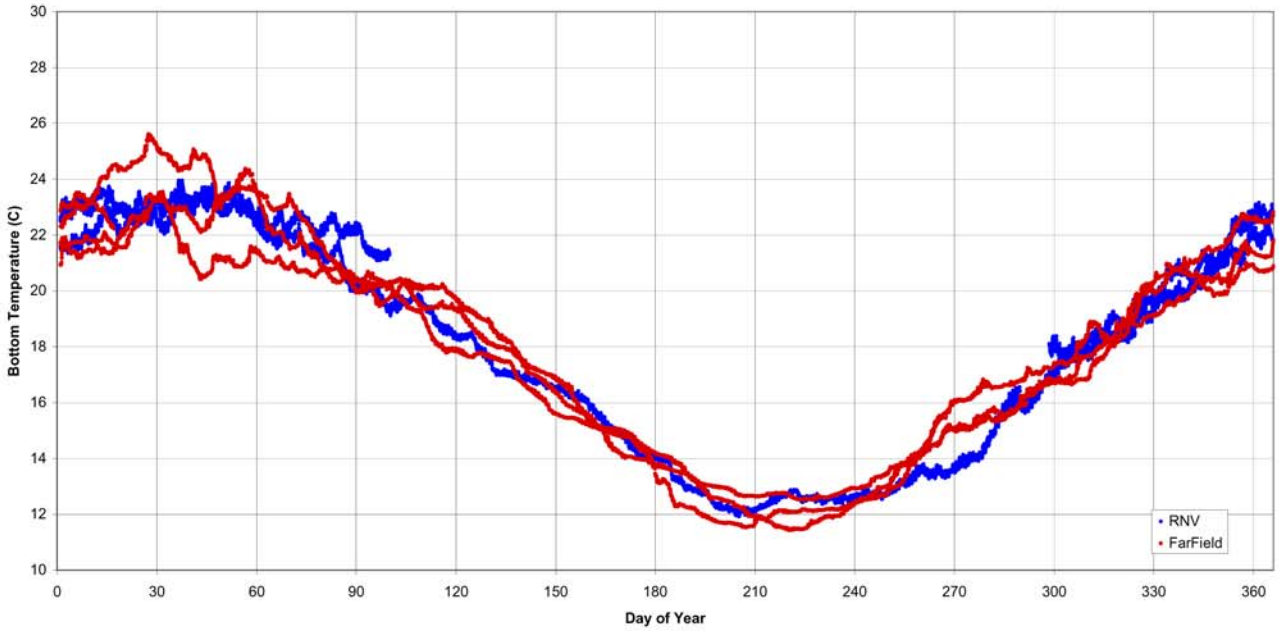

Figure 14 Bottom Temperature

The figures show that modelled and measured data sets are consistent.

Myponie

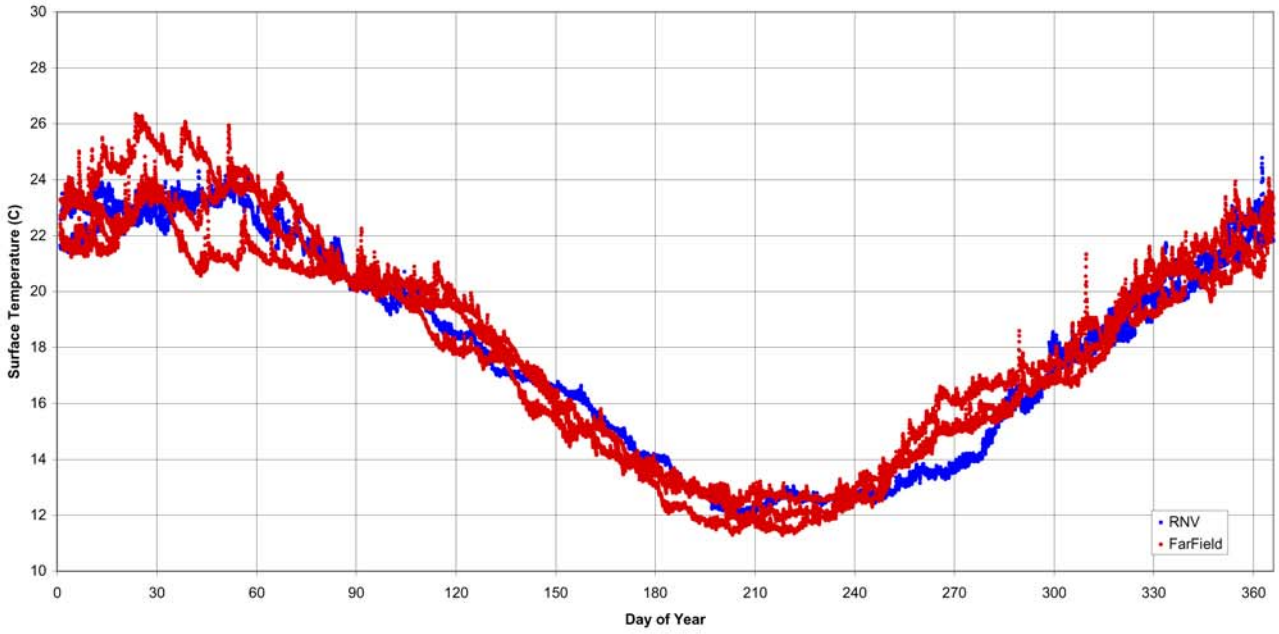

Figure 15 Mid Depth Temperature

The figures show that modelled and measured data sets are consistent.

Comparison Between Models

Hydrodynamic and physical water quality predictions of the mid and far field models were compared at three locations:

- Point Lowly
- Beacon 5
- Open water

The approximate location of the open water site is shown in Figure 16.

Figure 16 Open Water Site

Analysis included comparisons of:

- Water surface elevation
- Temperature
- Salinity
- Surface velocity magnitude
- Surface velocity direction

Results follow. Red and blue are always far and mid field model predictions, respectively.

Point Lowly

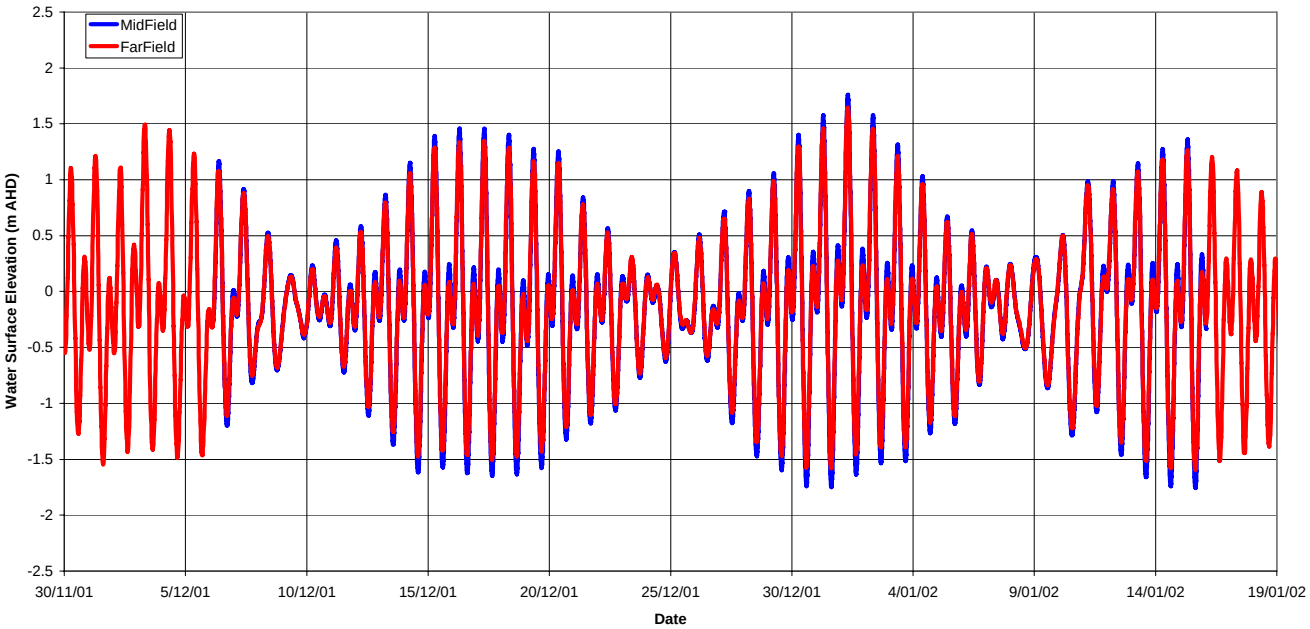

Figure 17 Water Surface Elevation – Point Lowly

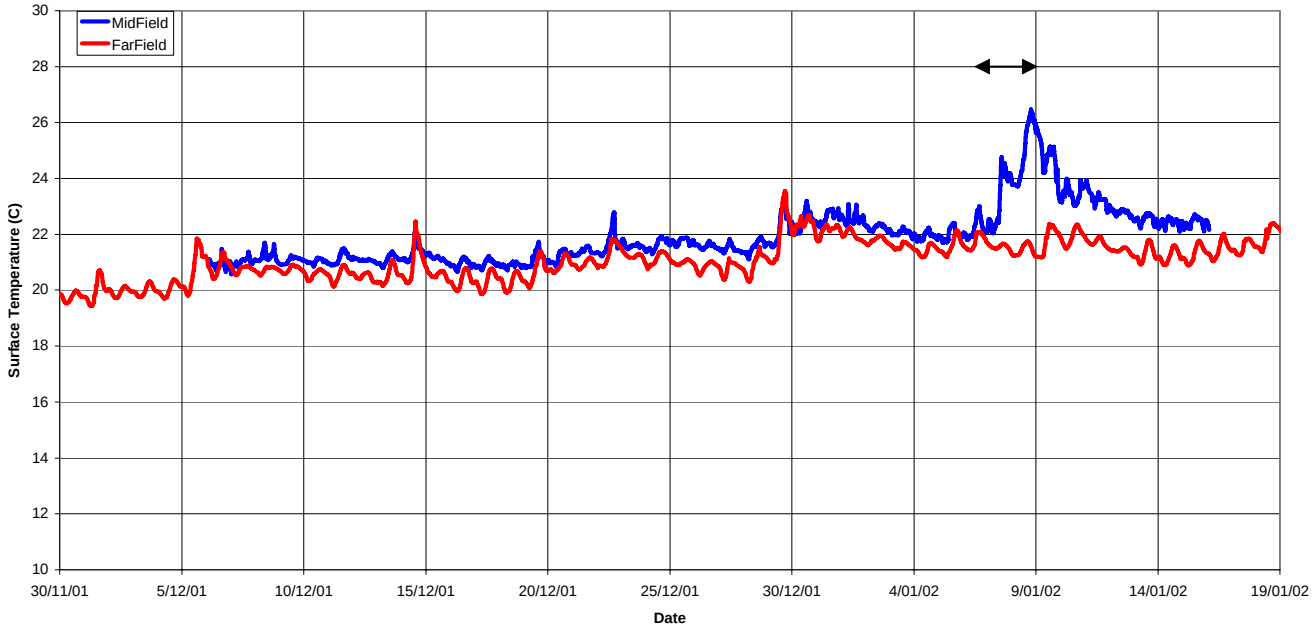

Figure 18 Surface Temperature – Point Lowly. The arrows mark approximate period for which mid field simulation was forced with no wind.

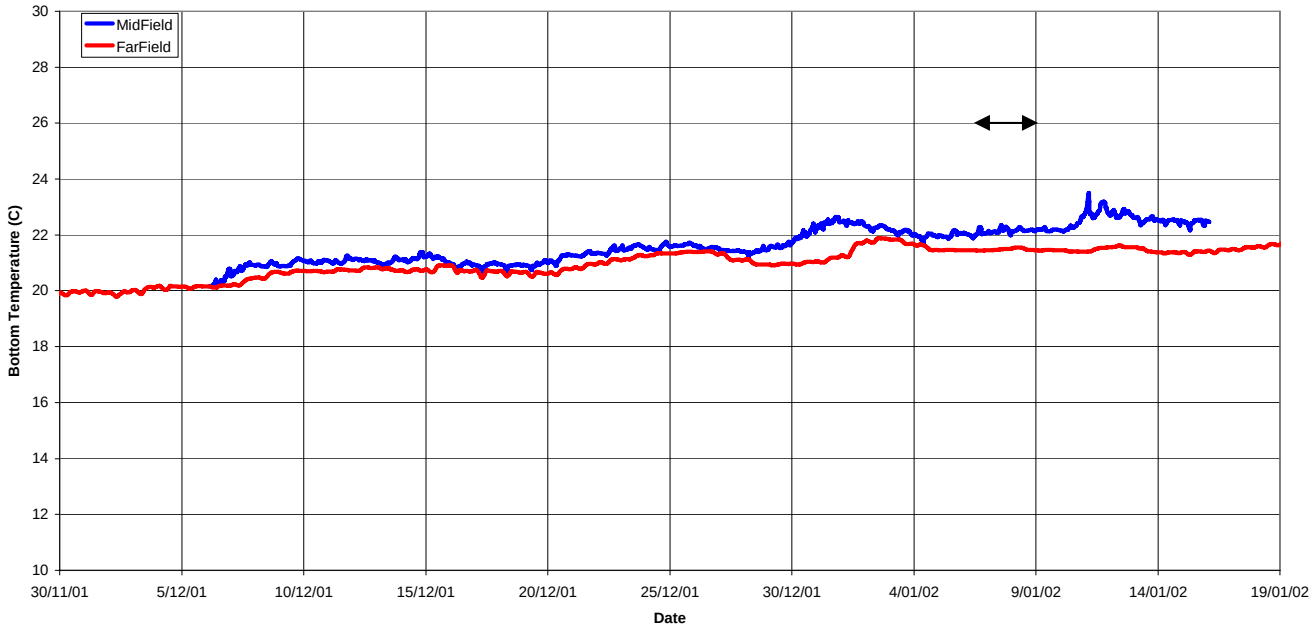

Figure 19 Bottom Temperature – Point Lowly. The arrows mark approximate period for which mid field simulation was forced with no wind.

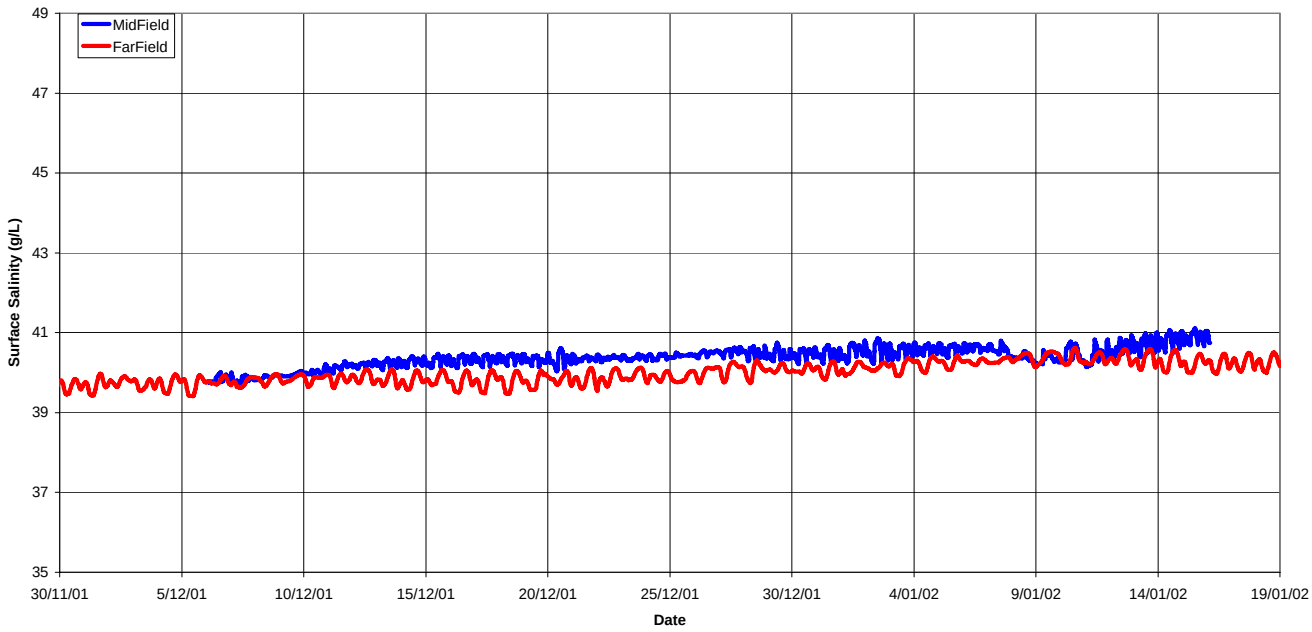

Figure 20 Surface Salinity – Point Lowly

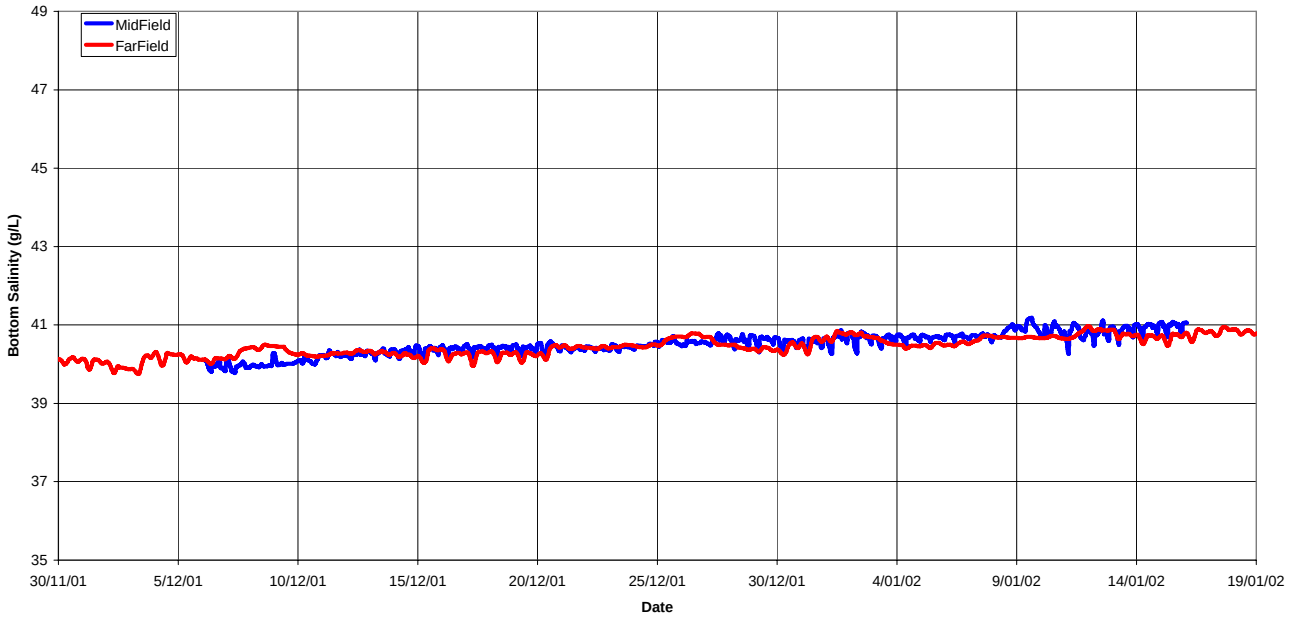

Figure 21 Bottom Salinity – Point Lowly

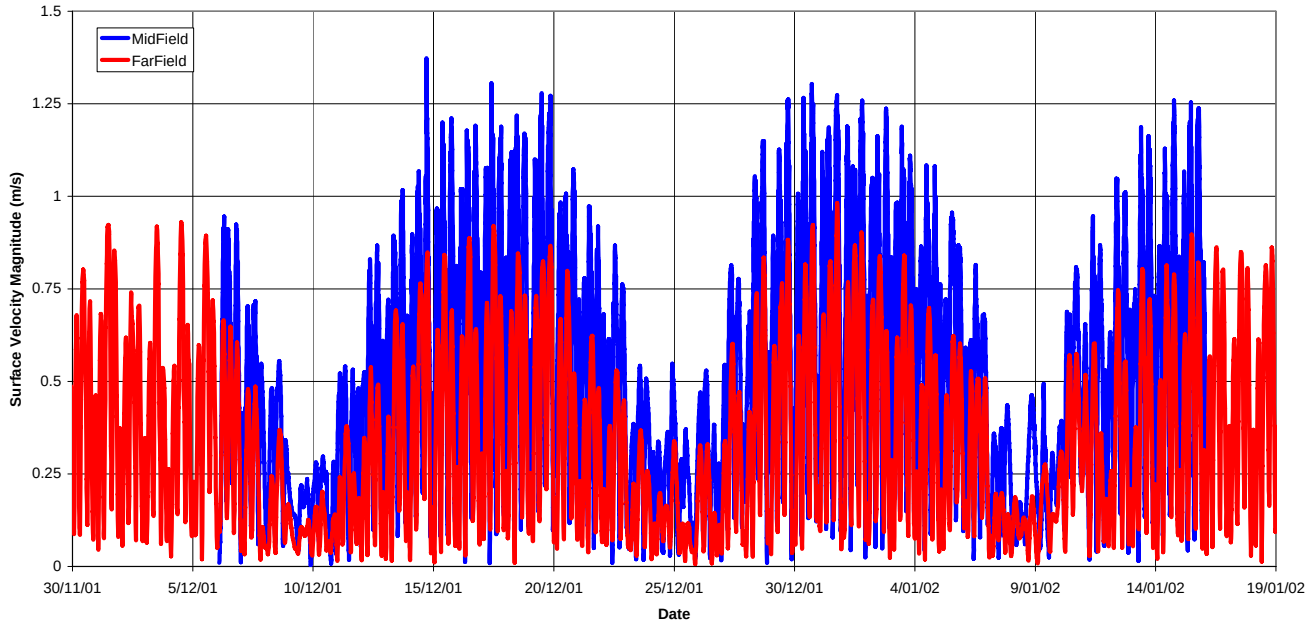

Figure 22 Surface Velocity Magnitude – Point Lowly

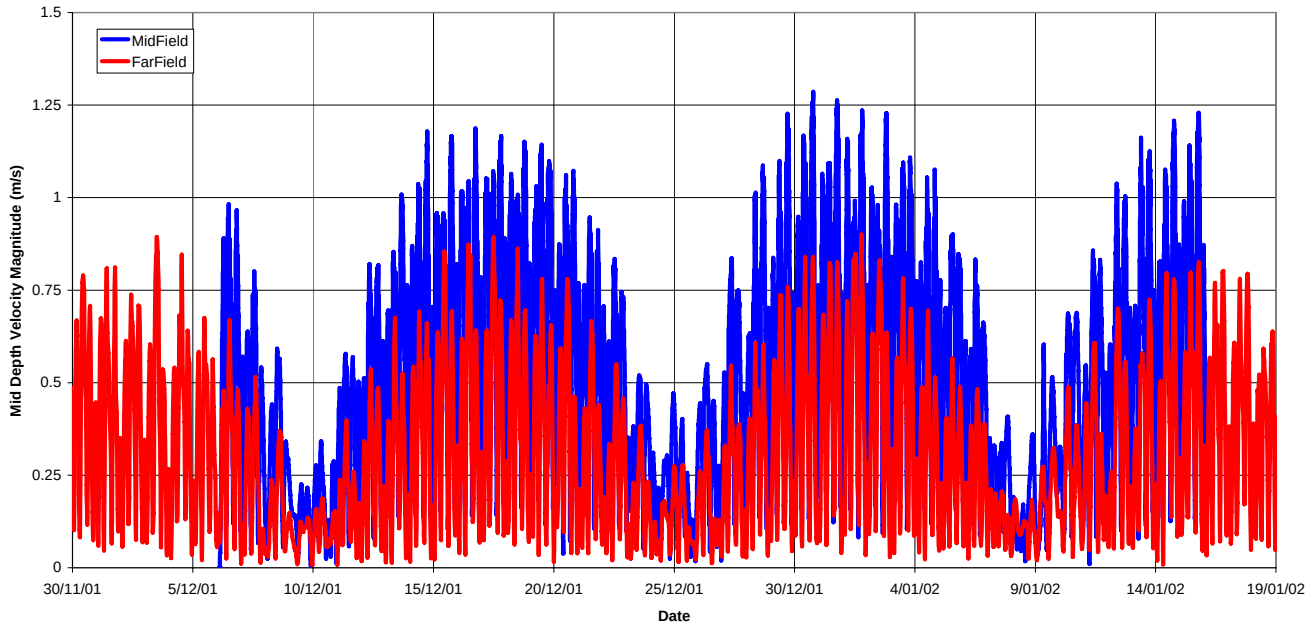

Figure 23 Bottom Velocity Magnitude – Point Lowly

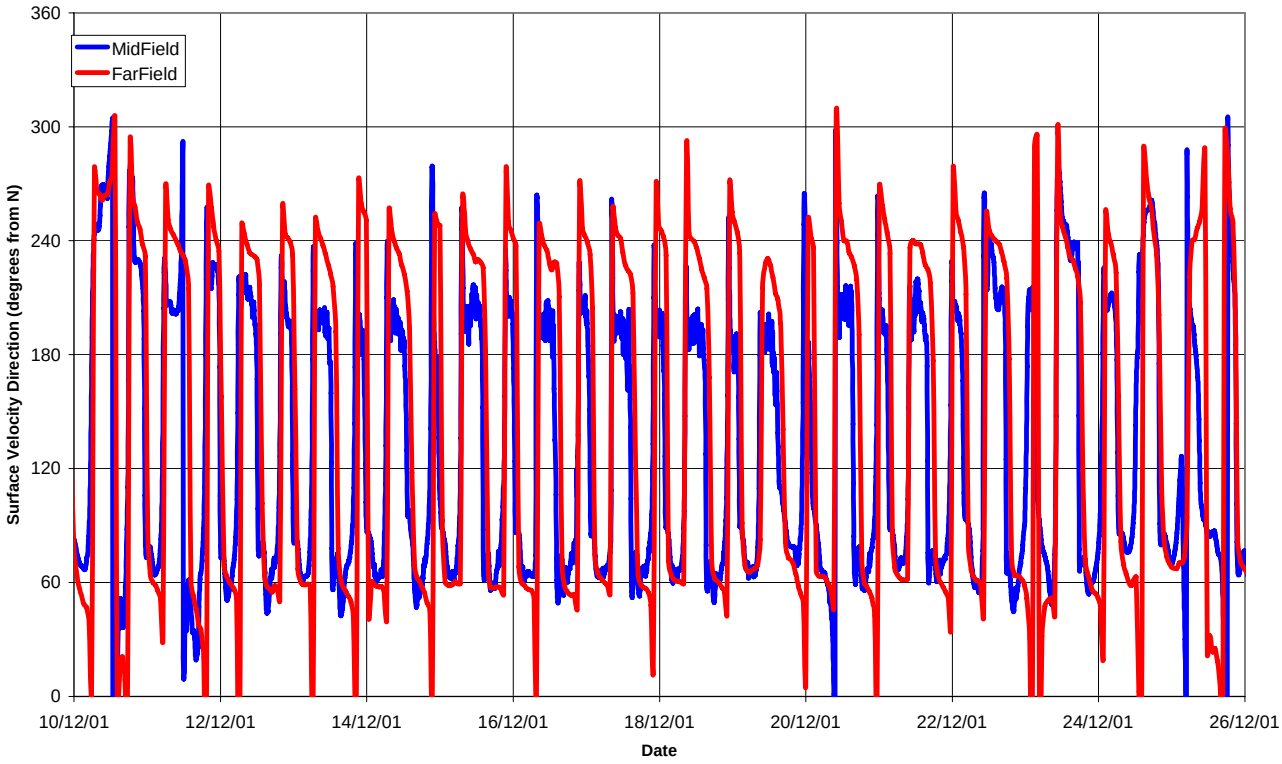

Figure 24 Surface Velocity Direction – Point Lowly

Figure 25 shows these directions schematically. The yellow arrow heading at approximately 60 degrees represents both mid and far field predictions for flooding tide directions. The light and dark blue arrows represent the mid and far field ebbing tidal direction predictions, respectively.

Figure 25 Surface Velocity Direction – Point Lowly

Other than the velocity magnitudes, the models compare well. It is noted that the temperature spike in the surface mid field results is due to the forced absence of wind during dodge tides, which was agreed during simulation scoping.

The primary reason for the divergence of the velocity magnitude predictions at Point Lowly is the presence of large lateral gradients of tidal velocity in the area. Specifically, large tidal velocities exist

near the point, and rapidly reduce away from it. These gradients are resolved by the mid field model so that it captures the highest velocities around Point Lowly, however the coarser 2km grid of the far field model 'smears' these high (localised) velocities over a larger grid cell and as such predicts lower tidal currents. The same applies to the directions – the mid field model can resolve relatively rapid direction changes around the point, whereas the far field model is less suited to doing so.

Beacon 5

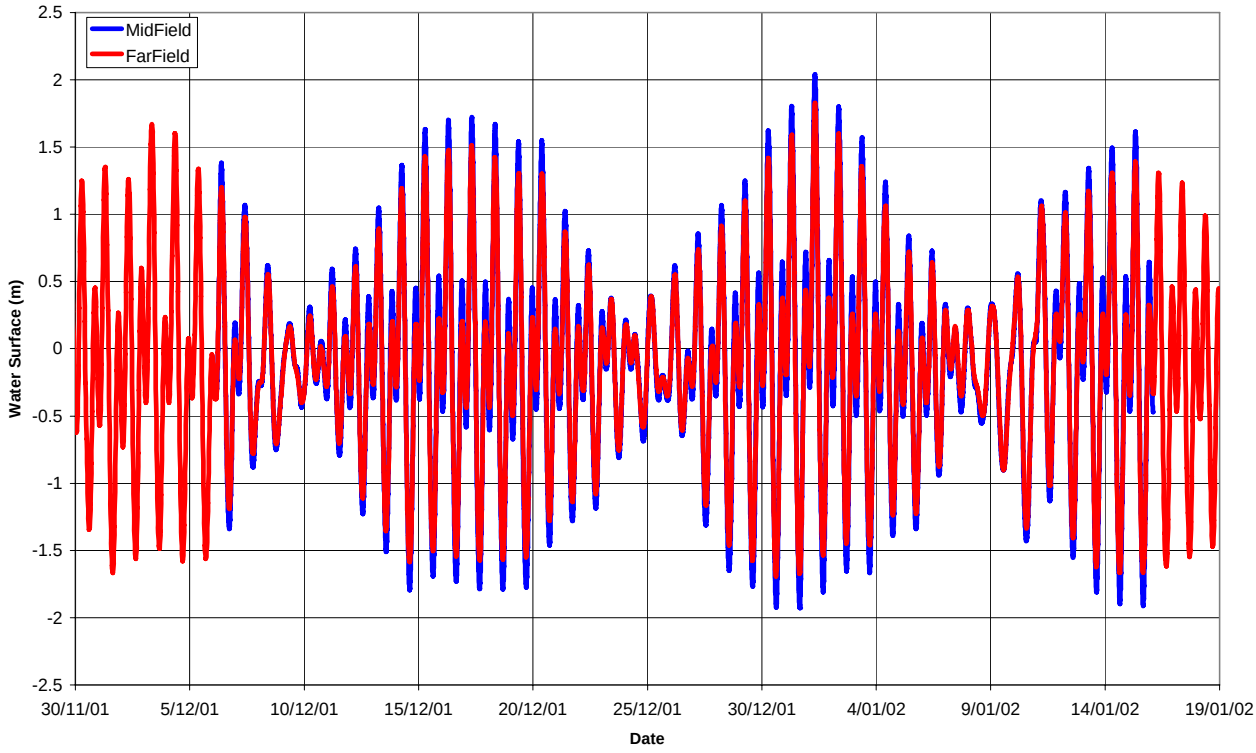

Figure 26 Water Surface Elevation – Beacon 5

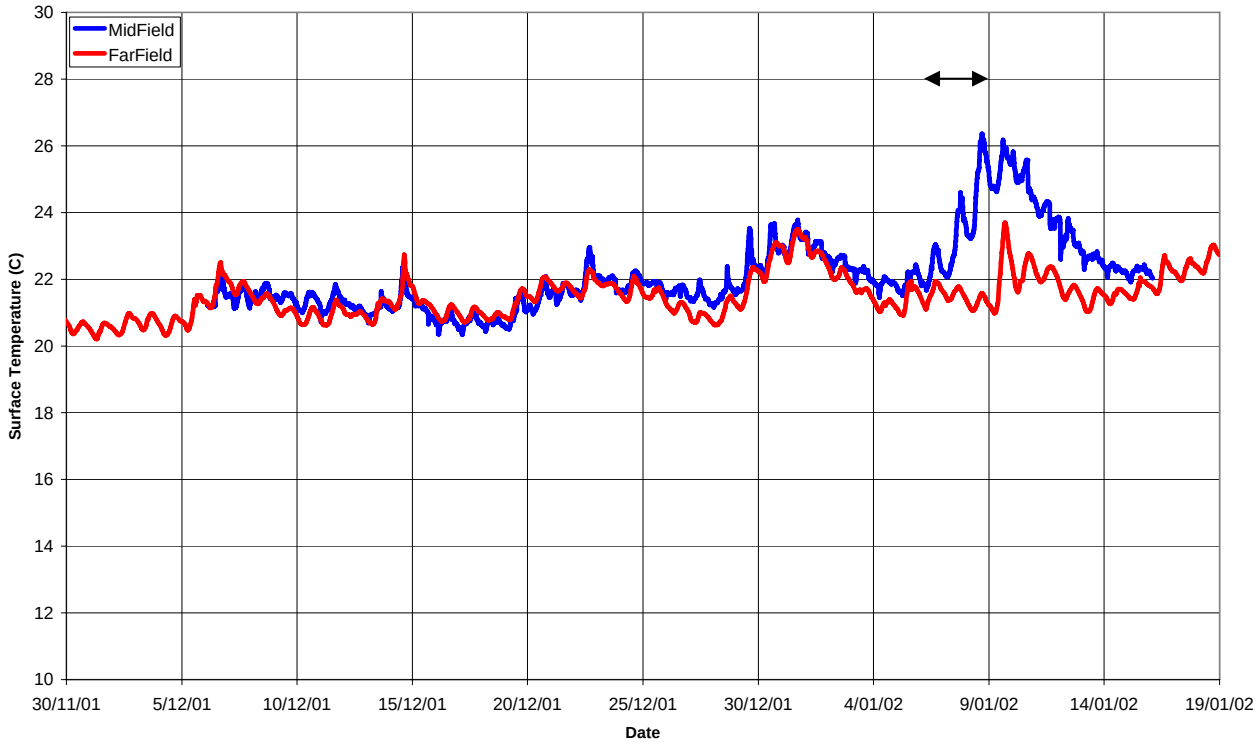

Figure 27 Surface Temperature – Beacon 5. The arrows mark approximate period for which mid field simulation was forced with no wind.

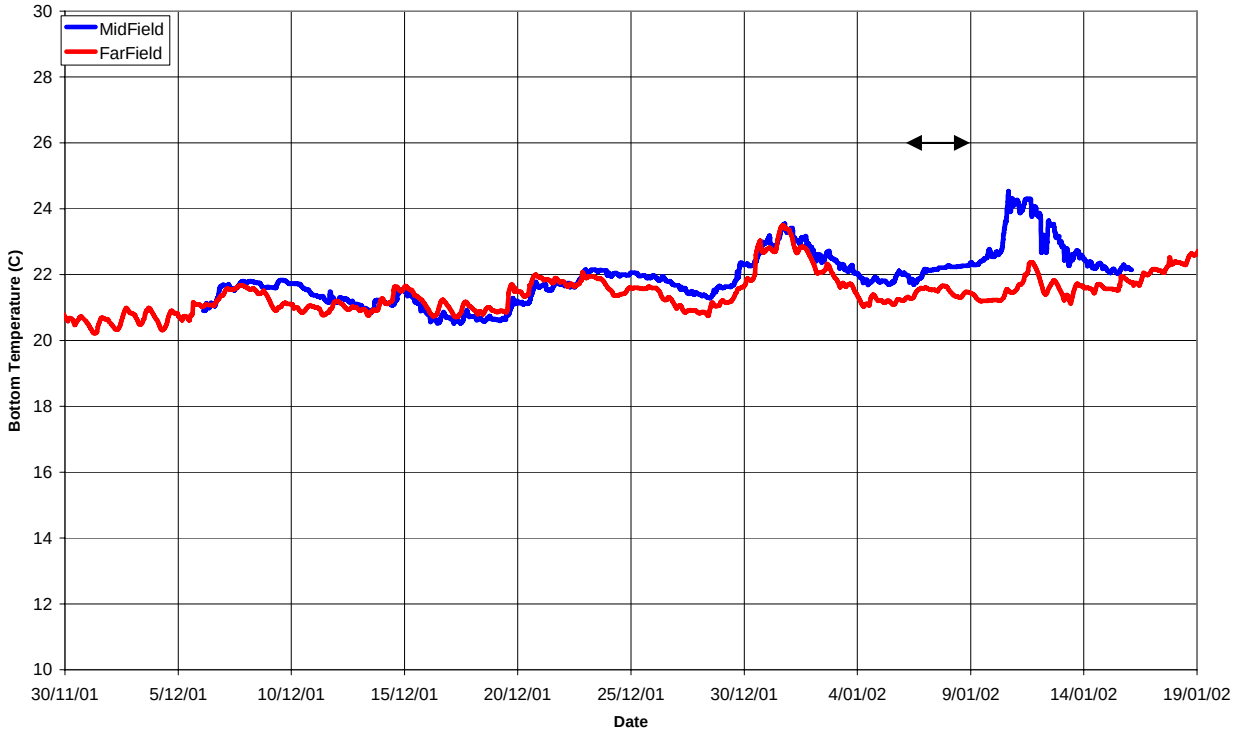

Figure 28 Bottom Temperature – Beacon 5. The arrows mark approximate period for which mid field simulation was forced with no wind.

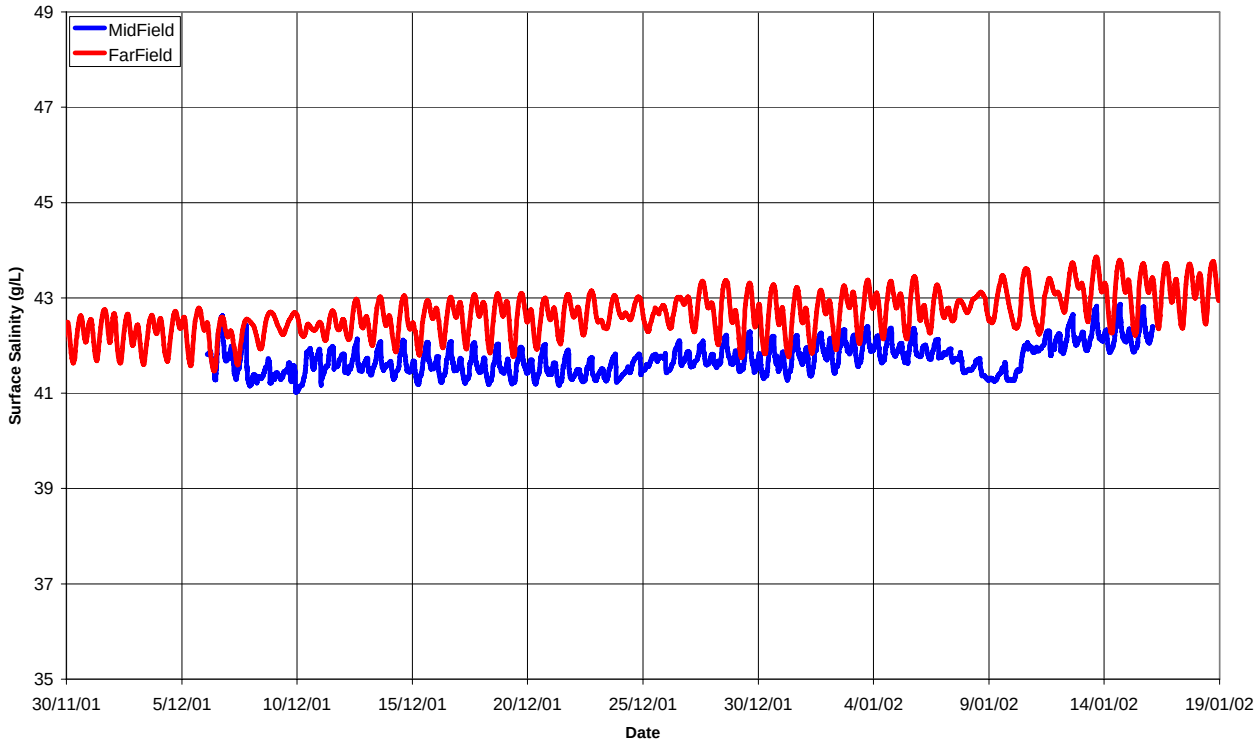

Figure 29 Surface Salinity – Beacon 5

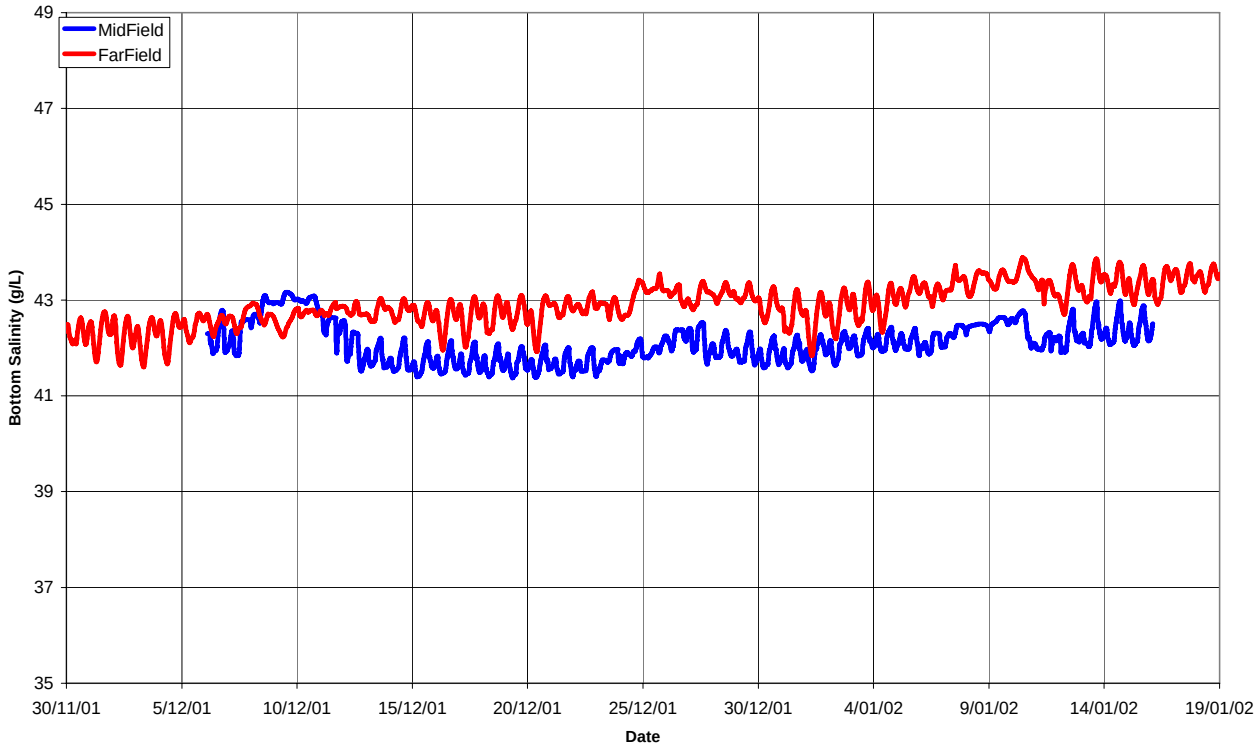

Figure 30 Bottom Salinity – Beacon 5

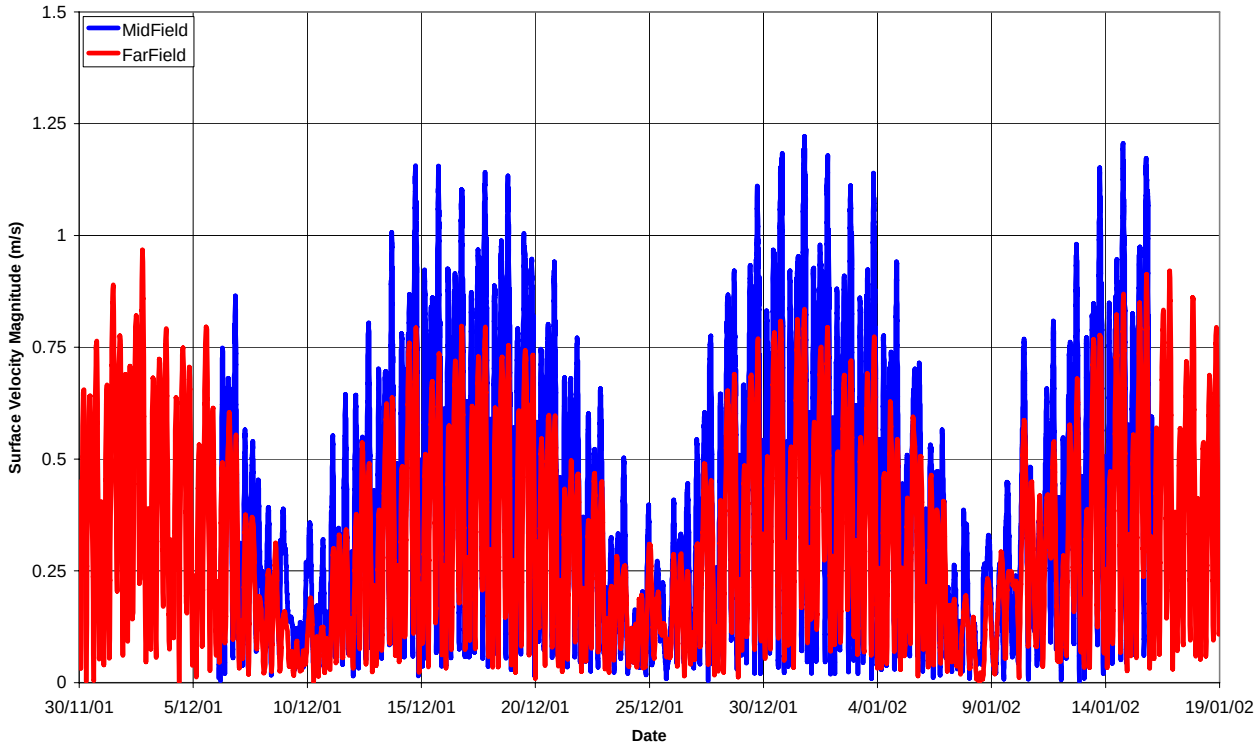

Figure 31 Mid Depth Velocity Magnitude – Beacon 5

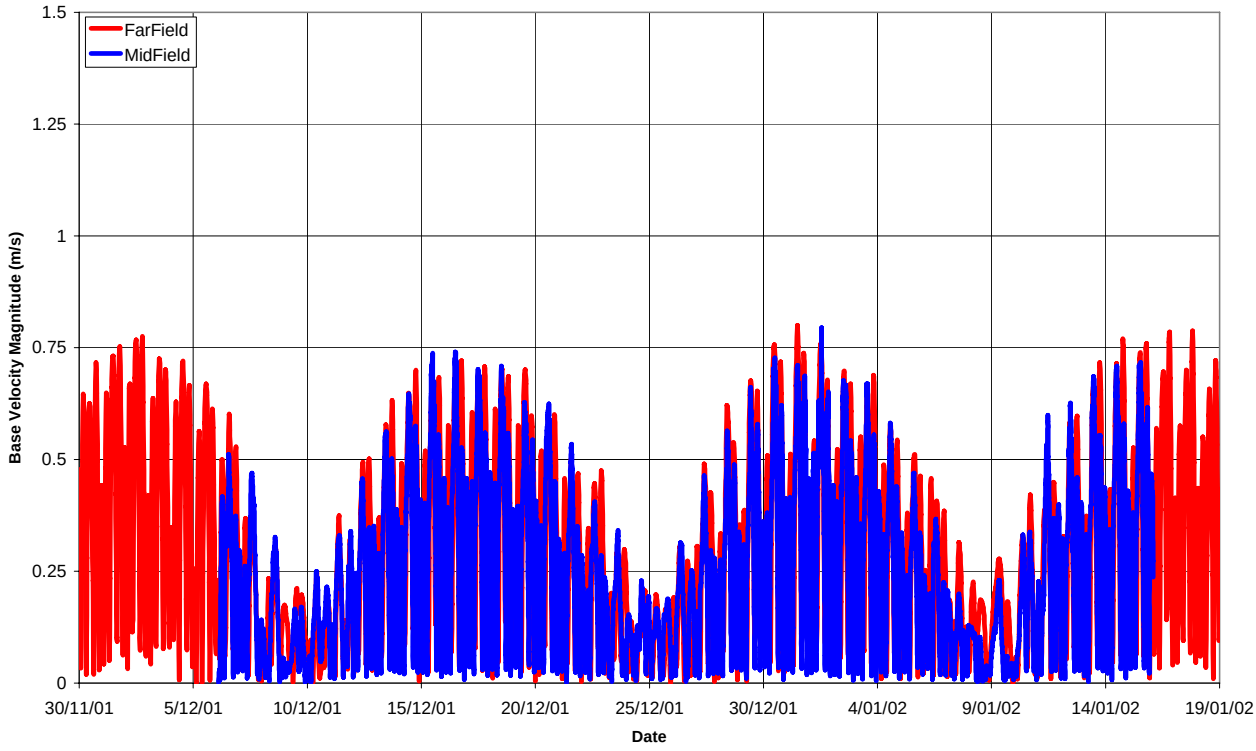

Figure 32 Bottom Velocity Magnitude – Beacon 5

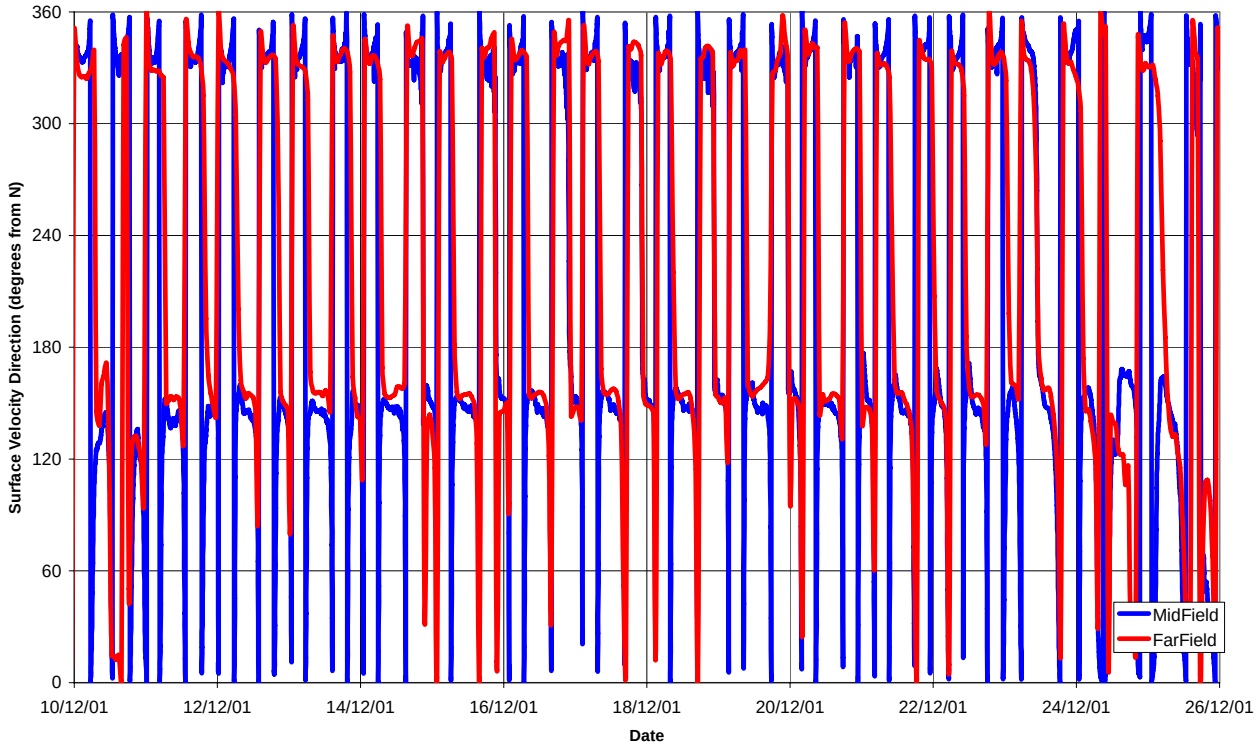

Figure 33 Surface Velocity Direction – Beacon 5

Figure 34 shows these directions schematically.

Figure 34 Surface Velocity Direction – Beacon 5

Other than the mid depth velocity magnitudes, the models compare well, with the greatest divergence being between salinity predictions, but with this being generally less than 1 g/L. It is again noted that the temperature spike in the surface mid field results is due to the forced absence of wind during dodge tides, which was agreed during simulation scoping.

The velocity predictions in the far field model at Beacon 5 are strongly influenced by the coarse grid. Specifically, it is noted that the complex bathymetry of the area is only captured via three computational cells across the width of the channel. As a result, it is expected that numerical artefacts will play a role in simulating velocities in this area, and most likely result in accentuated numerical drag, i.e. slowing of water flow due to the coarseness of model discretisation. Conversely, this effect appears to play a smaller role when bottom drag (bed effects) dominates, given the satisfactory agreement between the bottom velocity magnitudes. The velocity directions are in excellent agreement.

Open Water Site

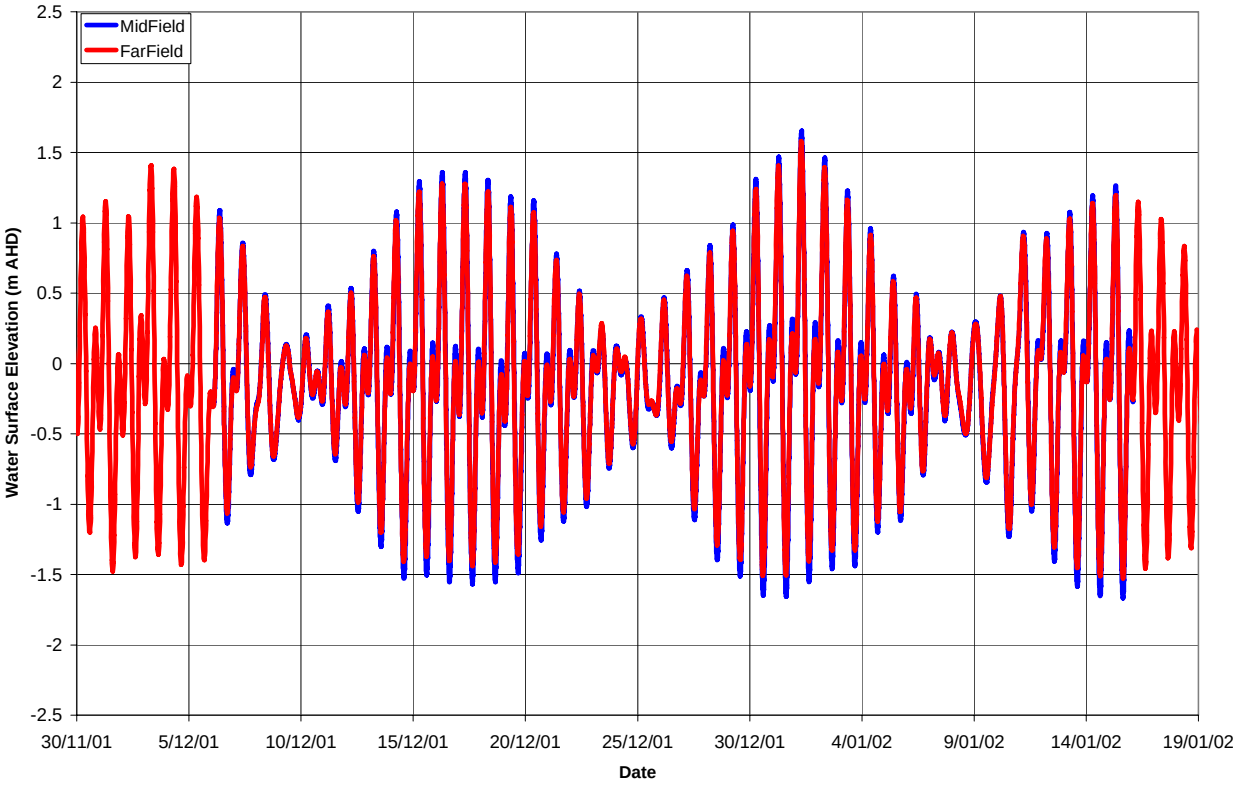

Figure 35 Greater Surface Elevation – Open Water

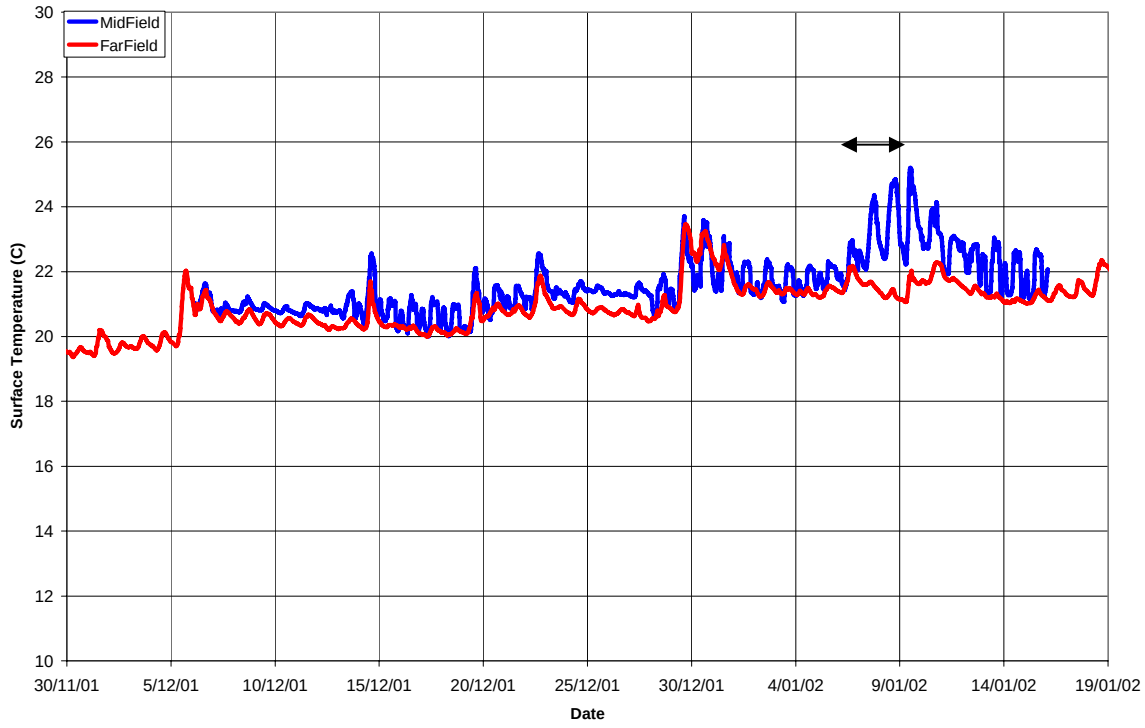

Figure 36 Surface Temperature – Open Water. The arrows mark approximate period for which mid field simulation was forced with no wind.

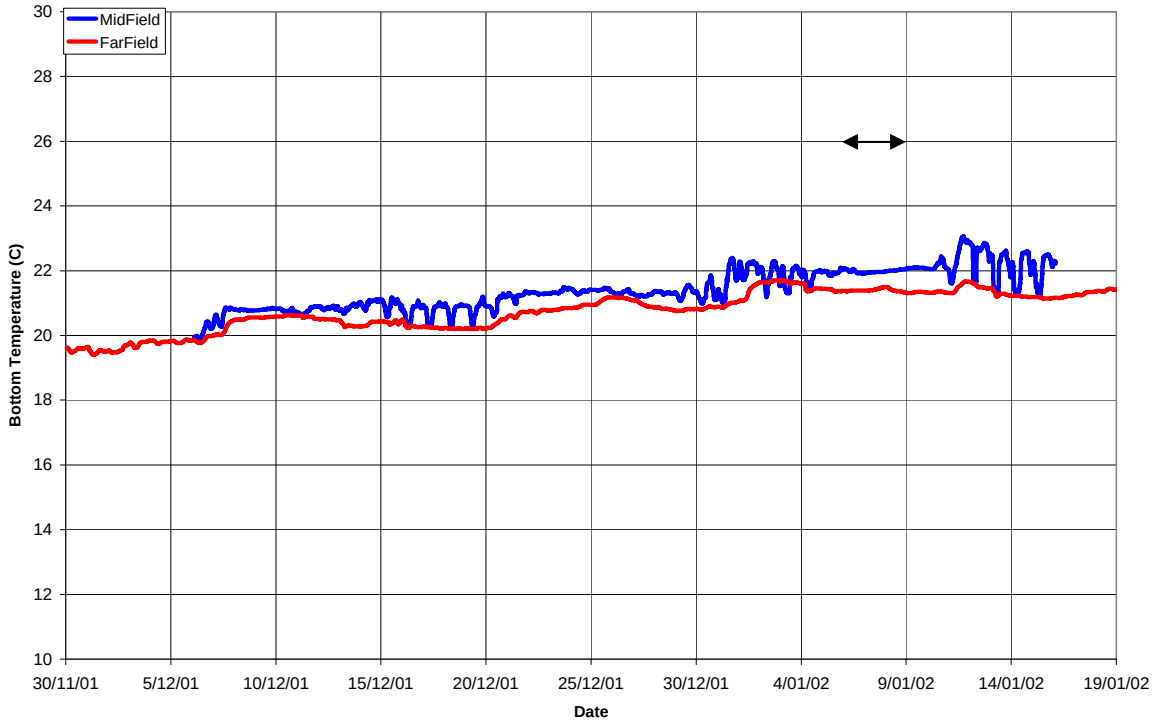

Figure 37 Bottom Temperature – Open Water. The arrows mark approximate period for which mid field simulation was forced with no wind.

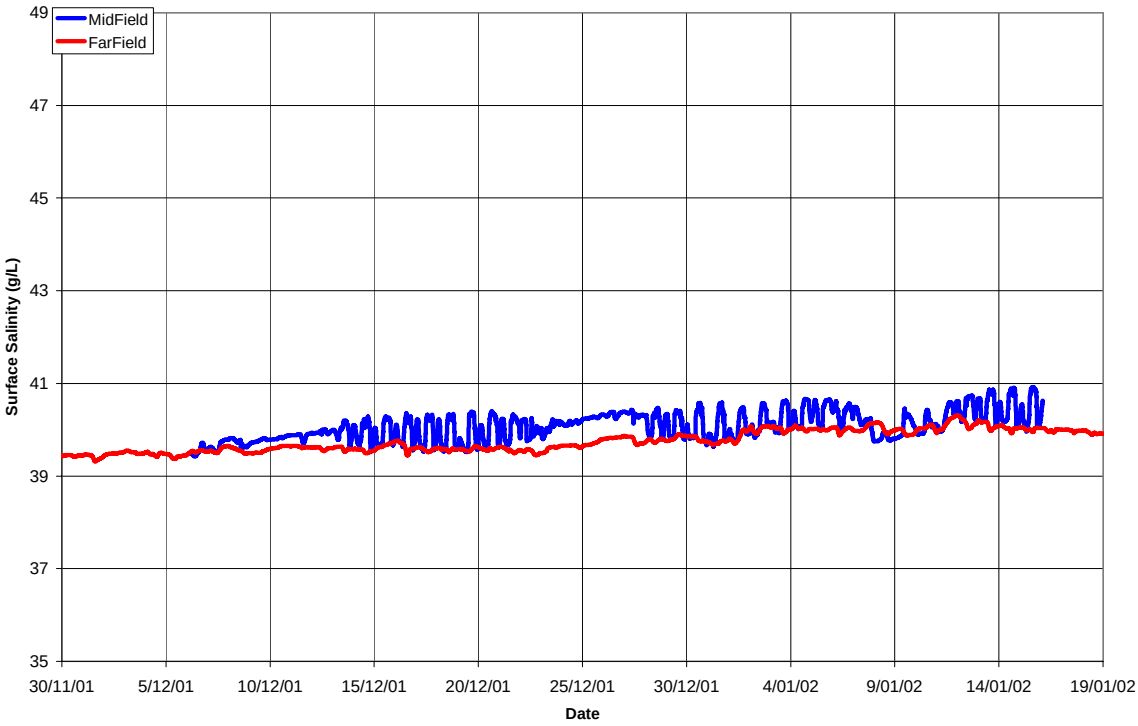

Figure 38 Surface Salinity – Open Water

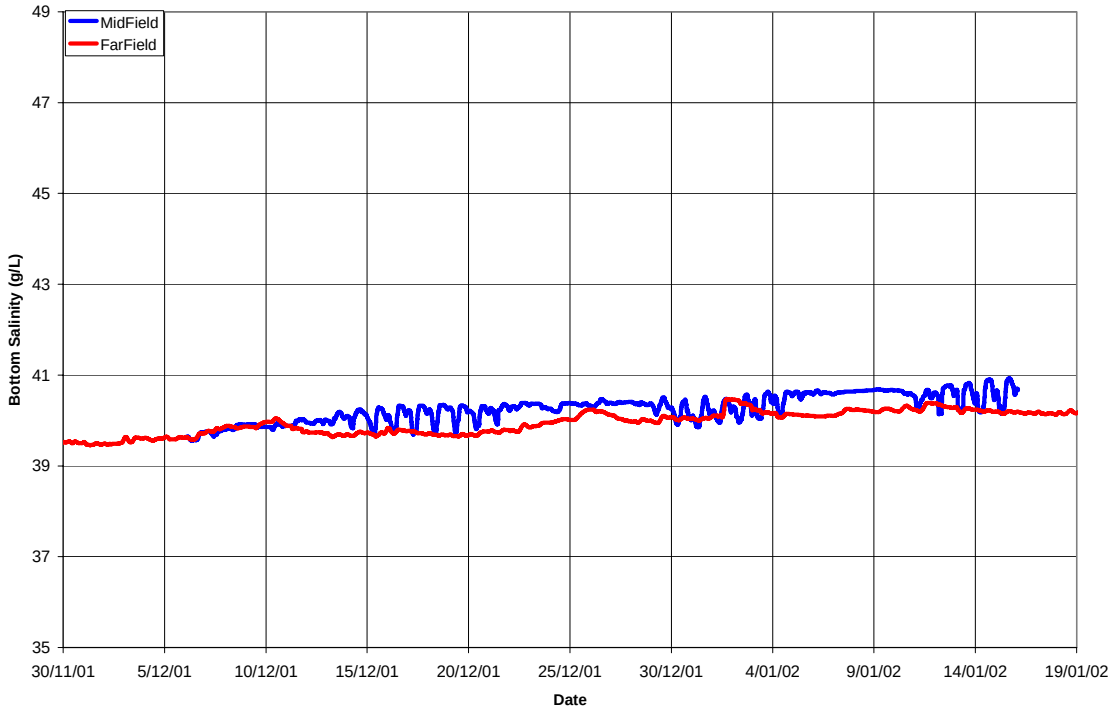

Figure 39 Bottom Salinity – Open Water

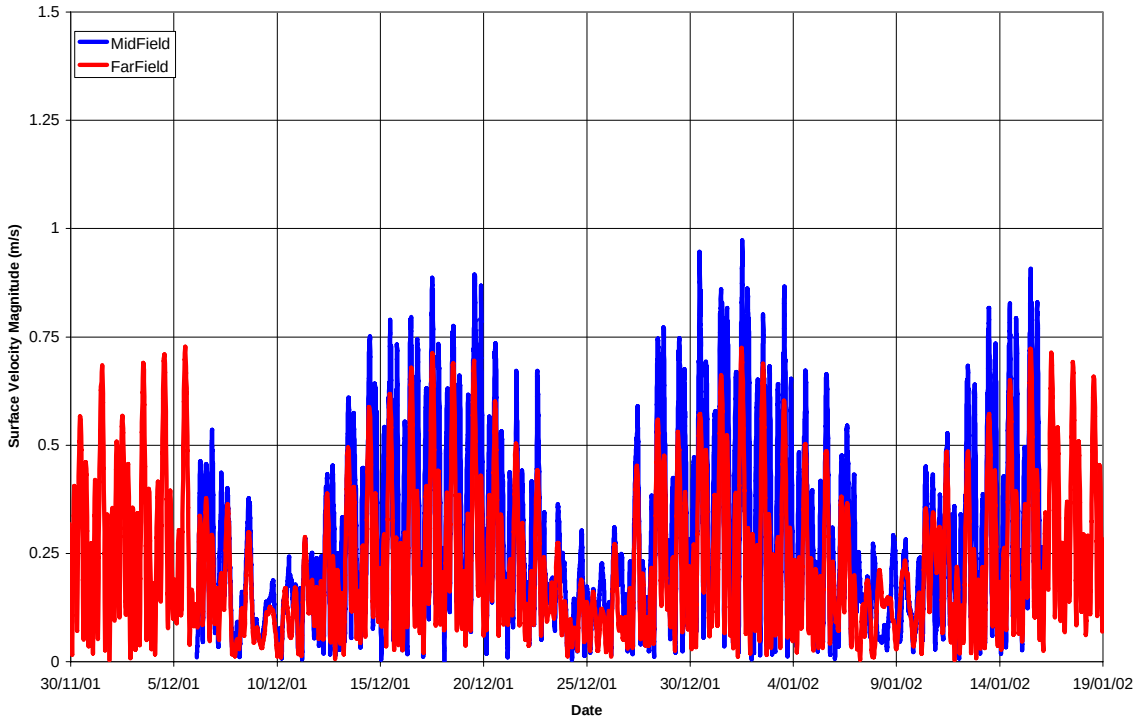

Figure 40 Surface Velocity Magnitude – Open Water

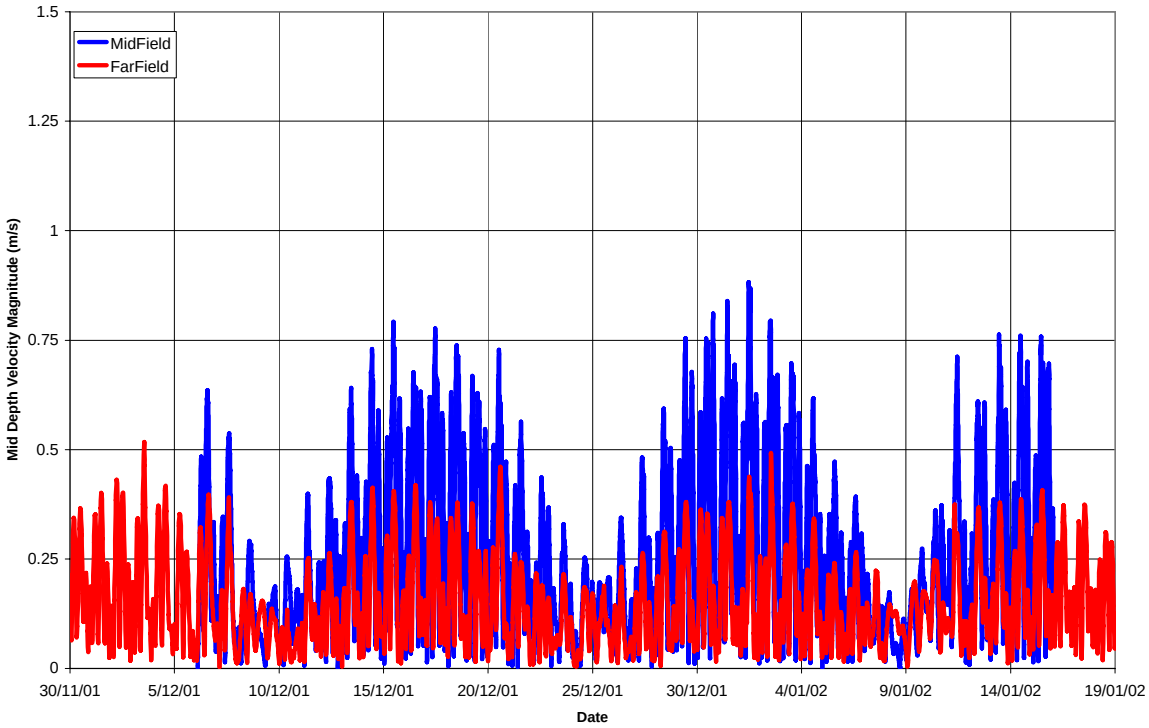

Figure 41 Mid Depth Velocity Magnitude – Open Water

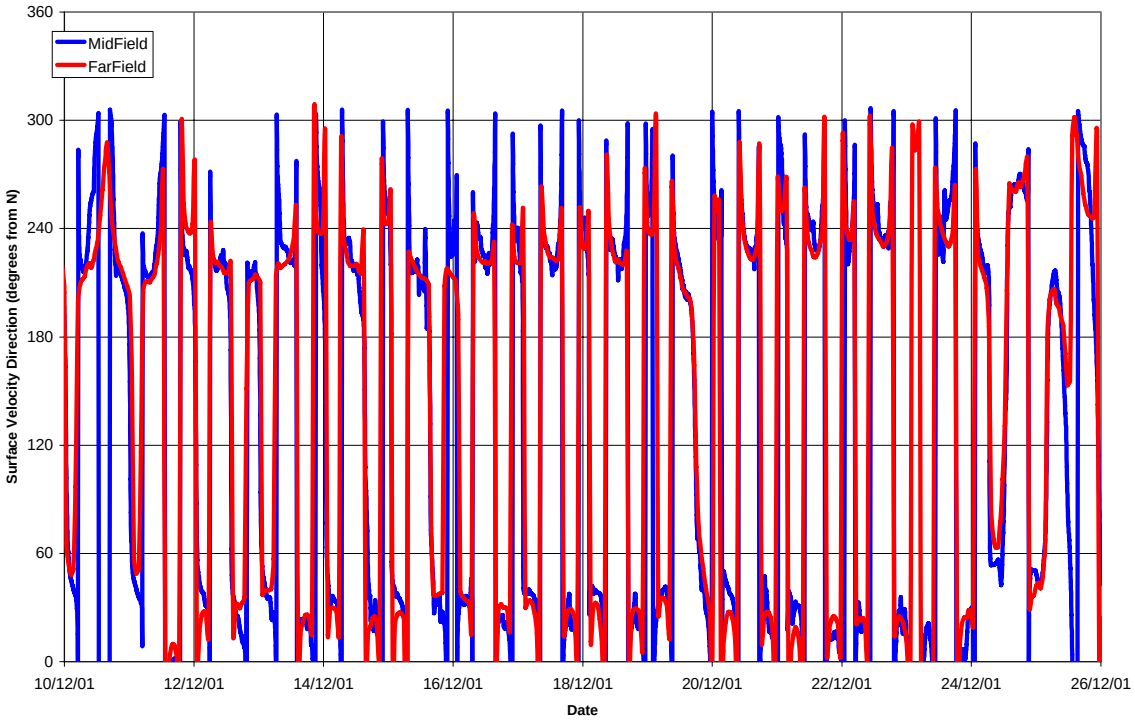

Figure 42 Surface Velocity Direction – Open Water

Figure 43 shows these directions schematically.

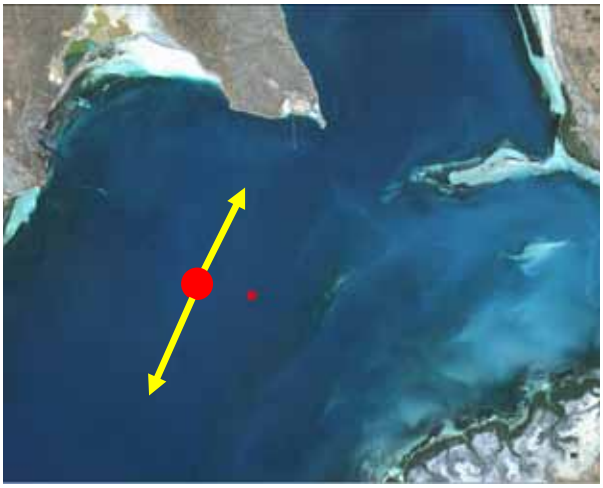

Figure 43 Surface Velocity Direction – Open Water

Again, other than the mid depth velocity magnitudes, the models compare well. Discussion has previously been provided on potential causes of this discrepancy. Another such cause may be potential differences in tidal storage volumes between the models, with the mid field model better resolving the intertidal zones (and thus providing a more refined representation of tidal storage) than the coarser far field model.

The Advection Dispersion Model Used in ELCOM

Gross et al. (1998) compared the performance of several conservative advection schemes and showed that the QUICKEST (Quadratic Upstream Interpolation for Convective Kinematics with Estimated Streaming Terms, Leonard 1991) presented the smallest errors amongst the schemes tested therefore, it was well suited to model advective transport, as long as the Courant condition of the velocity field is maintained below unity. However, a flux limiter (ULTIMATE - Universal Limiter for Transport Interpolation Modelling of the Advective Transport Equation) needs to be added to preserve monotonicity in the concentration gradient (Leonard 1991, Lin and Falconer 1997) to correct for non-physical oscillations that is inherent of the third-order spatial accuracy of the QUICKEST method (Gross et al. 1998). Although the implementation of the flux limiter introduces some numerical diffusion in the computation (Laval et al. 2003a), Fringer et al. (2005) showed that the ULTIMATE-QUICKEST presented good performance with respect to numerical error and conservation of background potential energy amongst the 14 schemes tested. ULTIMATE-QUICKEST was able to maintain both the monotonicity and the density gradients under different stratification conditions (i.e. relative thickness of the pycnoclyne).

The choice of ULTIMATE-QUICKEST for ELCOM ensures that:

- Transported variable conservation is maintained;
- High spatial accuracy is achieved (3^{rd} order);
- No unphysical oscillations occur; and
- Numerical diffusion does not affect the simulation considerably.

During the advection scheme, the solution in ELCOM is computed in sub-time steps, such that the Courant condition is maintained always below one in the grid cells of the highest velocities. This sub-time stepping ensures that the advection numerical scheme in ELCOM is always operating within the range of best performance. ELCOM can also apply a numerical anti-diffusion filter based on the background potential energy to counteract numerical diffusion (Laval et al. 2003b)

The scheme is competitive with the schemes used in other commonly used models. For example, the standard POM (Princeton Ocean model) codes uses a centred difference scheme that is only second-order spatially accurate and ROMS (Regional Ocean Modelling System) has options for second, third, and fourth order schemes. The scheme used in POM is not conservative, and does not preserve monotonicity, and is known to present problems with along-shore currents and large salinity gradients (http://www.aos.princeton.edu/WWWPUBLIC/htdocs.pom/FTPbackup/FAQ.html). POM, however, offers contribution codes for TVD advection schemes and an anti diffusion filter for an upwind scheme. Additionally, because POM and ROMS are terrain following coordinates, there is loss of resolution in the vertical direction within deeper regions of the domain.

The Role of Turbulent Horizontal Diffusion in the Model Framework

In advection-dominated systems and at the coarse grid resolutions, it is unlikely that turbulent horizontal diffusion has a dominant effect in the flow field (e.g. Odman 1997). Recent sensitivity in simulations of a river inflow entering a stratified reservoir showed that there was practically no difference between results without or including an explicit horizontal eddy diffusion coefficient of 10 m^2/s (Morillo et al. 2007). These tests indicate that either advection is a dominant process or

numerical diffusion completely masks the effect of the eddy diffusion. However, in the vertical, the scales are much smaller, such that a closure scheme representing the effects of vertical eddy diffusion is required.

The Role of Molecular Diffusion in the Model Framework

Consistent with the above, molecular diffusion is an insignificant process in geophysical flows. As such, it is not directly simulated by ELCOM.

Vertical Mixing Schematisation within ELCOM

The vertical mixing algorithm adopted in ELCOM is fully described in Hodges et al. (2000) and Laval et al. (2003a). The following is a brief explanation of the algorithm.

The method extends the mixed layer models based on the budget of Turbulent Kinetic Energy (TKE) (Kraus and Turner 1967; Spigel et al. 1986) to the 3D Eulerian structure of ELCOM. Noting that the spatial domain can be represented as a series of contiguous water columns, in short, the method works sequentially as follows:

- For each water column, starting at the free-surface, a TKE budget (see below) between two contiguous vertical cells is computed. A similar budget is successively carried out down to the cell adjacent to the bottom of the water column;
- The TKE budget computes two TKE components: E_A, the energy available for mixing, and E_M, the energy required for mixing;
- E_M is the energy required to completely mix the density gradient between the two contiguous cells. This is also called the buoyancy flux required to mix the cells or the work done against gravity required to mix the cells;
- E_A is the TKE originating from the following sources:
  - existing TKE in the cells;
  - wind stirring; and
  - bottom drag when the free-surface and bottom cells, respectively, are included in the calculation;
  - vertical shear production for cells in the water column; and
  - unstable density gradients (e.g. during convective cooling).
  - (See Hodges et al. (2000) and Laval et al. (2003b) for how E_A from each of these sources is computed);
- A mixing time scale T_m is calculated based on the gradient Richardson number (Laval et al. 2003a);
- When there is sufficient energy to mix the two cells ($E_A > E_M$), momentum and scalars in the two cells are fully mixed, as long as $dt<T_m$, where dt is the model time step. Otherwise, a mixing fraction dt/Tm is computed, and only this fraction of a complete mixing event takes place.
- Dissipation of TKE is subtracted from the E_A.
- The remaining E_A is transported throughout the domain, and constitutes the existing TKE in the cells for the next time step.

Turbulence Closure Scheme within ELCOM

The turbulent closure scheme has been used in several successful simulations of coastal seas basins such as the Red Sea, the Adriatic Sea, Marmion Marine Park, and Cockburn Sound. The method is well suited to situations where wind-driven mixing in stratified conditions plays an important role in the hydrodynamics, particularly in the dynamics of diurnal surface layers, which are quite important in shallow areas. Other turbulence closure schemes, such as the Mellor Yamada 2.5 level model were shown to under predict mixing under stratified conditions (Martin 1985, Kantha and Clayson 2000), particularly because of the lack of shear mixing. Kantha and Clayson (2000) suggested the inclusion of additional parameterisations to address these problems.

A comparison between the wind-mixing layer closure scheme in ELCOM with other closure schemes have so far not been devised. However, the comparisons for the upper layers of the ocean shown in Kantha and Clayson (2000) infer that both wind mixing layer models and the adjusted Mellor Yamada model perform similarly, and are able to predict the diurnal surface layer modulation induced by solar radiation and convective cooling during the night and storm events. Additionally, the results of McCormick and Meadows (1988) confirm that wind-mixed layer models are adequate for shallow seas.

Conservation of Tracer within ELCOM

The numerical schemes adopted in ELCOM are all mass conservative, ascertained with a divergent-free velocity field that is satisfied with the continuity equation for a Boussinesq fluid. The ULTIMATE-QUICKEST scheme used for advection is conservative (Leonard 1991). Horizontal mixing of scalars, if required, is also computed with an explicit three-point centred second-order spatial scheme that is also conservative in the ARKAWA-C grid design of ELCOM. The vertical mixing adopted in ELCOM (Hodges et al. 2000, Laval et al. 2003a) also conserves mass, as it considers the exchange of mass between adjacent vertical cells at a time, where the quantity C_1*Vol_1+C_2Vol_2 (where C_i is the scalar concentration in the cells – 1 for the upper and 2 for the lower cell) is enforced. Cells can either fully mix or mix partially depending on the time step and the estimated local mixing time (Laval et al. 2003a). Details of the mixing model are presented in Hodges et al. (2000) and Laval et al. (2003a).

Nett Seasonal Circulations

A suite of far-field simulations was undertaken over an annual period to investigate the model performance in this regard. In particular, the nett ("residual") circulation patterns over the surface and bottom sheets in the far-field model have been computed.

The far-field Base Case (no discharge) model was used to this end and was executed for an annual period from 1st December 2001. This simulation was hot-started with a restart file from the end of a previous simulation that spanned the preceding year. The three-month periods of December 2001 to February 2002, and June 2002 to August 2002 (all inclusive) were then interrogated as representative of summer and winter conditions, respectively. This approach was adopted as a more rigorous 'seasonal' approach than consideration of a one month period only.

The velocity outputs from the surface and bottom sheets from these periods were examined. In particular, the average longitudinal and meridional velocities were computed over each period. This averaging removed tidal signals and extracted residual velocities only. This method resulted in a

spatially variant data set of residual longitudinal and meridional velocities for each period and each of the surface and bottom sheets. These velocity components were then combined to give residual total directions and magnitudes. These results are presented below for the Upper Spencer Gulf, to allow for comparison with the Nunes-Vaz data, of which typical summer and winter data is also shown.

All ELCOM plots have colour bars to indicate the value of the plotted quantity, with +90 being due north and –90 being due south in the case of the direction plots. Note that the Nunes-Vaz maps have been scanned from hard copies and are at different zoom scales to each other, and the model data. Also note that although –180 and +180 are coloured blue and red, respectively, they represent the same direction.

Bottom Winter Direction and Speed

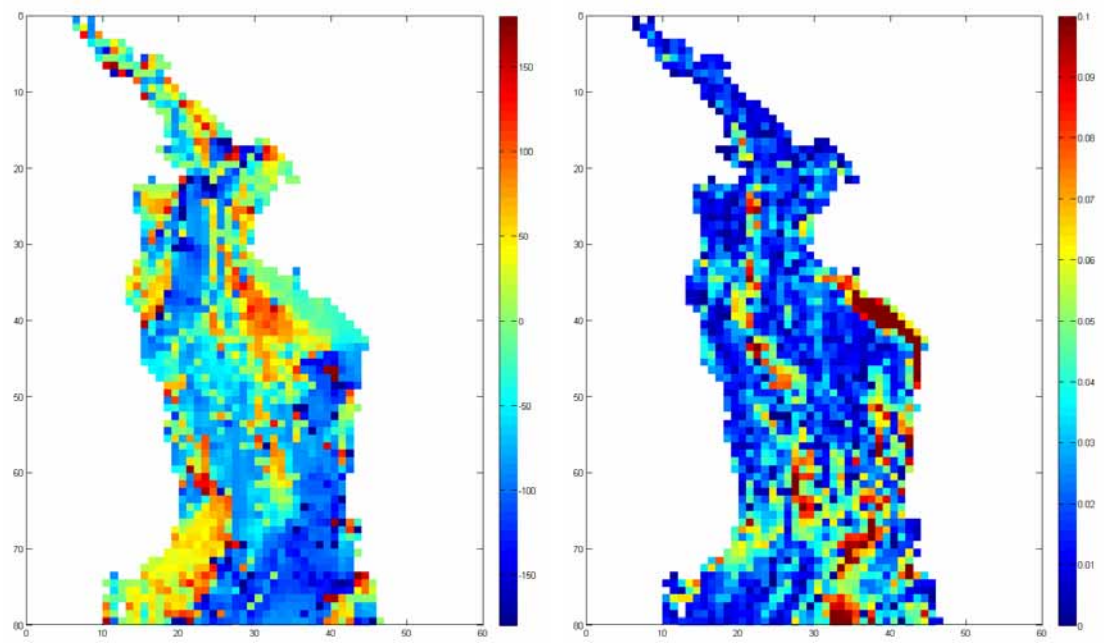

Surface Winter Direction and Speed

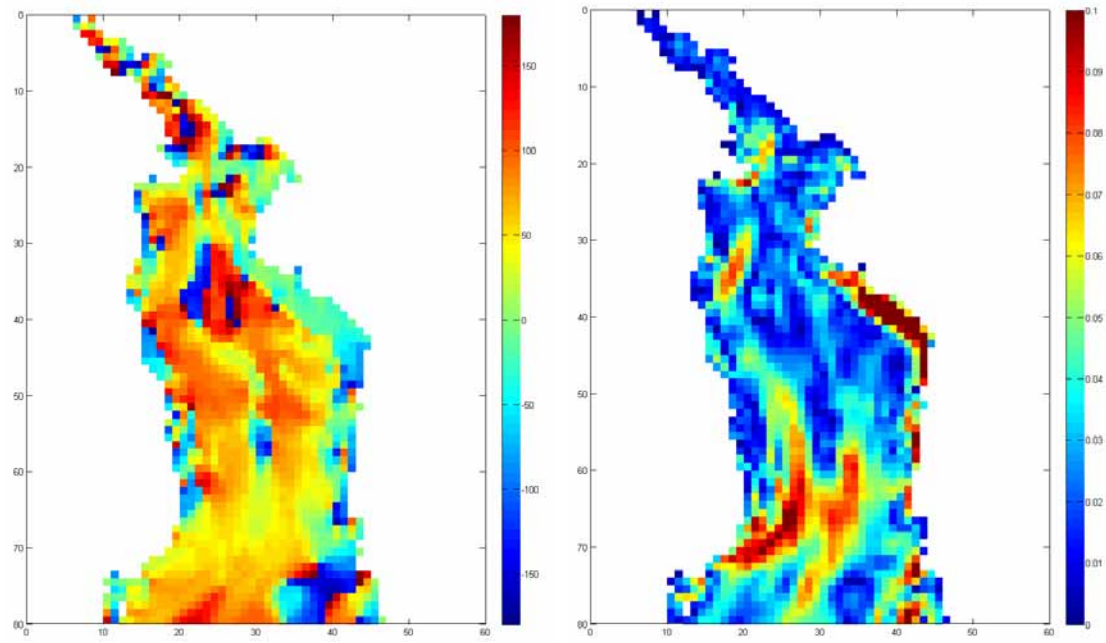

Figure 44 ELCOM Results: Winter

Nunes-Vaz Typical Winter Salinity Data

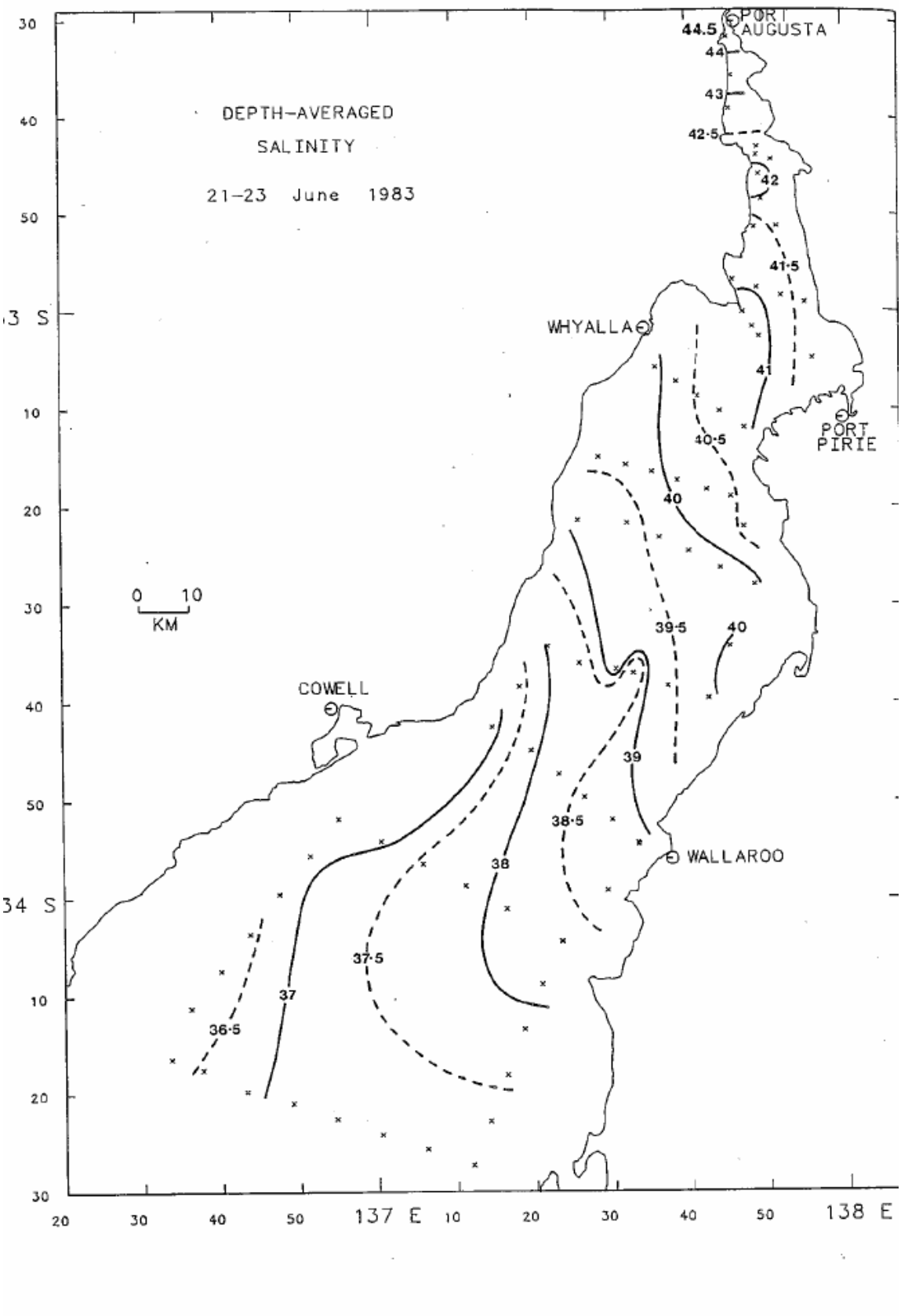

Figure 45 Nunes Vaz Data

Bottom Summer Direction and Speed

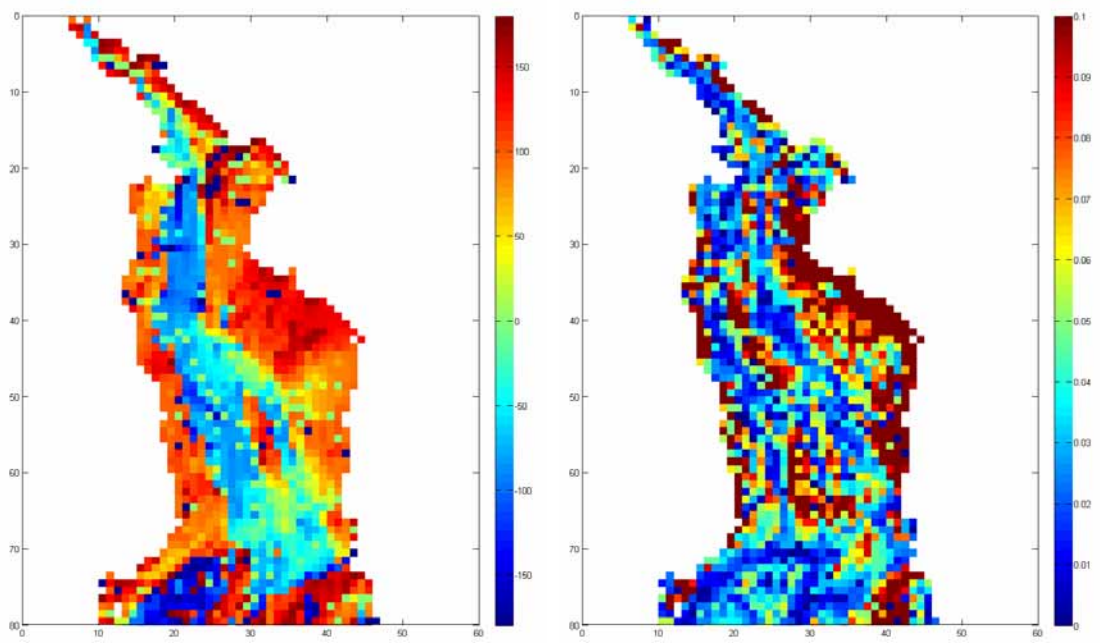

Surface Summer Direction and Speed

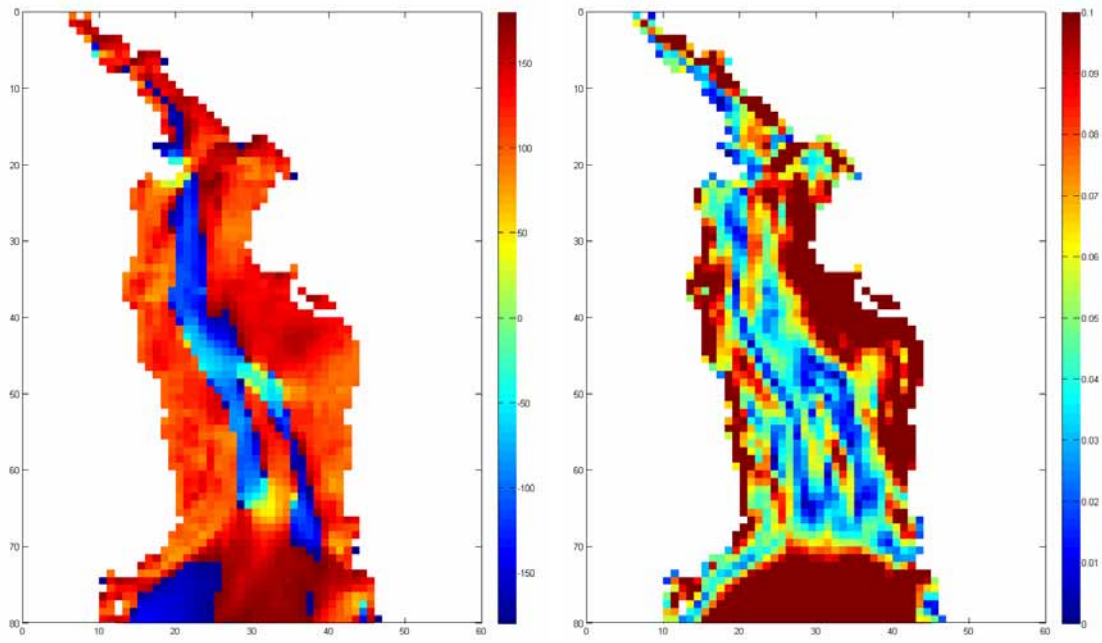

Figure 46 ELCOM Results: Summer

Nunes-Vaz Typical Summer Salinity Data

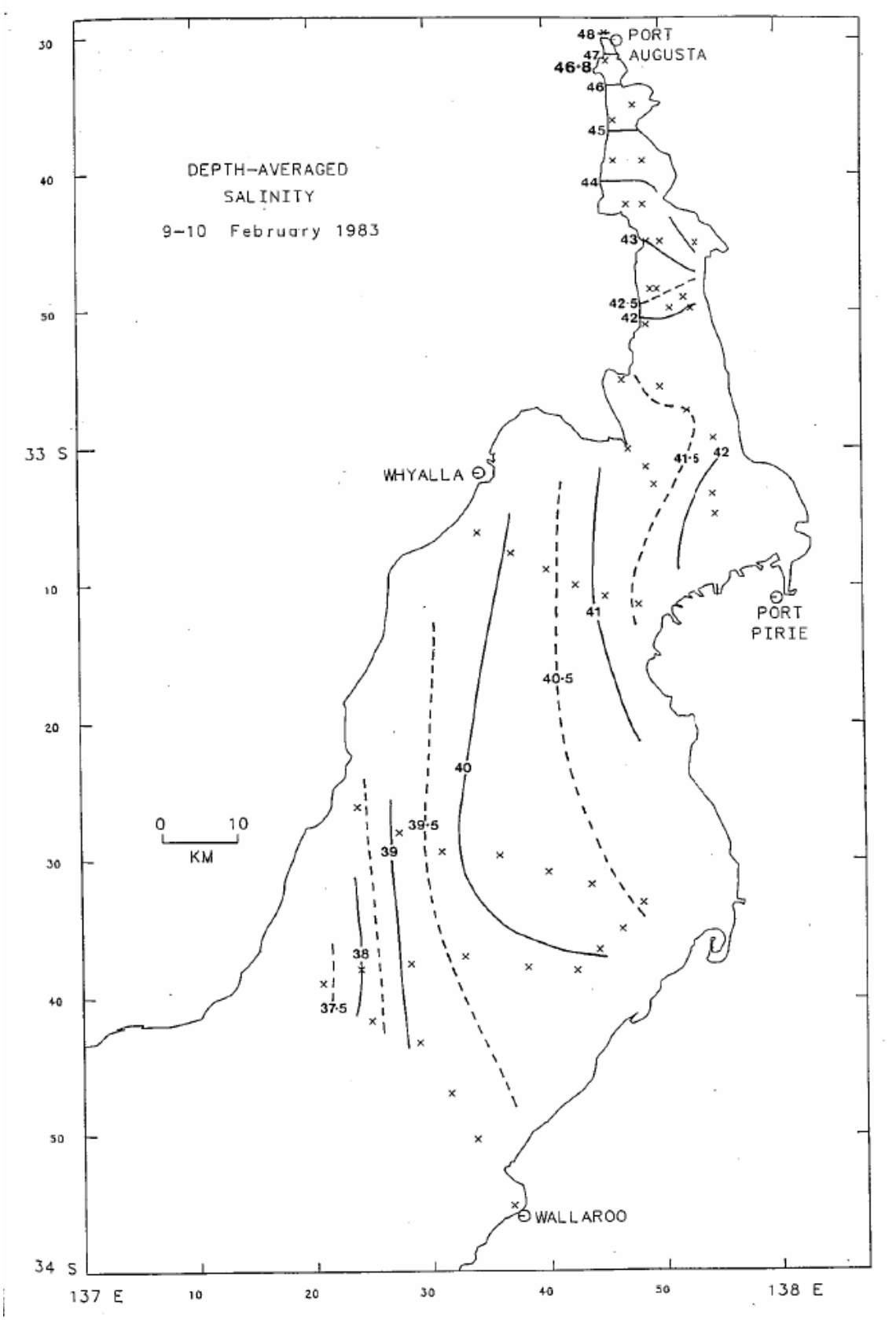

Figure 47 Nunes Vaz Data

Several key features of the above figures are apparent.

Firstly, both winter and summer bottom model residuals show a net southerly flow of water from Port Augusta along the deepest Gulf channels. In both seasons this is shown to be compensated for by surface return flows, to some extent, although the influence of wind-induced circulation on surface residuals has not been investigated. These bottom outflows are consistent with an ejection of saline water from the system at depth, as demonstrated elsewhere in this memo.

Secondly, the location of the nett southerly underflow during winter and summer is different in both the modelled and Nunes Vaz data sets (the latter is reflected in the curvature of the isohalines). In particular, the winter outflow is closer to the eastern shore of Spencer Gulf, consistent with Coriolis deflection, than the summer underflow. The above figures are repeated below with red circles indicating the location of the underflow in both the model and measured data.

Winter

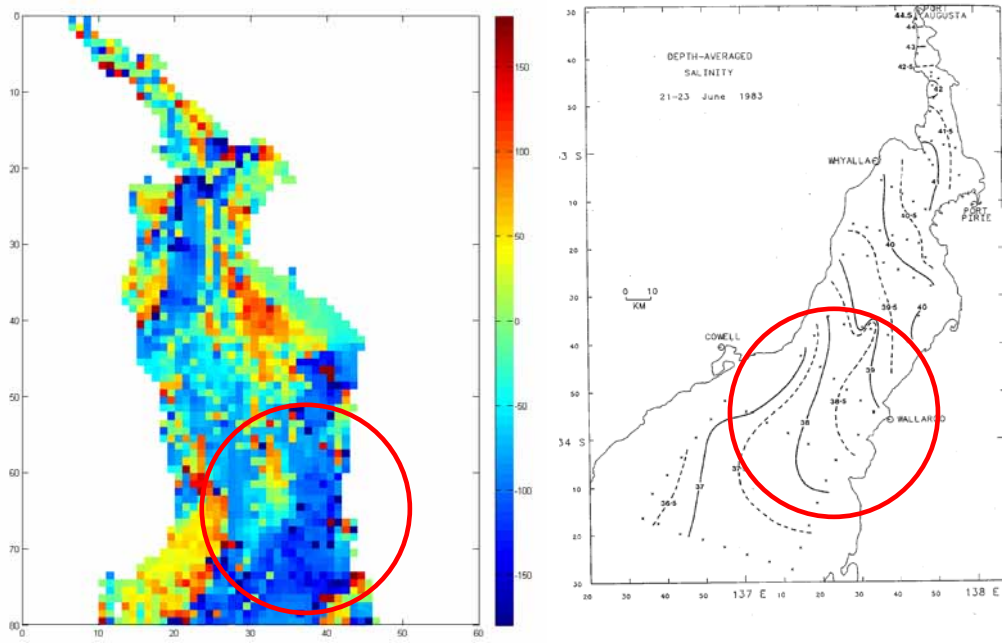

Figure 48 Winter Salt Ejection

Summer

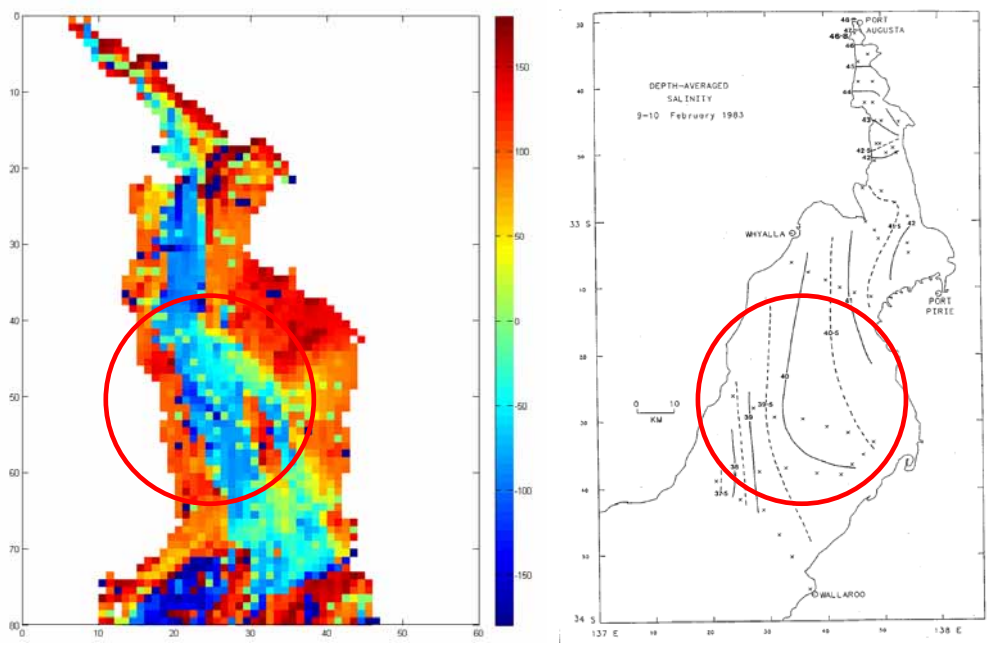

Figure 49 Summer Results and Data

Finally, there is some evidence of more uniform residual vertical velocity fields in summer, at least through the main channel, as evidenced by the directions in the top and bottom sheets. This may be related to a number of factors, including wind-induced mixing and atmospheric forcing, but the impact of these has not been investigated here.

Recent ADCP Data Collected at Point Lowly

Following the 2006 data collection program, a subsequent data collection exercise was undertaken over summer 2007-2008. Part of these measurements included deployment of a single bottom mounted ADCP at site B3 off Point Lowly. It was set to record current speed and direction at that location over several neap-spring tidal cycles. Model data (from the bottom layer) was also extracted at that location and the two were compared in a percentile sense. It is noted that this comparison is not strict in the sense that the model was not executed over the same period as the ADCP data. Nonetheless, results are presented in Table 1.

Table 1 Model and ADCP Velocity Magnitude Comparison (m/s) – Point Lowly

Percentile	0	1	5	10	25	50	75	90	95	99	100
Modelled	0.00	0.01	0.03	0.05	0.15	0.34	0.590	0.77	0.86	0.98	1.17
ADCP	0.00	0.05	0.12	0.19	0.38	0.70	1.00	1.26	1.38	1.54	2.11

The table shows that the model predictions are generally lower that the ADCP measurements. This may be due to numerical drag issues, the difference in the modelled and measured periods, the size of the grid cells, the very high ambient velocities in the area, or other calibration related matters. Based on this result, the need to undertake recalibration or re-configuration of the model was considered. It was determined, however, that this was not necessary at present as the model was

shown to provide a conservative estimate of dilution and mixing via its under-prediction of velocity magnitudes.

References

Bye, J.A.T. and I.P. Harbison. 1991. Transfer of inland salts to the marine environment at the head of Spencer Gulf, South Australia. *Palaeogeography, Palaeoclimatology, Palaeoecology*, 84: 357-368.

Fringer, O. B.,Armfield, S. W., Street, R. L. (2005). Reducing numerical diffusion in interfacial gravity wave simulations. *International Journal for Numerical Methods in Fluids* 49: 301-329.

Gross, E. S., Casulli, V., Bonaventura, L., Koseff, J. R. (1998). A semi-implicit method for vertical transport in multidimensional models. *International Journal for Numerical Methods in Fluids* 28: 157-186.

Hodges, B.R., Imberger, J, Saggio, A. A., Winters, K. B. (2000). Modeling basin-scale internal waves in a stratified lake. *Limnology and Oceanography* 45(7): 1603-1620.

Kantha, L. H., and Clayson, C. A. (2000). Small-scale processes in geophysical fluid flows. Academic Press.

Kraus, E. B., Turner, J.S. (1967) A one-dimensional model of the seasonal thermocline II. The general theory and its consequences. *Tellus* 19: 98-106.

Laval, B.E., Imberger, J. and Findikakis, A.N. (2003a) Mass transport between a semi-enclosed basin and the ocean: Maracaibo system. *Journal of Geophysical Research* (*Oceans*) 108 (C7): 3236.

Laval, B.E., Hodges, B. R., Imberger, J. (2003b) Reducing numerical diffusion effects with pycnoclyne filter. *Journal of Hydraulic Engineering*, *ASCE* 129(3) 215-224.

Leonard, B.P. (1991) The ULTIMATE conservative difference scheme applied to unsteady one-dimensional advection. *Computer Methods in Applied Mechanics and Engineering* 88: 17-74.

Lin, B. Falconer, R.A. (1997). Tidal flow and transport modelling using ULTIMATE QUICKEST scheme. *Journal of Hydraulic Engineering*, ASCE 123(4) 303-314.

Martin, P. J. (1985). Simulation of the mixed layer at OWS November and Papa with several models. *Journal of Geophysical Research* 90: 903-916.

McCormick, M. J., Meadows, G. A. (1988). An intercomparison of four mixed layer models in a shallow inland sea. *Journal of Geophysical Research* 93: 6774-6788.

Morillo, S., Imberger, J., Antenucci, J.P. and Woods, P. (2007) The influence of wind and lake morphometry on the interaction between two rivers entering a stratified lake. *Journal of Hydraulic Engineering, ASCE* (submitted).

Nunes, R.A. (1985). Catalogue of Data from a Systematic Programme of oceanographic Measurements in Northern Spencer Gulf from 1982 to 1985. School of Earth Sciences Flinders University of South Australia, *Cruise Report No. 9*.

Nunes, R.A., and G.W. Lennon. (1986). Physical property distributions and seasonal trends in Spencer Gulf, South Australia: an inverse estuary. *Australian Journal of Marine and Freshwater Research*. 37: 39-53.

Nunes Vaz, R.A., G.W. Lennon and D.G. Bowers. (1990). Physical behaviour of a large, negative or inverse estuary. *Continental Shelf Research*. 10(3): 277-304.

Odman, M. T. (1997). A quantitative analysis of numerical diffusion introduced by advection algorithms in air-quality models. *Atmospheric Environment*. 31(13): 1933-1940.

Spigel R. H., Imberger, J., Rayner, K.N. (1986) Modeling the diurnal mixed layer. *Limnology and Oceanography*. 31: 533-556.

BMT WBM Brisbane
Level 11, 490 Upper Edward Street Brisbane 4000
PO Box 203 Spring Hill QLD 4004
Tel +61 7 3831 6744 Fax +61 7 3832 3627
Email wbm@wbmpl.com.au
Web www.wbmpl.com.au

BMT WBM Denver
14 Inverness Drive East, #B132
Englewood Denver Colorado 80112 USA
Tel +1 303 792 9814 Fax +1 303 792 9742
Email wbmdenver@wbmpl.com.au
Web www.wbmpl.com.au

BMT WBM Melbourne
Level 5, 99 King Street Melbourne 3000
PO Box 604 Collins Street West VIC 8007
Tel +61 3 9614 6400 Fax +61 3 9614 6966
Email wbmmelbourne@wbmpl.com.au
Web www.wbmpl.com.au

BMT WBM Morwell
Cnr Hazelwood Drive & Miners Way Morwell 3840
PO Box 888 Morwell VIC 3840
Tel +61 3 5135 3400 Fax +61 3 5135 3444
Email wbmmorwell@wbmpl.com.au
Web www.wbmpl.com.au

BMT WBM Newcastle
126 Belford Street Broadmeadow 2292
PO Box 266 Broadmeadow NSW 2292
Tel +61 2 4940 8882 Fax +61 2 4940 8887
Email wbmnewcastle@wbmpl.com.au
Web www.wbmpl.com.au

BMT WBM Perth
1 Brodie Hall Drive Technology Park Bentley 6102
Tel +61 8 9328 2029 Fax +61 8 9486 7588
Email wbmperth@wbmpl.com.au
Web www.wbmpl.com.au

BMT WBM Sydney
Suite 206, 118 Great North Road Five Dock 2046
PO Box 129 Five Dock NSW 2046
Tel +61 2 9713 4836 Fax +61 2 9713 4890
Email wbmsydney@wbmpl.com.au
Web www.wbmpl.com.au

BMT WBM Vancouver
1190 Melville Street #700 Vancouver
British Columbia V6E 3W1 Canada
Tel +1 604 683 5777 Fax +1 604 608 3232
Email wbmvancouver@wbmpl.com.au
Web www.wbmpl.com.au